SLAPTON SANDS BEACH MANAGEMENT PLAN:

COASTAL PROCESSES BASELINE

Report provided by: Coastal Marine Applied Research, University of Plymouth Enterprise Ltd.

Report provided for: Slapton Line Partnership

Date: September 2017

Project code: 1609

Document code/version:1609_v4

COASTAL MARINE APPLIED RESEARCH WITH PLYMOUTH UNIVERSITY

A research-informed consultancy to address important issues in the coastal and marine environment

CMAR: Coastal Marine Applied Research

CMAR is a research-informed consultancy group based in the School of Biological and Marine Sciences at Plymouth University, south west UK, and contract our services through the university's wholly owned commercial subsidiary, University of Plymouth Enterprise Limited (UoPEL). We focus on coastal processes and marine physics, and aim to provide a first-class data collection, analysis and synthesis service to help address important issues in the coastal and marine environment. We strive to understand and predict the behaviour of coastal, marine and estuarine systems to support the appropriate management of resources and activities in these environments.

All queries related to this document should be directed to the CMAR Team:

School of Biological and Marine Sciences, Reynolds Building, Plymouth University, Drake Circus, Plymouth, Devon PL4 8AA

Email: cmar@plymouth.ac.uk

Telephone: +44 1752 586177

Web: www.plymouth.ac.uk/cmar

Twitter: @pu_cmar

COASTAL MARINE APPLIED RESEARCH WITH PLYMOUTH UNIVERSITY

Document Information

Document permissions	CH2M HILL
Project number	1609
Project name	SLAPTON SANDS BEACH MANAGEMENT PLAN: COASTAL PROCESSES BASELINE
Report date	September 2017
Report number	1609_v4
Client	Slapton Line Partnership
Client representative	CH2M HILL, Emma Allan
Project lead	Dr Christopher Stokes
Project manager	Prof. Gerd Masselink

Document history

Date	Issue	Prepared	Approved	Authorised	notes
07/09/17	Revised Draft	CS	GM	GM	
30/08/17	Revised Draft	CS	GM	GM	
14/06/17	Revised Draft	CS	GM	GM	
07/06/17	Draft	CS	GM	GM	

Document authorisation

Prepared	Approved	Authorised
Dr Christopher Stokes	Prof. Gerd Masselink	Prof. Gerd Masselink

Slapton Sands Beach Management Plan: Coastal Processes Baseline

Executive Summary

This Coastal Processes Baseline Report has been prepared to support the Slapton Sands Beach Management Plan (BMP). Studies covering defences, the environment and economics are being undertaken separately and a detailed options appraisal will be completed as part of the BMP process.

The purpose of this report is to provide an up-to-date understanding of the coastal processes operating along the coastline at Slapton Sands, and to the north at Blackpool Sands, and to the south at Hallsands and Beesands. The content and findings of this report aim to provide an update to the Slapton Coastal Zone Management Study (SCZMS) (Scott Wilson, 2006) and draws upon Plymouth University's recent research of Slapton Sands and the wider Start Bay, to ensure that the options appraisal process is underpinned by the best possible evidence and analysis of coastal processes and shoreline change.

In this report, coastal processes and morphological change acting over three key time-scales (long-term, medium-term, and short-term) in Start Bay have been examined, with a detailed focus on Slapton Sands. The key findings are:

- Over long time-scales, relative sea level rise gradually increases the vertical reach of waves; this increasingly allows for short-term events (storm waves) to cut-back the upper beach profile and for wave run-up to overtop/overwash the crest of the beach.
- Meanwhile, alongshore-oriented waves cause beach rotation (where sediment that is lost from one section of the beach migrates either north or south) over medium time-scales, which reduces the sediment volume along certain stretches of Start Bay. Those sections are then vulnerable to short-term wave attack and overwashing.
- Short-term storm wave attack results in vulnerable sections of Start Bay being cut-back even further, and allows wave run-up to overtop and overwash sections of the beaches.
- These episodic, short time-scale overwashing events are the mechanism for long-term barrier roll-back, and allow the barrier to retreat in response to sea level rise.
- As Slapton Barrier retreats, its overall length is expected to increase as a result of the barrier conforming to the embayed shape of the Ley during its retreat.

- Eventually, the decreasing cross-sectional area of Slapton Barrier, caused by the lengthening of the shoreline as it retreats, will make the barrier increasingly vulnerable to breaching. Once significant breaching occurs, the barrier could begin to break down into a series of tidal inlets.

These interacting coastal processes cause a number of coastal management challenges. In the short-term, storm wave attack is the main concern to coastal management, as this can cause barrier erosion/cut-back in response to wave run-up, overtopping or overwashing, as well as coastal flooding and undermining of the A379 road, storm defences (seawalls and rip-rap), and other engineered structures. Over medium time-scales (weeks – years), the alongshore supply of sediment and resulting vulnerability of the different sections of Start Bay is a concern for coastal management as it will make certain sections of the barrier more vulnerable to short-term storm processes (barrier erosion and overwashing). Over the long-term (decades – centuries), without appropriate mitigation, the retreat of Slapton barrier could potentially expose Torcross village to the sea, and will require consideration to be given to the future of the Slapton line section of the A379 road. This may involve gradual realignment, to maintain the roads position on the barrier, or eventually to complete re-routing or re-engineering of the road in the extreme case of barrier breaching/breakdown. In the long-term, barrier retreat and potential breaching of the barrier road may also have significant implications for the freshwater status of Slapton Ley.

In Start Bay, wave conditions arrive from both a southerly direction and an easterly direction. The southerly waves originate in the Atlantic Ocean, and refract into Start Bay as they propagate up the English Channel, whereas the easterly waves originate from local storms occurring in the Channel itself. Net alongshore sediment transport in Start Bay is from south to north, driven by Atlantic waves arriving from the south of the bay. Drift reversals occur from north to south, when waves originating in the English Channel arrive from the east. Alongshore sediment transport and beach rotation is shown to be strongly related to the magnitude and direction of the incident wave power, and that the cumulative effects of powerful waves refracting around Start point and arriving obliquely from the south drives the net sediment transport to the north. This has subsequently resulted in erosion of the beaches to the south and accretion of the beaches to the north. This pattern effectively causes the shoreline in Start Bay to rotate in an clockwise direction.

Alongshore sediment transport has led to an overall net loss of volume at all profiles in Start Bay south of Strete Gate since at least 1972, with net gains seen at the Strete end of Slapton Sands, and at Blackpool Sands. Statistical modelling suggests that, since at least 1980, periods of rapid northward (clockwise) beach rotation, caused by northward alongshore transport, have occured every 1 – 2 years over winter, interspersed by more gradual southward (anti-clockwise) beach rotation, caused by southward alongshore transport.

In the last 30 years, there has been a 75% reduction in the 10-year averaged activity of easterly storms with wave height (H_s) greater than 2.5 m arriving at Start Bay. In contrast, southerly storm activity remained relatively constant over that period. This is attributed to shifts in the distribution of atmospheric pressure and resulting storm tracks across the Atlantic Ocean, with easterly storm conditions only developing during periods of negative North Atlantic Oscillation (NAO), which have declined in the last 30 years. This has created a bias towards net northward sediment transport in Start Bay.

The total volume of sediment transported northward in Start Bay during the extremely energetic winter of 2013/2014 (which featured 26 days of stormy wave conditions from the south) was approximately 745,000 m^3, equating to an average alongshore transport rate of 28,654 m^3 per day, equivalent to around 48,000 metric tonnes of gravel per day. This provides some estimate of the maximum alongshore transport rate likely to occur in Start Bay, given the magnitude and return period of the storms experienced during that winter. Modelling indicates that Slapton Sands now has more sediment in the north, and less sediment in the middle and south, than at any other time since at least 1980. Embayment-wide surveys conducted before and after the 2013/2014 winter indicate that no sediment volume was lost from Start Bay during that period, and as such we conclude that, for all practical purposes, Start Bay can be considered a closed sediment cell.

The most significant erosion in Start Bay is likely to occur due to the sequential action of southerly and easterly storm wave conditions. Southerly waves have the potential to drive significant alongshore sediment transport to the north, which results in beach narrowing to the south, widening to the north and resultant beach rotation in a clockwise direction. This leaves the coast to the south of Strete vulnerable to waves from the east, which can cause further profile cut-back and overwashing.

A number of erosional hot-spots have been identified within Start Bay. The most vulnerable sections are at the south of Hallsands beach and at the south of Slapton Sands in front of Torcross village. The middle of the Slapton barrier (around the location of the 2001 road collapse) is shown to be the most vulnerable section of the barrier to overwashing of sediment, and to potential future undermining of the road, or even breaching of the barrier. Further modelling is required in order to better understand the vulnerability of each section of Start Bay to future potential storm events.

Under all UKCP09 emissions scenarios, the rate of sea-level rise will increase in the future, and local sea levels are likely to be 42 – 59 cm higher than their 1990 levels by the year 2100. Coastal flooding in Start Bay will therefore become more likely in the future, and in the first instance is most likely to affect parts of Hallsands and Beesands, which have the lowest profiles in Start Bay. At present, skew surge can super-elevate the height of the still water level during a storm by 85 – 104 cm during 20-year to 100-year return period events, and is therefore a major potential contributor to coastal flooding.

Using a barrier retreat formula developed specifically for gravel barriers, it is predicted that, on average, the Slapton barrier will naturally attempt to migrate landward 3.4 – 4.5 m by the year 2036, 9.6 – 12 m by the year 2065, and 22 – 28 m by the year 2117. These migration rates may be exceeded due to increasing storminess in the future, and due to a reducing cross-sectional area as the barrier retreats. Therefore, under all UKCP09 emissions scenarios, the barriers position is predicted to migrate inland over the next 100 years, and the majority of the Slapton Line section of the A379 road and southwest coast path could be affected within this period. However, the actual rate of barrier retreat will be lower where human interventions (engineered sea defences and post-storm sediment re-charges) act to stop sediment from migrating from the front of the barrier to the back of the barrier.

Detailed modelling is now required in order to better understand the inshore wave conditions along the length of Start Bay under different scenarios. This can then feed into detailed alongshore transport modelling which will enable the quantification of alongshore transport rates and sediment gains/losses along the bay under different wave scenarios. To fully assess the vulnerability of the barrier system, and hence the A379 road, to overwash and breaching under different wave and sea-level scenarios, process-based morphodynamic modelling is required. An outline methodology for such a study is proposed in Section 7.2 of the report.

Contents

COASTAL MARINE APPLIED RESEARCH WITH PLYMOUTH UNIVERSITY

Table of Figures

1. Introduction

1.1. Background and Study Area

This report has been prepared for South Hams District Council (SHDC) and their partners, including the Slapton Line Partnership (SLP), the Environment Agency and Devon County Council (DCC), as part of the Slapton Beach Management Plan (BMP).

The BMP study area covers the coastline from Torcross in the south, to Strete Gate in the north, as shown in Figure 1.1. For the purpose of the Coastal Processes Baseline Report, the study area has been extended to include Blackpool Sands, Beesands and Hallsands.

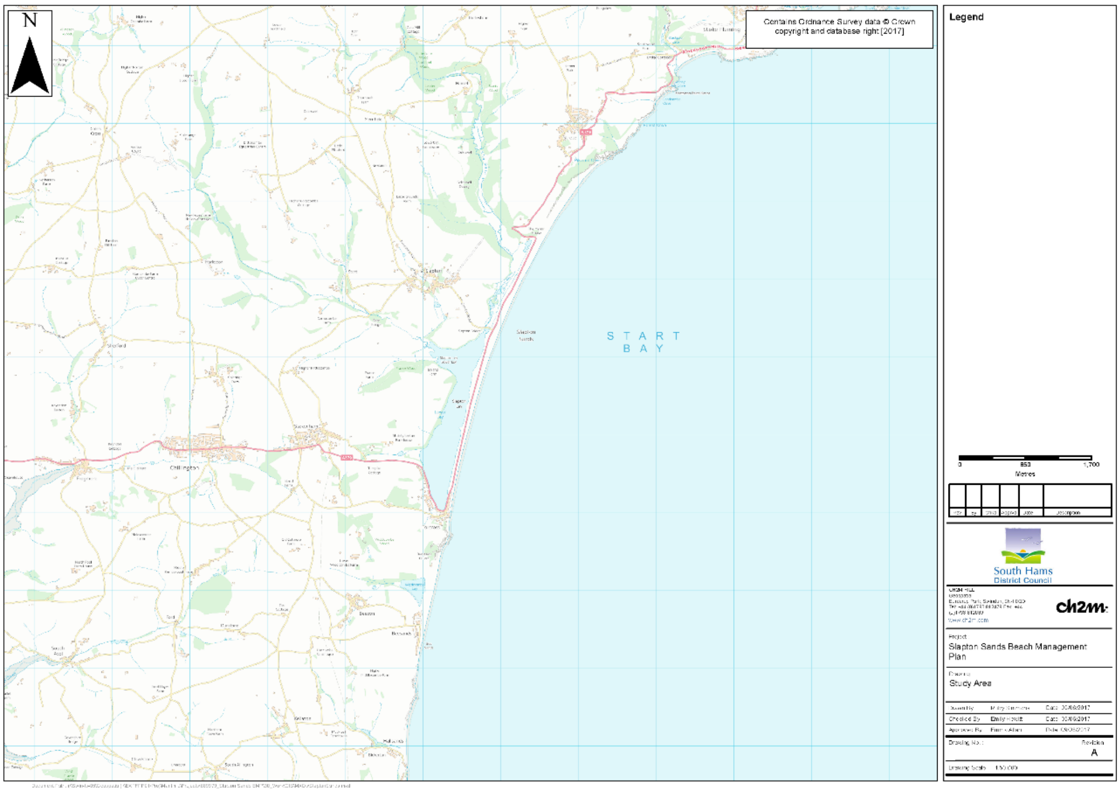

Figure 1-1. Slapton Sands BMP Study Area

1.2. The Basis of this Report

This Coastal Processes Baseline Report is a supporting document to the BMP. Studies covering defences, the environment and economics are being undertaken separately and a detailed options appraisal will be completed as part of the BMP process.

The purpose of this report is to provide an up-to-date understanding of the coastal processes operating along the coastline at Slapton and to the north at Blackpool Sands and to the south at Hallsands and Beesands. The content and findings of this report aim to provide an update to the Slapton Coastal Zone Management Study (SCZMS) (Scott Wilson, 2006) (*specifically Chapters 5 and 10 – beach dynamics, trends and understanding; and Chapter 11 – conceptual process model and predictions of future evolution*) and draws upon the Plymouth University's recent research of Slapton Sands and the wider Start Bay, to ensure that the options appraisal process is underpinned by the best possible evidence and analysis of coastal processes and shoreline change.

1.3. Information Reviewed and New Analysis

A key aim of the Slapton Sands BMP and objective of this report is to provide an update to the coastal processes information presented in the SCZMS. This report draws from existing literature, which is still highly relevant, but also focusses on using new information and data that have become available since 2006. Where there are data gaps, new analysis has been undertaken to improve the existing understanding, specifically:

- Wave climate and water levels,
- Climate change and sea level rise,
- Beach profile analysis and morphological change,
- Estimates of sediment transport volumes and longshore transport rates; and
- Erosional hot-spots.

2. Physical Setting

This section considers the controls on the coastal behaviour and shoreline evolution within the BMP study area. It discusses the morphology of the coastline, as it is today, and how it has evolved over time, and includes a summary of the key influences driving coastal processes and shoreline change. The information presented in this section of the report draws from the existing literature reviewed for the SCZMS (Scott Wilson, 2006), and the related publication by Chadwick *et al*. (2005), which are still highly relevant. Recent literature relevant to the studies undertaken for this coastal processes baseline is also provided within each section of the report.

2.1. The Study Area Today

Slapton Sands is a southeast facing gravel barrier beach in Start Bay, on the south coast of Devon, UK (Figure 2-1, Figure 2-2 and Figure 2-3). To the northeast of Slapton Sands lies Blackpool Sands, and to the southwest lies Beesands and Hallsands beaches (Figure 2-3). These beaches make up a semi-connected (tidally cut-off) system of beaches within Start Bay (Buscombe, 2008). The beach at Slapton Sands is approximately 4.5 km long, and extends continuously between headlands at its southwestern (Torcross) and northeastern (Strete) extents (Figure 2-1). The central section of Slapton Sands fronts the Slapton Ley lagoon, the largest freshwater lake in southwest England, which is a national nature reserve and is of considerable ecological importance (Barne *et al.*, 1996). Between the lagoon and the beach runs a section of the A379 road (Figure 2-2, the 'Slapton line'), which provides an important thoroughfare for local traffic, and running parallel to the road on the barrier is a stretch of the southwest coast path.

The gravel barrier at Slapton Sands is between 50 and 100 m wide at high tide and widens between Torcross and the northeast extent of the barrier. The barrier crest sits at approximately 6 m above Ordnance Datum Newlyn (ODN, 3.32 m above highest astronomical tide) at Torcross, and increases to 8 m ODN at the northeastern extent of the beach (Buscombe, 2008). Median gravel sizes on Slapton Sands coarsen from 1.9 mm at Strete, to 7.0 - 9.5 mm at Torcross.

Over the years, the shingle barrier has become constrained by the installation of short lengths of coastal defences, and by the A379 road itself. The defences, which are comprised of rock armour and concrete block mattresses, defend Torcross village and the road and car parks along the Slapton line. The presence of these engineered structures slows the erosion of the barrier crest and influences the adjoining beach profiles (Chadwick *et al.*, 2005). The road has a significant influence on the evolution of the barrier, preventing gravel thrown landwards of the beach crest from forming a new crest further landward (i.e. rolling back). Instead, gravel is cleaned off the road after a storm and deposited back on the seaward side. These effects, however, only play a role at the sections of the beach where the road is close to the active beach crest.

Figure 2-1. Slapton Sands and Slapton barrier/Ley from above. At the left and right hand sides of the beach, Strete Gate and Torcross village can be seen, respectively. Slapton village is inland, just left of centre. Image courtesy of the Slapton Line Partnership (http://www.slaptonline.org/).

Figure 2-2. Slapton Sands and Slapton barrier/Ley from the Torcross (south) end of the beach. The A379 road can be seen in the centre of the barrier. Relic gravel wash-over fans from historic storm events can be seen on the lagoon (left) side of the barrier. Image courtesy of the Slapton Line Partnership (http://www.slaptonline.org/).

COASTAL MARINE APPLIED RESEARCH WITH PLYMOUTH UNIVERSITY

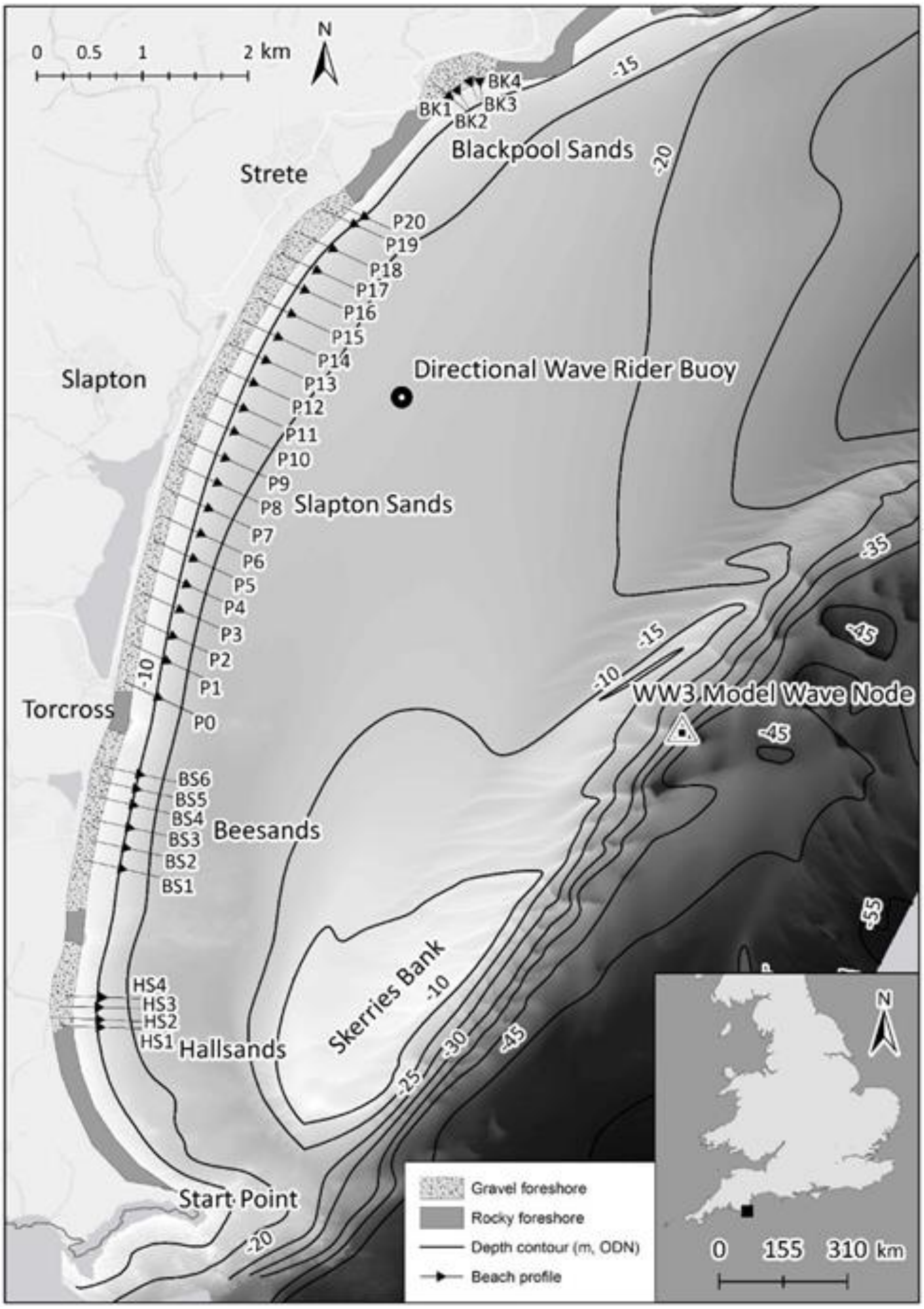

Figure 2-3. Location map showing Start Bay, South Devon, UK (from Wiggins *et al.*, 2017). Nearshore bathymetry from 2013 (UKHO, http://aws2.caris.com/ukho/) and associated contours (m, ODN) highlight the location of Skerries Bank. Survey profile locations for each beach are shown as arrows pointing offshore and are labelled accordingly. The foreshore is identified as either gravel or rock, and the location of the Directional Wave Rider Buoy (PCO, http://southwest.coastalmonitoring.org/), and the WaveWatch III (WW3) model node is shown to the east of Slapton Sands.

2.2. Key Coastal Process Influences and Long-Term Morphological Evolution

2.2.1. Key Coastal Process Influences

As was identified in the previous SCZMS, coastal processes influence the beaches of Start Bay on three main time-scales (Table 2-1). These are: the long-term effects of sea-level rise, including barrier roll back and shoreline retreat, acting over decades to centuries, medium-term alongshore transport, acting over weeks to years, and short-term storm impacts, which act over a matter of days. Coastal processes acting on these three time-scales are examined in this report in more detail in Sections 4 (long-term), 5 (medium-term), and 6 (short-term), respectively. The sections/time-scales are presented in this order to highlight the relative order in which the processes occur – processes acting on the medium time-scale are superimposed on the long-term changes, and processes acting on short time-scales are superimposed on the medium and longer term changes.

Table 2-1. The three key time-scales of morphological change in Start Bay.

Time-scale	Time-frame	Morphological forcing
Long-term	decades – centuries	sea-level rise and barrier rollback
Medium-term	weeks – years	alongshore transport gradients
Short-term	hours – days	storm impacts

2.2.2. Start Bay

Based on a set of tidal current data collected within Start Bay, Hails (1975) suggested that the submarine topography of the bay is formed by tidal streams and that waves are less effective than currents in transporting bottom sediment. He also suggested that little sediment from offshore reaches the beaches of Start Bay and identified three distinct sediment units within the bay, described as bay, bank and barrier deposits. The bay deposits were medium to fine sands with varying concentration of silts and shells. The bank deposits were coarse, shelly sands and approximately occupy the area of Skerries Bank. The barrier deposits were shingle or beach gravels and occupy a relatively narrow zone extending from the backshore of the beach to about 200 m beyond low water mark.

Robinson (1961) found that Skerries Bank has been relatively stable for over a century and there has been very little change in the planform of the bank from 1825 to 1951. He also found that apart from the shingle found on the barrier and the immediate foreshore very little shingle was found elsewhere. The materials on Skerries Bank, mobilised by moderate to high seas, is redistributed by tidal currents running parallel to the coast rather than being carried shoreward. However, there is no more-recent evidence to suggest whether there has been any net change to Skerries Bank as a result of such transport.

By analysing a number of sediment samples within Start Bay, Gleason *et al*. (1975) found that beach material at Slapton Sands is predominantly granules and small pebbles and has a pronounced alongshore grading with coarser beach material towards Torcross, and finer material to the north. They noticed a reversal of alongshore sediment grading along Slapton Sands at different times of the year. It was also noted that greatest accretion and depletion of sediment occurred at Torcross Point and Strete Head where coarse materials accumulated against the headlands.

The Shoreline Management Plan Review (SMP2) for Durlston Head to Rame Head (Halcrow Group, 2011) identified Start Bay as a closed sediment cell and Skerries Bank as a wave and sediment barrier. The report states that Skerries Bank focuses wave energy onto the southern sector of Start Bay, modifying the wave direction by diffraction and refraction. A limited net northward drift was identified within the bay from which Slapton Sands is likely to benefit. According to their calculations, the net northward alongshore transport at Slapton Sands is 61,500 m^3/year. The calculations were based on a theoretical analysis, comprising transformation of an offshore average annual wave climate to the shoreline and the determination of the alongshore transport rate at a single point using the Delft UNIBEST package. However, the results were not validated against reliable estimates of beach volume changes.

2.2.3. Slapton Sands

Futurecoast (2002) identified Slapton Sands as a self-contained beach that does not have significant sediment sources or sinks. The River Dart was not recognised as a major influence on coastal evolution as it is separated from the rest of Start Bay by hard rock headlands. Sediment exchange between Slapton beach and Skerries Bank was also thought not to occur (Futurecoast, 2002). Futurecoast (2002) recognised that beach materials move alongshore in north and south directions, depending on the incident wave direction, and that widening of the beach to the north, as identified by historical maps, implies a net northward drift. It also identified that frequent storms from the east and southeast can have a significant impact on alongshore transport.

Through a comprehensive analysis of different transport formulae, previously reviewed for their applicability to coarse-grained beaches, Chadwick *et al*. (2005) modelled alongshore transport rates on Slapton Sands. The results showed that high rates of net annual sediment transport can occur (of the order of 150,000 m^3 per annum), but that the rate and direction varies from year to year and with location along the frontage. The results from their one-line model demonstrate that quite large changes in the shoreline position (of the order of 5 to 10 m) can occur over medium time-scales (weeks – months).

2.2.4. Slapton Barrier

A barrier beach is a narrow, elongated ridge of sand or gravel sitting slightly above high tide level. Generally, a barrier beach lies parallel to the coast, but is separated from it by a wetland, lagoon or estuary. Barrier beaches act as a natural means of coastal protection. In addition, the low-lying areas behind barriers provide shelter for many coastal habitats and are therefore of considerable environmental significance.

Barrier beaches are constantly changed and modified by coastal processes acting over different time-scales (Table 2-1). Short-term changes in barrier beaches are related to the local wave and current climate, tidal variations, storminess and barrier geometry. Over medium and long time scales, sea-level change, changes in alongshore sediment transport and sediment sources/sinks are the primary factors for barrier beach evolution. A barrier beach can respond to these factors by landward or seaward migration, reshaping and realignment and crest breakdown or build-up (Scott Wilson, 2006).

A barrier beach can respond to these factors by landward or seaward migration, reshaping and realignment and crest breakdown or build-up. Long-term barrier evolution associated with processes such as sea-level rise is well documented. Orford *et al*. (1991; 1995a; 1995b; 1996) found that landward migration of the seaward shoreline of a barrier beach is linearly proportional to annual sea-level change and the short-term sea-level rise is influential in the rate of barrier breakdown. Zhang *et al*. (2002) found that hydraulic conditions such as wave climate and storm intensity are more significant to barrier-beach evolution than barrier geometry.

Coarse-grained barrier beaches with steep seaward slopes possess distinct morphodynamic and hydrodynamic characteristics that differ from those on sandy barrier beaches. For instance, the high seepage potential in coarse-grained barrier beaches greatly reduces offshore sediment transport, thus creating barrier migration only in the onshore direction (Carter and Orford, 1984). However, barrier beaches with a steep seaward slope are found to be relatively stable under wave attack. Sediment particles in a coarse-grained barrier are entrained only by high-energy waves and have low landward migration in comparison with their sandy counterparts.

Three stages in the evolution of the Slapton barrier were identified by Massey (2004). These stages (Figure 2-4) are part of a general model of barrier evolution in south Devon, which is not only based on the three cores collected from Slapton Sands, but also on eight additional cores collected in South Devon at Blackpool Sands, Bantham, and Salcombe:

- Stage 1. With lower sea levels prior to 3000 years ago, barrier islands and/or spits are located east of the present shoreline. Tidal inlets allow marine waters to enter the back-barrier lagoon. The lagoon is fringed by salt marshes.
- Stage 2. Around 3000 years ago, sea-level rise slows down and the tidal inlets are 'choked' with sediments. The saline lagoon changes to a freshwater environment and the present Ley becomes established.
- Stage 3. The Ley fills in with sediments. This stage has been completed at Beesands and Hallsands.

COASTAL MARINE APPLIED RESEARCH WITH PLYMOUTH UNIVERSITY

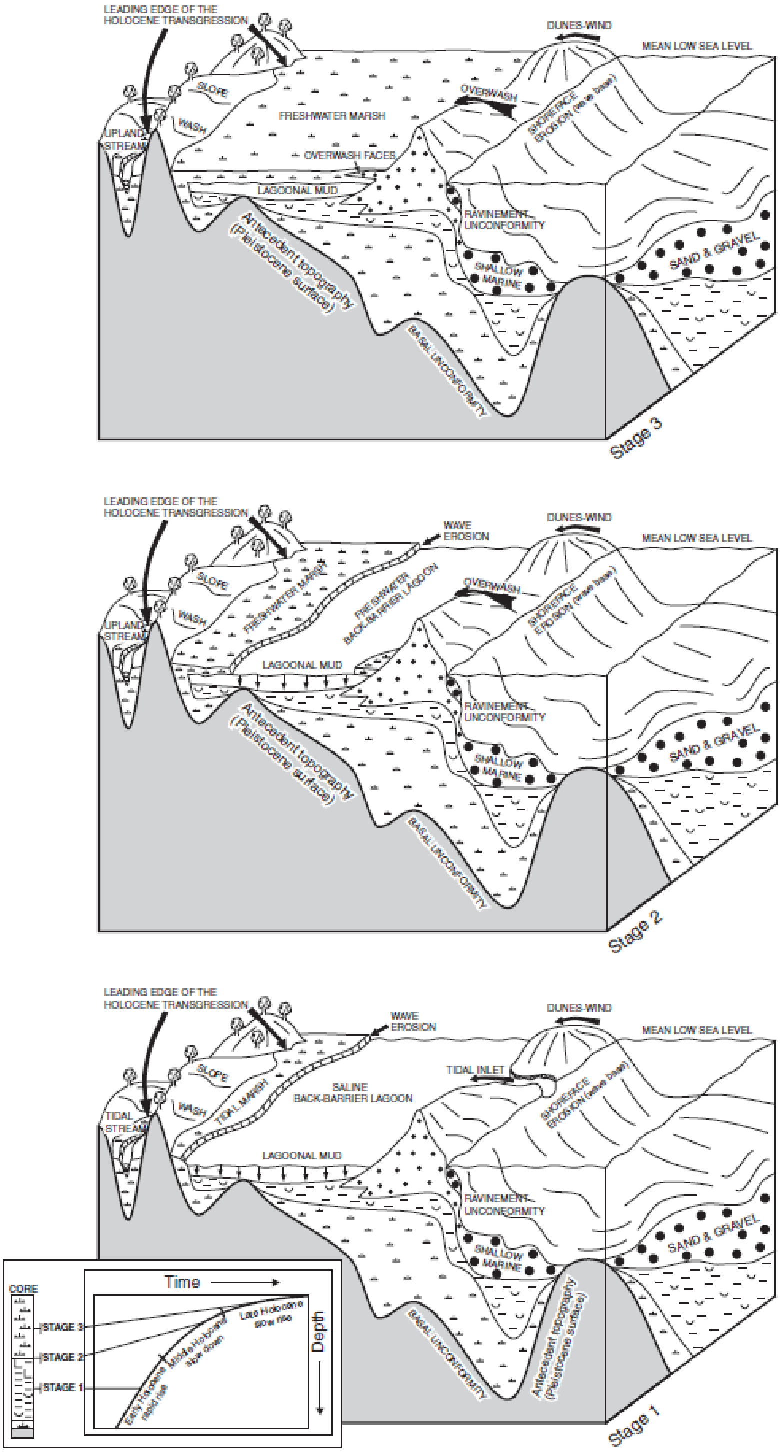

Figure 2-4. The three stages in the evolution of Slapton Sands, reconstructed from core data (from Massey, 2004). The inset shows the generalised sea-level curve and associated schematic stratigraphy. Stage 1 (bottom panel): discontinuous barrier system in early Holocene under rapid rates of sea-level rise. Stage 2 (middle panel): closure of barrier system under decelerating sea level rise. Stage 3 (top panel): filling in of back-barrier basin during slow sea-level rise.

Slapton Ley is still in a transition zone between stages 2 and 3, although the Higher Ley has already reached an advanced state of terrestrialisation. Under slow rates of sea-level rise it is be expected that the Ley would fill in completely. The transition from stage 1 to stage 2 is the critical phase in the evolution of Slapton Sands. This transition occurred when the average rate of sea-level rise slowed to less than 3 m per 1000 years (3 mm/year).

Analysis of three cores taken on Slapton barrier by Massey (2004) shows that the transition between the upper unit of gravel and underlying silts and clays occurs at a level of approximately 4 m below ODN. The thickness of the gravel unit varies between 7.65 and 9.42 m. The cores show changes in pebble size through the core, reflecting variations in energy conditions and/or sediment availability. The silt and clay unit is between 3.58 and 10.20 m thick. All cores reached bedrock between 8.34 and 14.83 m below OD.

On the basis of a radiocarbon date on the lowest peat in the Ley, Morey (1976, 1983) concluded that tidal influence in the Slapton back-barrier ceased about 3000 years ago. The silts and clays found in Massey's (2004) cores extend under the Ley and further offshore. They contain microfossils (foraminifera) that are characteristic of salt-marsh and tidal flat environments. From this litho- and biostratigraphical evidence, Massey (2004) concluded that, prior to 3000 years ago, the Ley was an intertidal environment, fronted by a discontinuous barrier system.

The barrier beach ridge has experienced periodic wash-over caused by storm waves and this has allowed the whole landform to transgress landward (roll-back) and increase in crest height, in response to rising sea levels. Wash-over fans are seen along the length of the barrier (Figure 2-2), although these are poorly developed in comparison with other similar systems (e.g. Chesil Beach). A number of contemporary processes are at work on the Slapton shoreline, identified by Chadwick *et al*. (2005).

(a) Short-term changes in beach profile due to storms, acting over a period of several days. These storms may cause cut-back of the seaward edge of the shingle crest, or changes in crest elevation.
(b) Overtopping, in which wave action throws sediment and water onto the crest.
(c) Overflowing, or overwashing, where extremely high water levels coincident with wave action cause water to flow over the crest of the ridge. This can cause significant changes to the crest and backslope of the ridge.
(d) Medium-term changes in beach width and profile due to alongshore transport, occurring over a period of months or several years.

(e) Long-term landward retreat in which the barrier beach responds to sea level rise by 'roll-over' and by increasing its crest height. This process involves overwashing, transferring sediment from the shore-face to the back barrier area. This is an episodic rather than a continuous process.
(f) Planform change; as the barrier beach is pinned by hard rock cliffs at either end (Strete and Torcross), landward retreat results in a gradual increase in both curvature and length. Pethick (2001) noted that since the total volume of sediment is fixed, so the volume of sediment per unit beach length will decrease as the barrier extends.

Evidence from historic mapping in Futurecoast (2002) suggests that the general alignment and integrity of the Slapton barrier has changed very little until recently. It was found that a part of the barrier beach does not appear to have been retreating in response to sea-level rise, whereas the remaining part has been shown to have a slow retreat. In a report to English Nature, Orford (2001) stated that the landward retreat of Slapton barrier is a function of rising sea level, variation in nearshore wave climate such as storminess, ratio of wave overtopping to over-washing and variation in alongshore spatial position of over-washing. He suggested that the beach stabilisation by rock armouring, which took place in 2001, would reduce the local rollover rate of the barrier at the potential breach point, but will not inhibit rollover rate at either end of the rock armouring. He mentioned that rock armour would also alter the anticipated geomorphological change of the barrier in response to sea-level rise and storminess in the longer term.

Contemporary beach behaviour involves brief episodes of overwashing and erosion, followed by longer periods of recovery during which the 'damage' caused by storm events is 'healed' during overtopping events (Orford, 2001). The extent to which the beach can recover from a particular storm is conditional on the precise timing and sequence of subsequent storm events. Areas of 'damage' (i.e. crest lowering) can be the focus of future overwashing events and, ultimately, become vulnerable to erosion events.

As this system is believed to be a closed sediment system, receiving no additional beach-building material, the changes in beach height and curvature that occur in response to sea-level rise are at the expense of changes in beach width. The volume of beach material stays the same; it is simply reorganised to adjust to changing sea level. Pethick (2001) suggested that the Slapton beach system is entering the breakdown stage of the Carter–Orford model for gravel barriers (Orford *et al.*, 1996). The barrier would become increasingly vulnerable to crest erosion, as breakdown is generally associated with a lack of sediment volume in the beach face that can be mobilised to 'heal' the effects of storm action. In the short-term there would be considerable uncertainty about the potential for crest erosion, reflecting the random nature of storm event sequences. Over the next 50-year period there will be periods of barrier stability separated by over-washing events during major storms which may cause localised crest erosion (Chadwick *et al.*, 2005). The probability of this erosion will increase over time because of the progressive decline in beach width and the probable increase in the rate of sea-level rise.

Chadwick *et al*. (2005) used the breach prediction model of Bradbury (2000) to determine that at the time of the road collapse in January 2001, the loss of road was probably due to beach cut-back and not due to the mechanism of overwashing and rollback. The storm event of October 2004, which did produce overtopping, confirmed that the breach prediction model is a reasonably reliable estimator for determination of incipient breaching (Chadwick *et al.*, 2005). The overall assessment of the January 2001 event is that it was caused by a combination of beach line recession due to northward alongshore transport in the preceding autumn, and the occurrence of a 1-in-25-year easterly storm event lasting four days, which further cut back the profile, with the beach crest reaching road level.

It has been postulated by various authors that the shingle bank is likely to break down irreversibly and breach, forming tidal inlets, within the next 30 to 50 years. Chadwick *et al*. (2005) considered this to be unlikely, as recent storm events had not had a major impact on the shingle barrier height or width, and none had come close to causing a breach of the barrier. They concluded that future sea-level rise and increased storminess will increase the rate of erosion and the risk of a major recession event, but that the risk of a breach of the shingle bank would remain low over the next 30 to 50 years. Thereafter, with no intervention measures and expected rates of sea-level rise, it is anticipated that the barrier beach will eventually be breached forming tidal inlets (Chadwick *et al.*, 2005). This would represent a reversed evolutionary sequence from stage 3 back to stage 1 (Figure 2-4).

3. Hydrodynamics

3.1. Introduction

This section provides an overview of the waves and water levels affecting coastal processes in Start Bay, including average and extreme conditions, and discusses the impacts that climate change may have on sea levels and wave heights. The information presented here is based on new analyses of measured and modelled data, which provide an update to chapter 11 of the SCZMS, and have been completed for the present study to provide:

- Improved characterisation of the average wave climate,
- Characterisation of extreme wave conditions,
- Improved characterisation of average and extreme water levels; and
- Description of extreme joint wave and water level events.

3.2. Wave Climate

In Start Bay, wave conditions arrive from both a southerly direction and an easterly/south-easterly direction. The southerly waves originate in the Atlantic Ocean, and refract into Start Bay as they propagate up the English Channel, whereas the easterly waves originate from local storms occurring in the Channel itself.

The wave climate in Start Bay was examined using two main data sources. The first is a nearshore directional wave rider buoy, situated in approximately 15 m depth directly offshore of Slapton Sands (Figure 2-3), which has been collecting directional spectral wave observations since April 2007. The second data source is the Met Office WAVEWATCH III hindcast wave model (herein, Met Office WWIII), which predicts spectral wave conditions at 8 km resolution around the coast of the UK, and covers the period between 1980 and 2017. The nearest Met Office WWIII node to Slapton Sands is situated at approximately 35 m depth just outside of Start Bay and seaward of Skerries Bank (Figure 2-3).

Although the WWIII data node is located outside of Start Bay, it provides a long time series of wave data for the site, and is therefore used alongside the wave buoy data in this report to examine the local wave climate, and to undertake an extreme value analysis. One month of wave conditions from the two data sources are compared in Figure 3-1. This indicates that the WWIII data generally have higher wave heights and more of a southwesterly approach than the wave buoy data because they haven't yet undergone refraction and shoaling over Skerries Bank. They also lack the distinct tidal signal that is evident in the wave buoy data, which occurs as a result of the varying effect of Skerries Bank on wave conditions throughout a tidal cycle.

Regardless of these differences, both data sources are useful for describing the wave conditions around Start Bay: the WWIII data represent waves arriving at the edge of Start Bay, and the inshore wave buoy represent wave conditions that have refracted into Start Bay, including southwesterly waves that have propagated across the shallow waters over Skerries Bank (Figure 2-3). Breaking wave heights will not be estimated from either data set, as this is likely to introduce significant errors due to the complexity of wave refraction and shoaling in Start Bay. To fully quantify the inshore wave climate in Start Bay, including the height and direction of breaking waves, high-resolution wave modelling which can capture the effects of Skerries Bank is required. This is outside the scope of this report (see Section 7.2).

From examination of the wave buoy data in Figure 3-2, and the WWIII data in Figure 3-3, the wave climate within Start Bay is clearly bi-directional, with a dominant component from the south/southwest, and a secondary component from the east. The longer peak wave periods ($T_p \geq 10$ s) evident in the southerly component indicate that the S-SW waves originate from the Atlantic and refract into Start Bay, giving them a southerly direction at the coast. As the waves from the east originate from the English Channel, they are comprised of shorter period ($T_p < 10$ s), locally-generated waves due to the reduced fetch in the Channel. Despite the lower occurrence and shorter periods of waves from the east compared to waves from the south, significant wave heights larger than 2 m occur almost as frequently from the east as they do from the south, confirming that energetic conditions occurred from both directions during the 10-year wave buoy monitoring period.

The wave roses in Figure 3-2 and Figure 3-3 demonstrate the degree of refraction that southwesterly waves undergo as they propagate from 35 m to 15 m depth. As these waves arrive at Start Bay they refract and shoal across Skerries Bank, which re-directs the waves to a more southerly approach as they propagate across the bay. Easterly waves arriving at Start Bay are less influenced by Skerries Bank, and are therefore less impeded as they propagate into the bay. Because the WWIII data cover a considerably longer time-period, they are of more use in describing the long term wave climate at Start Bay, and the remaining analysis therefore focusses on the WWIII data (Figure 3-4).

From the WWIII data shown in Figure 3-5 and Figure 3-6, around 70% of all wave conditions arriving at Start Bay have $H_s = 0 - 1.5$ m, and $T_p = 2 - 10$ s, with around 45% of these waves arriving from the southwest, and around 15% arriving from the east. More detailed assessment (Table 3-1) shows that the average waves arriving from the S-SW have significant heights of 0.7 m ($H_{s50\%}$ - the height exceeded 50% of the time) and that the largest waves have significant heights exceeding 2.2 m ($H_{s5\%}$ - the height exceeded 5% of the time). Wave heights from the east are not dissimilar, with average and largest significant heights of $H_{s50\%}$ = 0.8 m and $H_{s5\%}$ = 2.0 m, respectively. The average ($H_{s50\%}$) and highest ($H_{s5\%}$) wave heights are lower in summer and are higher in winter (Table 3-1 and Figure 3-7).

Table 3-1. Wave height statistics from the WWIII model hindcast in Start Bay, output at a water depth of approximately 35 m, for the entire dataset (‘All’), as well as for winter months (ONDJFM), summer months (AMJJAS), Southerly waves (145° – 270° from North), and Easterly waves (35° – 145° from North). $H_{s50\%}$, $H_{s10\%}$, and $H_{s5\%}$ are the significant wave heights exceeded only 50%, 10%, and 5% of the time, respectively. $H_{s50\%}$ is the average (median) wave height, while $H_{s10\%}$ and $H_{s5\%}$ indicate the largest wave heights experienced.

	All	Winter	Summer	Southerly	Easterly
$H_{s50\%}$	0.70	0.97	0.51	0.71	0.75
$H_{s10\%}$	1.76	2.09	1.21	1.81	1.68
$H_{s5\%}$	2.15	2.48	1.49	2.22	2.03

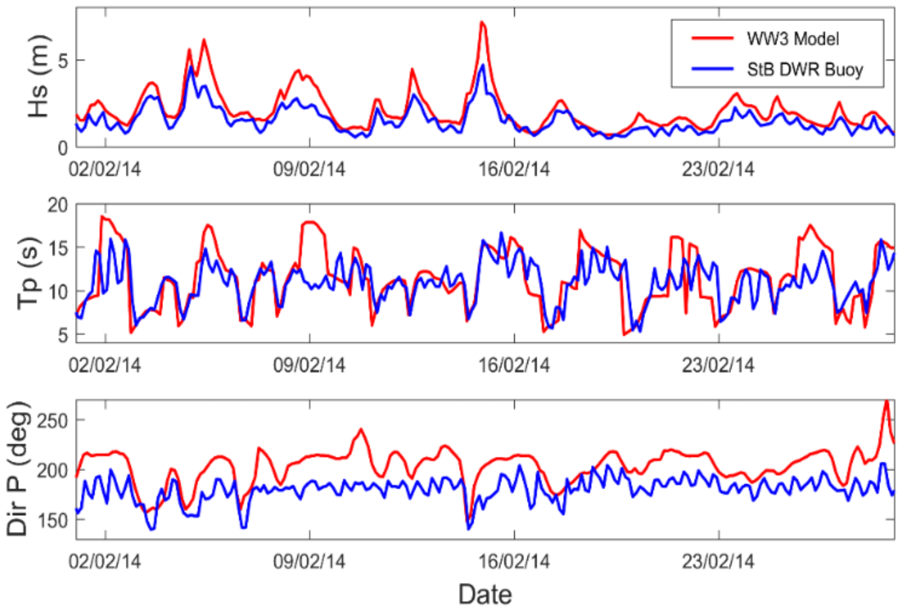

Figure 3-1. Comparison of one month of wave data from the Start Bay wave buoy, collected in approximately 15 m water depth, and WWIII model hindcast data, output at approximately 35 m water depth (from Wiggins *et al.* (2008)). The location of the two data sources is given in Figure 2-3.

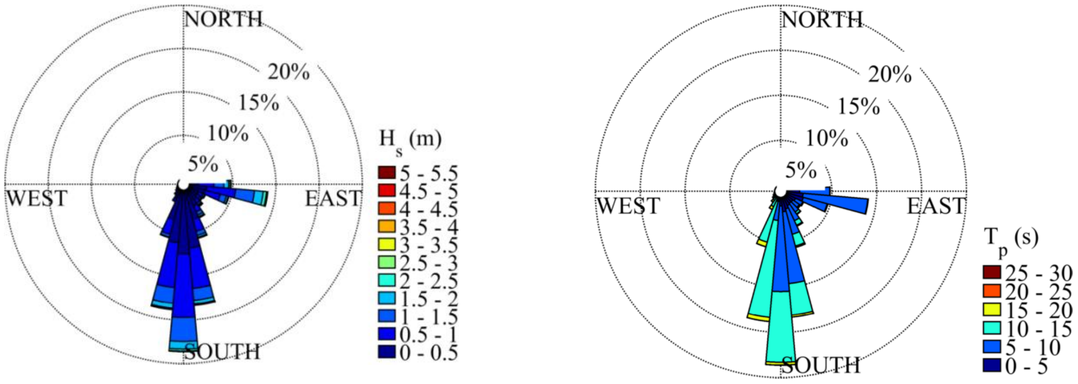

Figure 3-2. Directional wave roses of significant wave height (left panel) and peak wave period (right panel), measured by the Start Bay wave buoy in approximately 15 m water depth, between 01-Apr-2007 and 30-Apr-2017.

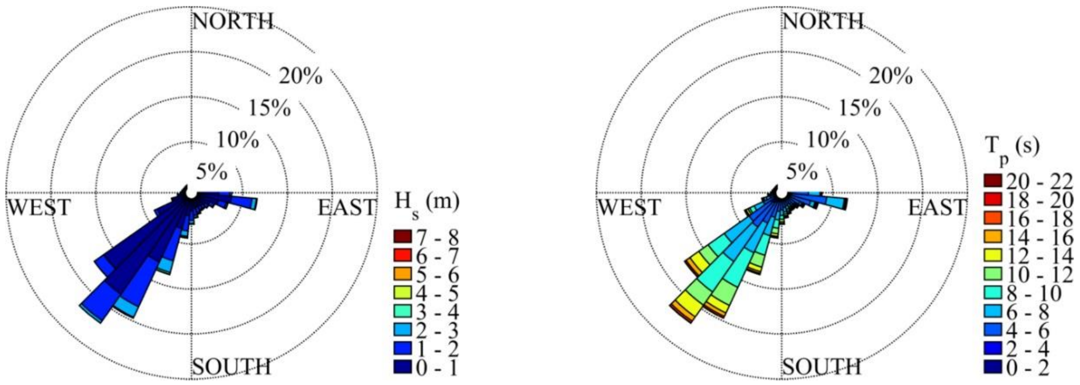

Figure 3-3. Directional wave roses of significant wave height (left panel) and peak wave period (right panel), as determined from the WWIII model hindcast in Start Bay, output at a water depth of approximately 35 m, between 01-Jan-1980 to 31-Dec-2016.

COASTAL MARINE APPLIED RESEARCH WITH PLYMOUTH UNIVERSITY

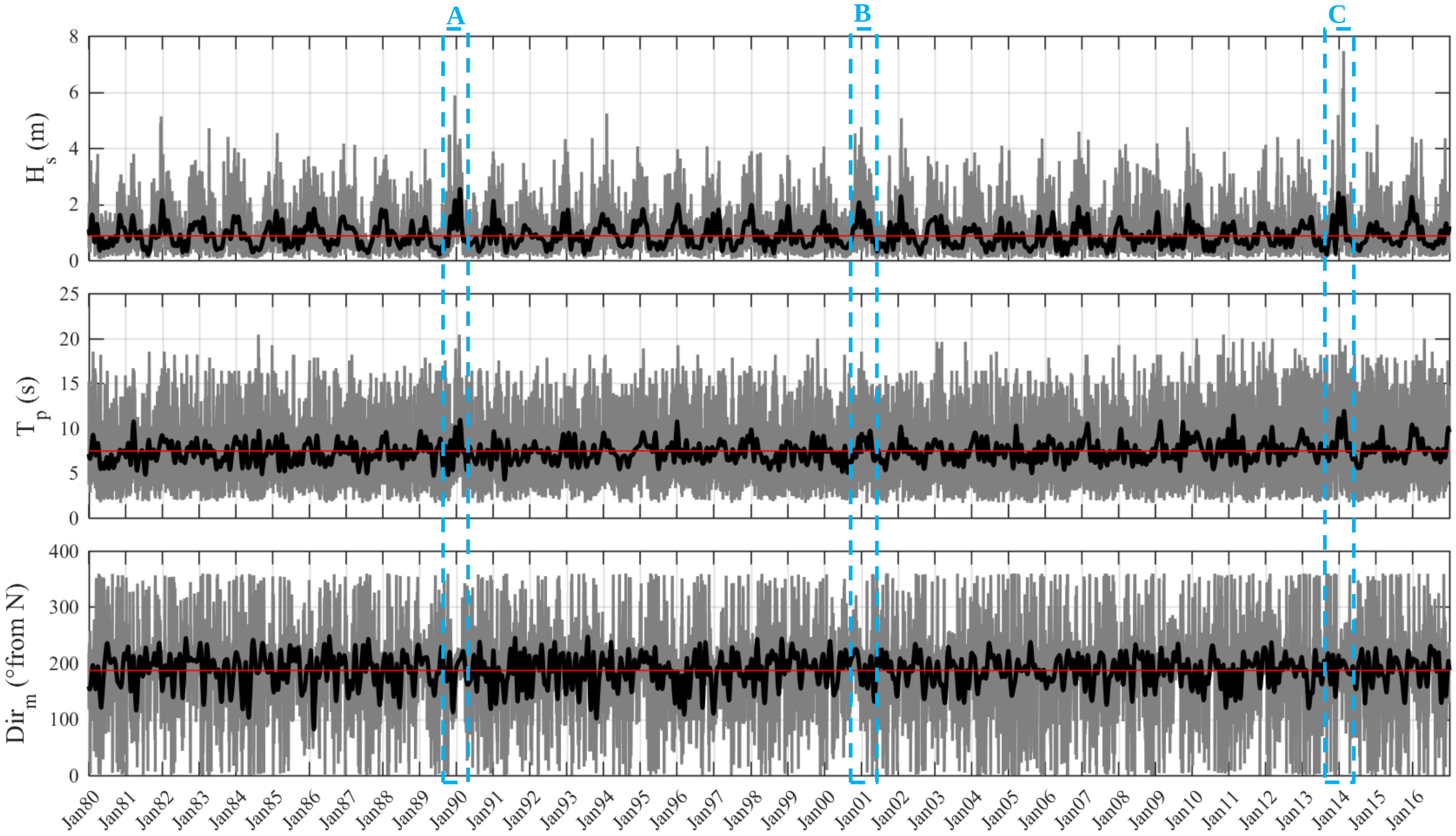

Figure 3-4. Time series of 36 year WWIII model hindcast in Start Bay, output at a water depth of approximately 35 m. In each panel the grey line is the hindcast data, the black line shows the low-pass-filtered seasonal signal in the data, and the red line shows the time series mean. Boxes A, B, and C indicate significant storm events described in the text.

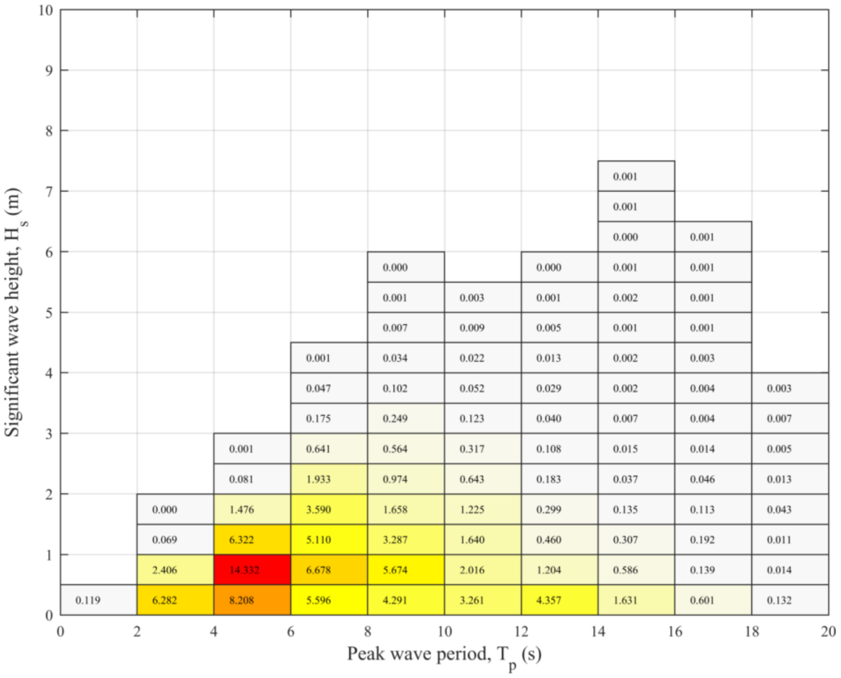

Figure 3-5. Percentage occurrence of significant wave heights (H_s) and peak wave periods (T_p) from the from the WWIII model hindcast in Start Bay, output at a water depth of approximately 35 m.

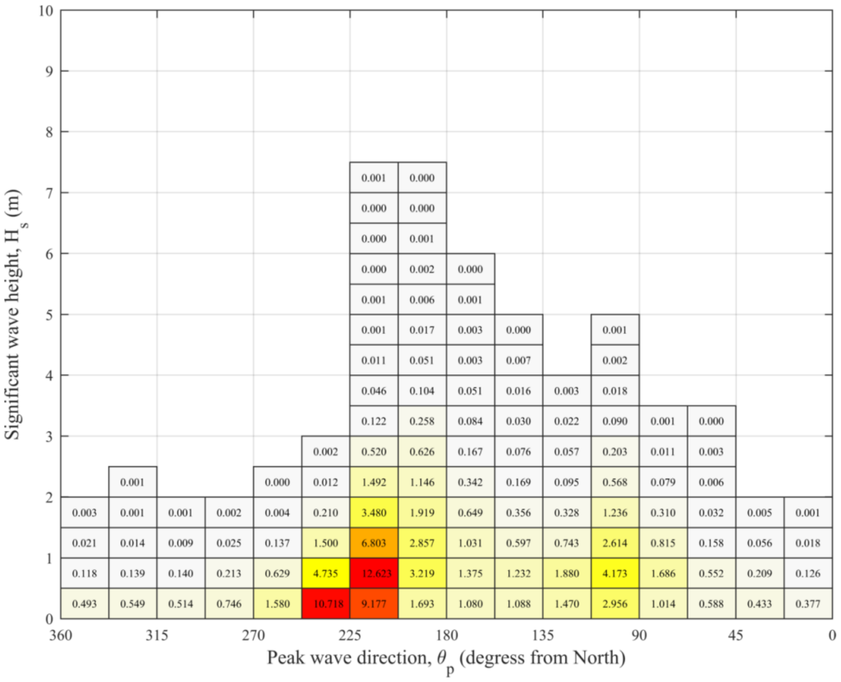

Figure 3-6. Percentage occurrence of significant wave heights (H_s) and peak wave directions (θ_p) from the WWIII model hindcast in Start Bay, output at a water depth of approximately 35 m.

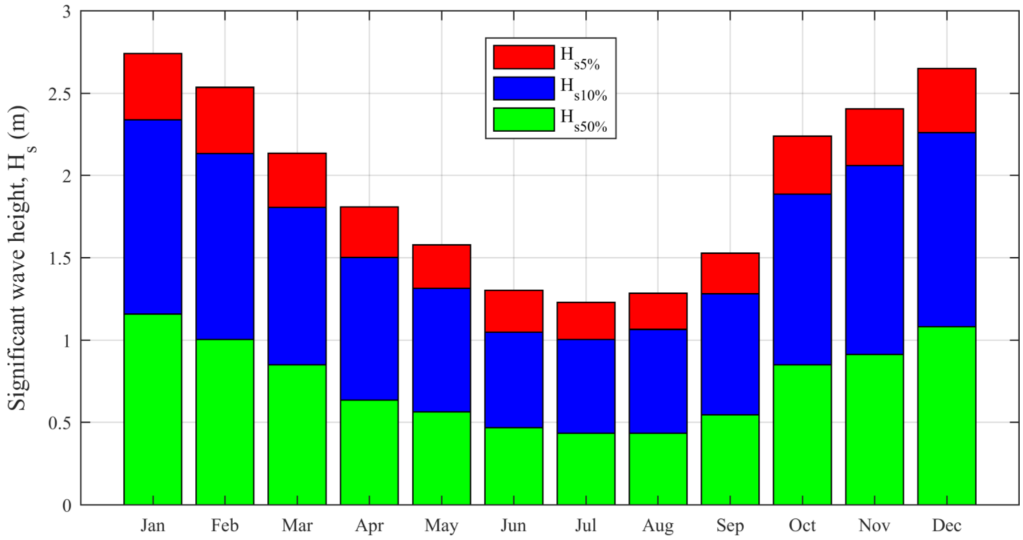

Figure 3-7. Monthly wave height statistics from the WWIII model hindcast in Start Bay, output at a water depth of approximately 35 m. The top of each bar indicates the value of $H_{s50\%}$, $H_{s10\%}$, and $H_{s5\%}$ for each month, which are the significant wave heights exceeded only 50%, 10%, and 5% of the time, respectively. $H_{s50\%}$ is the average (median) wave height, while $H_{s10\%}$ and $H_{s5\%}$ indicate the largest wave heights experienced.

3.3. Extreme Wave Conditions

The 36-year time series of WWIII hindcast wave height, period, and direction shown in Figure 3-4 shows a seasonal variation in wave height (larger waves in winter, smaller waves in summer), and reveals a number of energetic events that occurred over this period. The most notable is the highly energetic winter of 2013/2014, when long-period (~20 s) southwesterly waves with significant wave heights in excess of 7 m arrived at Start Bay (Figure 3-4, 'C'). The winter of 1989 also stands out, showing long-period southwesterly waves with heights of around 6 m (Figure 3-4, 'A'). January 2001 is also highlighted in Figure 3-4 ('B'), when part of the A379 road towards the Strete end of Slapton Barrier was undermined and collapsed due to storm waves from the east.

Maximum wave heights for the winter and summer months of each year shown in Figure 3-8 and Figure 3-9, which confirm that the largest waves occurred in the winters of 1989 and 2014 and originated from the south-southwest. The largest waves from the east occurred in 1985, and exceeded 4.5 m H_s. Interestingly, the 2001 road collapse event does not stand out in this figure, suggesting that the height of the waves was not unusual, and was therefore not the sole cause of the road collapse (see Section 6.3).

3.3.1. The 2013/2014 Winter

Between December 2013 and February 2014, an unprecedented series of long period, high energy swell events occurred (Figure 3-4, 'C'), making it the most energetic 8-week period of waves in at least the last 65 years (Masselink *et al.*, 2015). One storm swell, 'Hercules', featured offshore wave heights and periods of H_s = 9.6 m and T_p = 22 s, respectively (Castelle *et al.*, 2015), and the 8-week mean wave height measured offshore of southwest Cornwall was H_s = 4.4 m. This extremely energetic winter had a significant impact upon beach morphology along large parts of the Atlantic European coastline (Castelle *et al.*, 2015; Masselink *et al.*, 2015; Scott *et al.*, 2016), and markedly different beach responses were observed between exposed and semi-exposed beaches in the southwest of England. Because of the significance of the 2013/2014 winter, the impact the sequence of storms had on beach morphology in Start Bay is discussed throughout this report.

3.3.2. Extreme Value Analysis

To characterise extreme wave conditions in Start Bay, a suitably long wave record featuring a number of relatively extreme events is required in order to provide a robust analysis. Although the Start Bay wave buoy record is of sufficient duration to conduct an extreme value analysis (EVA), the longer length of the Met Office WWIII hindcast data, which includes a number of large wave events not present in the wave buoy time series (e.g. the winters of 1985 and 1989), makes it more robust for the present analysis. These data were divided into southerly and easterly directional sectors, and the EVA was performed separately for the two subsets of data. EVA values were also determined from the wave buoy data for comparison.

The analysis was used to determine the 20, 50 and 100-year return period wave heights at the site. A peaks-over-threshold (POT) approach was used, whereby wave height measurements larger than a given threshold height were used to examine the distribution of extreme wave heights in the WWIII time series. A Generalised Pareto Distribution (GPD) was then fitted to these peak values, resulting in a statistical characterisation of the extreme tail of the wave height data from which wave heights of various return periods can be calculated. The GPD is now a well-established marginal distribution model for assessing extreme values of waves and water levels (Hamm *et al.*, 2010; Jonathan and Ewans, 2013).

An assumption of this method is that the selected peaks are independent (and therefore originate from independent storms). To ensure this was the case, a minimum period of 4 days between storm peaks was required for each peak to be considered independent (Caires, 2011). The threshold that was selected for the POT method was determined from the mean of the data plus one standard deviation, which resulted in stability of the GPD parameters and return period estimates in each case. The extreme return period estimates are given in Table 3-2. A demonstration of the peaks over threshold method and the fitted GPD models are shown in Figure 3-10, providing evidence of the suitability of the fitted models in representing the extreme data values from each directional sector.

From the Met Office WWIII extreme wave heights in Table 3-2, there is little variation in the heights of waves with return periods of 20, 50, and 100 years. However, extreme waves from the south (ranging from 5.99 m to 6.60 m) are predicted to be larger than extreme waves from the east (ranging from 4.28 m to 4.76 m). Interestingly, extreme waves from the east are predicted to loose less of their energy as they propagate into Start Bay, with the 100-year wave height reducing by only 11% between the depths of 35 m and 15 m, compared to a 20% reduction for a 100-year wave height from the south (Table 3-2). This is likely to be due to the effects of refraction and shoaling, as waves arriving from a south-southwest direction propagate across Skerries Bank.

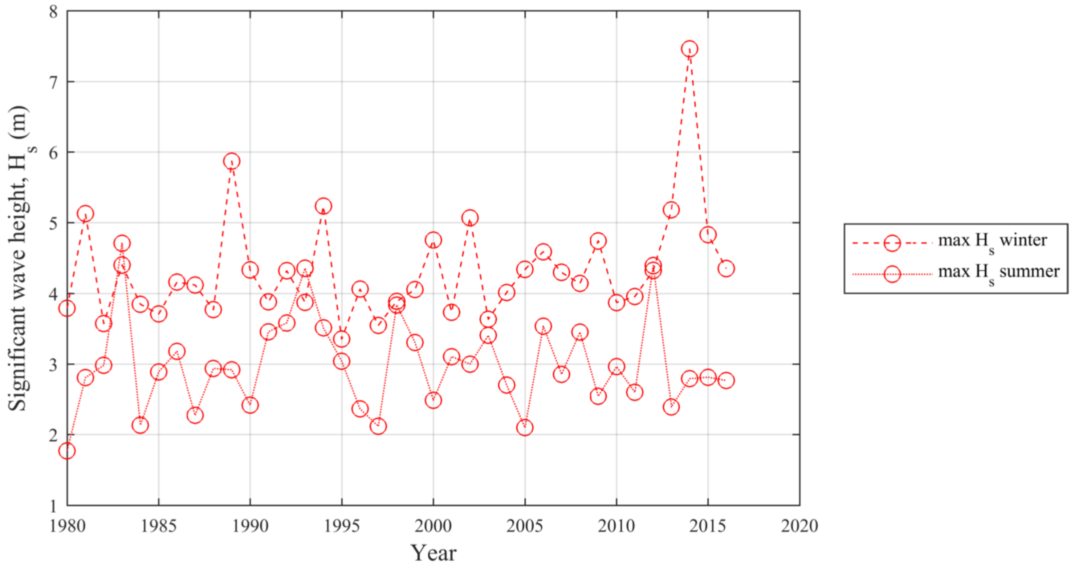

Figure 3-8. Annual wave height statistics for waves arriving from the south (145° – 270°) from the WWIII model hindcast in Start Bay, output at a water depth of approximately 35 m. Maximum values of H_s across the winter months (ONDJFM) and the summer months (AMJJAS) of each year of the time series are shown.

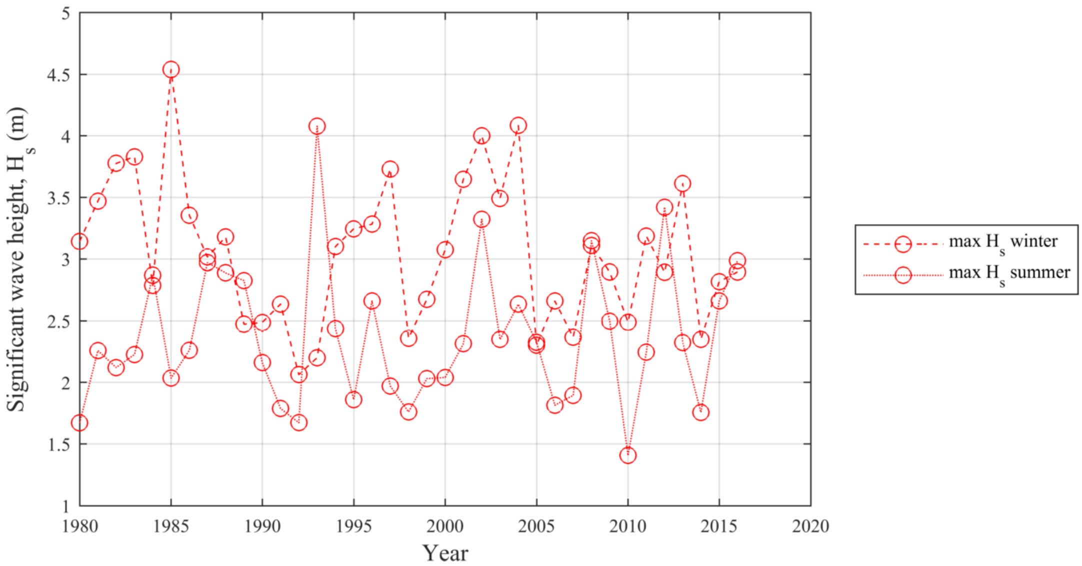

Figure 3-9. Annual wave height statistics for waves arriving from the east (35° – 145°) from the WWIII model hindcast in Start Bay, output at a water depth of approximately 35 m. Maximum values of H_s across the winter months (ONDJFM) and the summer months (AMJJAS) of each year of the time series are shown.

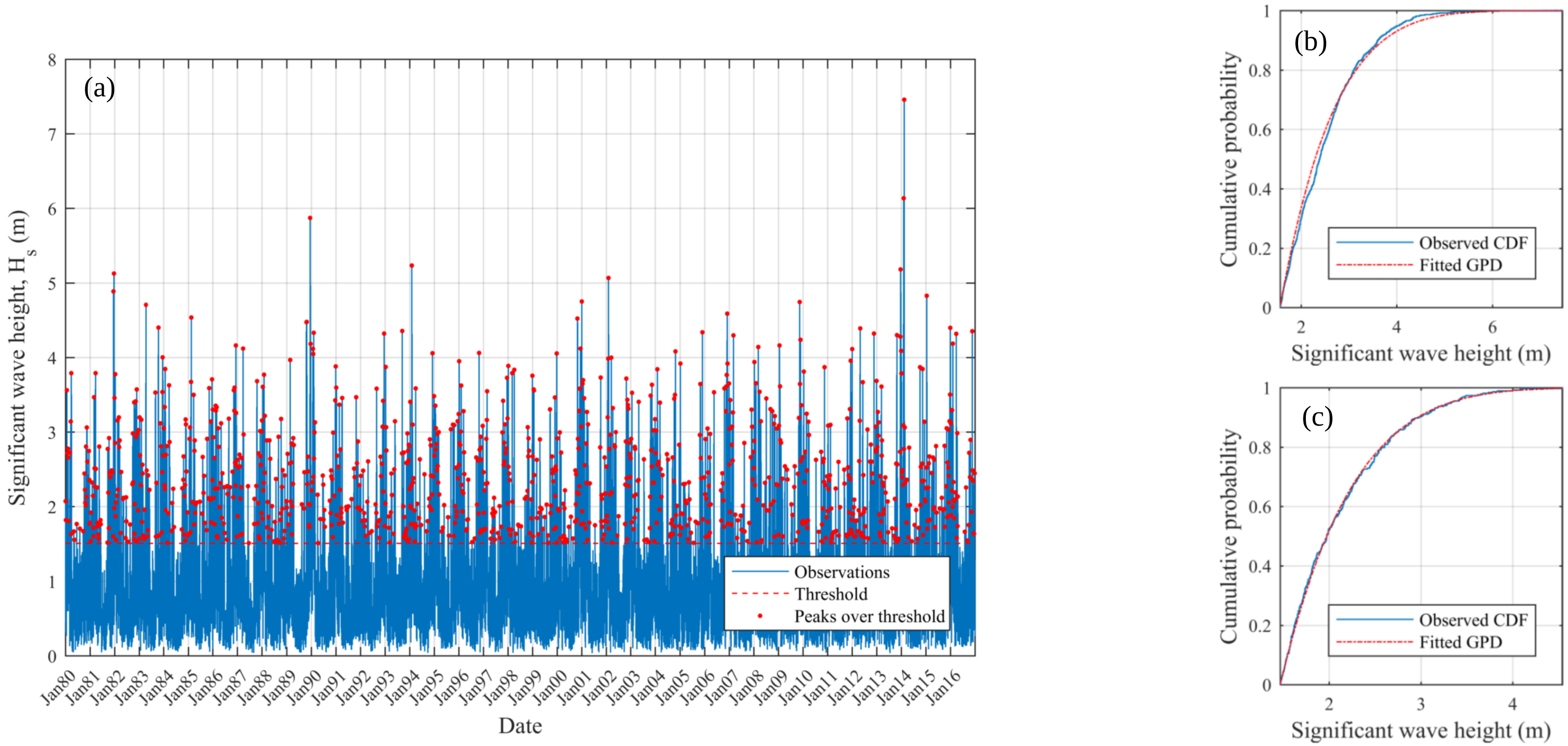

Figure 3-10. Demonstration of the Extreme Value Analysis (EVA) methodology. (a) Time series of significant wave height from the WWIII model hindcast in Start Bay, output at a water depth of approximately 35 m, and independent wave events determined from a Peaks-Over-Threshold (POT) analysis using a threshold of 1.5 m. (b) Generalised Pareto Distribution (GPD) fitted to the marginal wave height distribution from from southerly waves (145° – 270°). (c) GPD fitted to the marginal wave height distribution from easterly waves (35° – 145°). The fitted GPDs were subsequently used to determine the extreme return period wave heights in Table 3-2.

Table 3-2. Results of Extreme Value Analysis (EVA) performed on the the WWIII model hindcast data, and the Start Bay wave buoy data. Extreme significant wave heights are given for southerly waves (145° – 270°), and easterly waves (35° – 145°).

Return period	Met Office WWIII, 35 m depth		Start Bay wave buoy, 15 m depth	
	Southerly waves, H_s (m)	Easterly waves, H_s (m)	Southerly waves, H_s (m)	Easterly waves, H_s (m)
1-in-20 year	5.99	4.28	4.85	4.01
1-in-50 year	6.36	4.57	5.13	4.14
1-in-100 year	6.60	4.76	5.31	4.23

3.4. Water Levels

Water levels in Start Bay were derived from data collected by the nearby class-A tide gauge situated at Devonport in Plymouth (Figure 3-11). From Admiralty tide charts (Table 3-3) based on these data, the mean spring and neap tide ranges in Start Bay are 4.70 m and 2.20 m, respectively. Time series of water level, storm surge, and skew-surge are provided in Figure 3-11. The surge magnitude is derived from the observed water level, minus the predicted astronomical tide level, and represents the super-elevation of the water surface due to the effects of extreme weather conditions (storm surge), including the inverse barometric effect (low pressure) raising the elevation of the sea, and wind set up (Pullen *et al.*, 2007; McMillan *et al.*, 2011). Skew surge is defined as the difference between the highest predicted tidal elevation during a given tidal cycle and the highest recorded water level during that particular tide, and therefore represents how much higher the highest water level was than the expected tide level. From Figure 3-11, the largest surge and skew surge magnitudes since the start of the record in 1991 occurred in 2014, exceeding 1 m and 0.9 m, respectively, but typically both values range between +0.5 m and -0.5 m.

Table 3-3. Astronomical tide levels for the Devonport tide gauge, Plymouth, from Admiralty tide charts (2017). Water levels are given for HAT (highest astronomical tide), MHWS (mean high water springs), MHWN (mean high water neap), MSL (mean sea level), MLWN (mean low water neaps), MLWS (mean low water springs), and LAT (lowest astronomical tide).

Water level	Water level elevation, m above Chart datum (m CD)	Water level elevation, m above Ordnance Datum Newlyn (m ODN)
HAT	5.90	2.68
MHWS	5.50	2.28
MHWN	4.40	1.18
MSL	3.31	0.08
MLWN	2.20	-1.02
MLWS	0.80	-2.42
LAT	0.00	-3.22

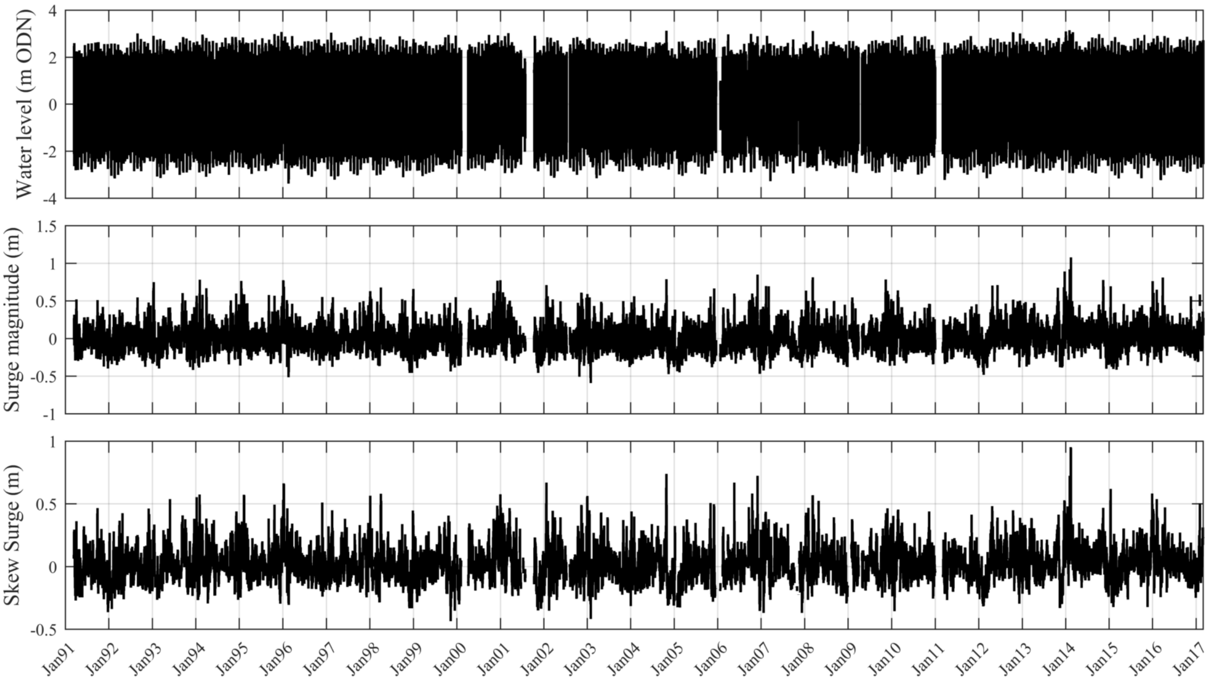

Figure 3-11. Time series of observed water level elevation (upper panel), surge magnitude (middle panel) calculated from the observed water level minus the predicted astronomical tide level, and daily skew surge magnitude (lower panel), from Devonport tide gauge data recorded between 01-Jan-1991 to 28-Feb-2017.

3.5. Extreme Water Levels

To predict the water level during an extreme storm surge event, an extreme value analysis (EVA) was conducted using the observed water level data, as well as using the skew surge data from the Devonport tide gauge. The same POT and GPD methodology as described in Section 3.3 was used to conduct the analysis on the tide gauge data, and the fitted GPD models are shown in Figure 3-12 to demonstrate that the GPD distributions represent the observed water levels very well. From these curves, the magnitude of extreme water level events with 20, 50, and 100-year return periods were derived (Table 3-4). These values indicate that water levels could reach 3.2 m above ODN during a 100-year event, and that storm surge could super-elevate the water level more than 1 m above the predicted highest tide level once in a 100 year period. The values in Table 3-4 indicate that the extreme storm surge event that occurred on the 14th of February 2014 (Figure 3-11) had a return period of around 50 years.

The heights of mean neap and spring high tide levels from the Devonport tide gauge, as well as the predicted 1-in-100 year water level, are projected onto the latest beach profiles at Blackpool Sands (measured on 15/11/2016), Slapton Sands (measured on 23/03/17), Beesands (measured on 16/11/16), and Hallsands (measured on 16/11/16) in Figure 3-13 to Figure 3-16. These plots show that a 100-year water level would not be sufficient alone to cause coastal flooding in Start Bay, as the water surface would not exceed the height of the beach berm at any of the profiles in Start Bay. However, with some level of wave run-up occurring at the same time as this water level, it is very likely that overtopping or overwashing of the beach profiles would occur, which could cause flooding and damage to the properties, infrastructure, and ecology along the beaches of Start Bay.

Along engineered or cliff-backed stretches of coast, where beaches and barriers are not able to roll-back in response to rising sea level, flooding events will become more likely in the future, as the total water level necessary to overtop natural and man-made sea defences will gradually reduce. For example, in 100 years time, UKCP09 has predicted that local sea levels may have risen by between 0.2 and 0.9 m compared to the 1990 sea level (Figure 3-18), depending on the level of global emissions that occur during that period. Taking this into consideration, coastal flooding in Start Bay may become more likely in the future. The sections of Start Bay most susceptible to flooding are currently Hallsands and Beesands, which have the lowest profiles in Start Bay (Figure 3-15 and Figure 3-16). The north end of Blackpool Sands may also be at risk of overtopping, given the uncharacteristically low level of profile BK4 (Figure 3-13). The susceptibility of the beaches in Start Bay to coastal flooding in the future will depend in part on each beaches ability to accommodate sea-level rise through roll-back.

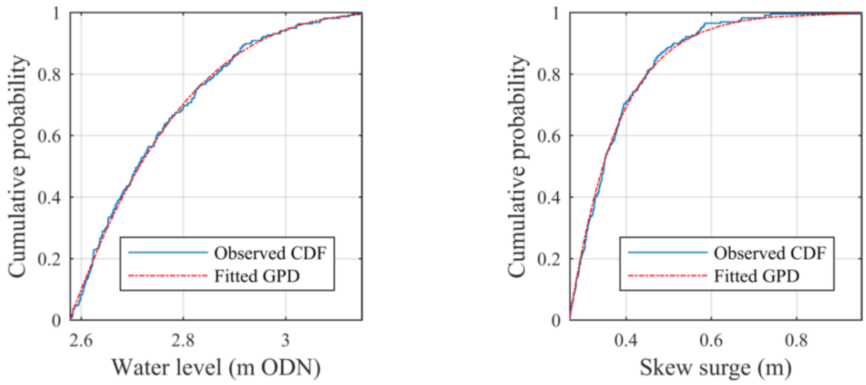

Figure 3-12. Generalised Pareto Distributions (GPD) fitted to the observed water level (left panel) and skew surge (right panel) distributions from the Devonport tide gauge data. The fitted GPDs were subsequently used to determine extreme return period values Table 3-4. The marginal distributions were determined using a Peaks-Over-Threshold (POT) analysis of independent water level and skew surge events, with thresholds of 8.6 m and 0.16 m for water level events and skew surge events, respectively.

Table 3-4. Results of the Extreme Value Analysis (EVA) performed on the Devonport tide gauge data.

Return period	Extreme water level elevation (m ODN)	Extreme skew surge magnitude (m)
1-in-20 year	3.15	0.85
1-in-50 year	3.19	0.96
1-in-100 year	3.21	1.04

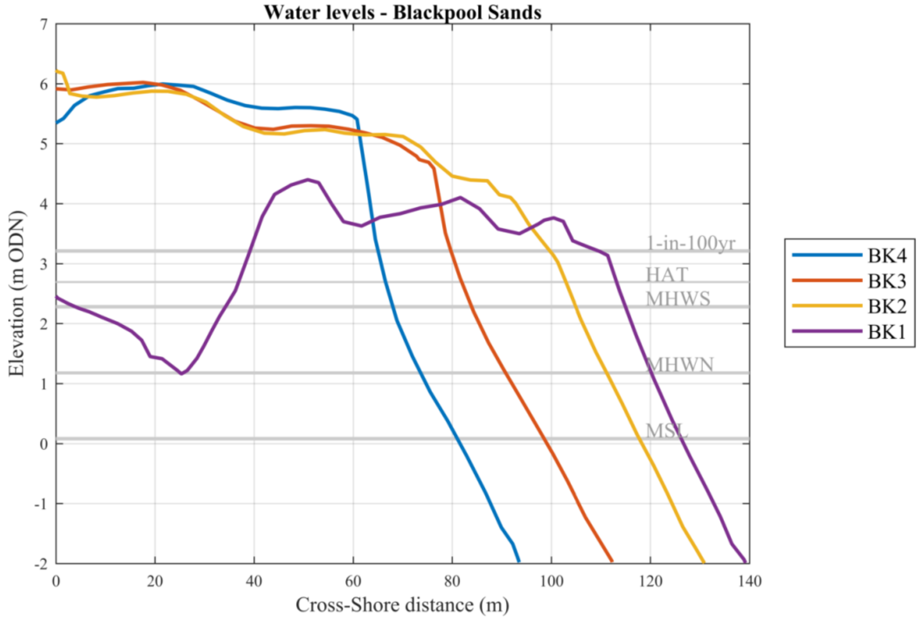

Figure 3-13. High water levels projected onto the latest beach profiles (as measured on 15/11/16) at Blackpool Sands. The geographic location of each profile is shown in Figure 2-3. The water levels are (from top to bottom): 1-in-100 year water level including storm surge and wind set-up (from Table 3-4), Highest Astronomical Tide (HAT), Mean High Water Springs (MHWS), Mean High Water Neaps (MHWN), Mean Sea Level (MSL).

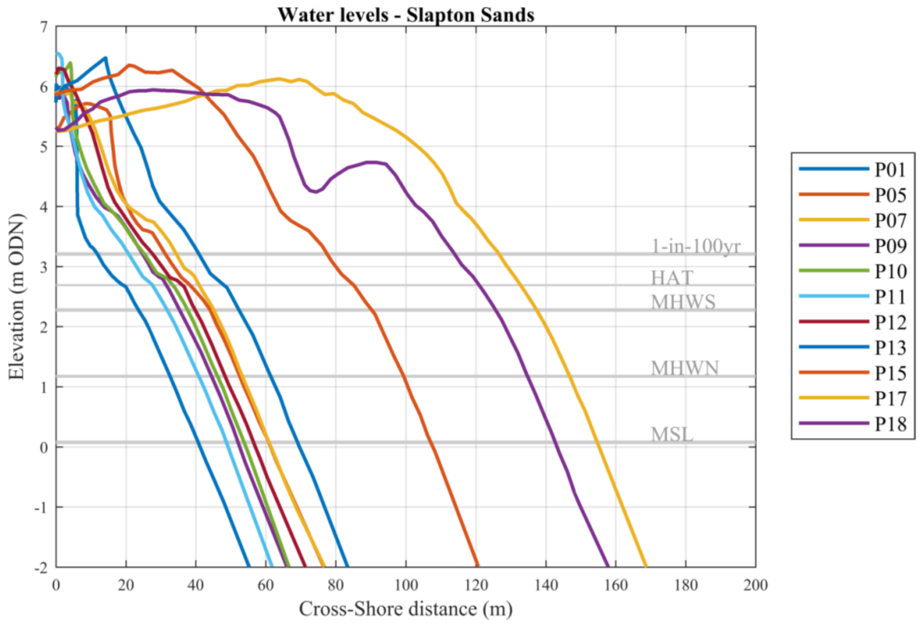

Figure 3-14. High water levels projected onto the latest beach profiles (as measured on 23/03/17) at Slapton Sands. The geographic location of each profile is shown in Figure 2-3. The water levels are (from top to bottom): 1-in-100 year water level including storm surge and wind set-up (from Table 3-4), Highest Astronomical Tide (HAT), Mean High Water Springs (MHWS), Mean High Water Neaps (MHWN), Mean Sea Level (MSL).

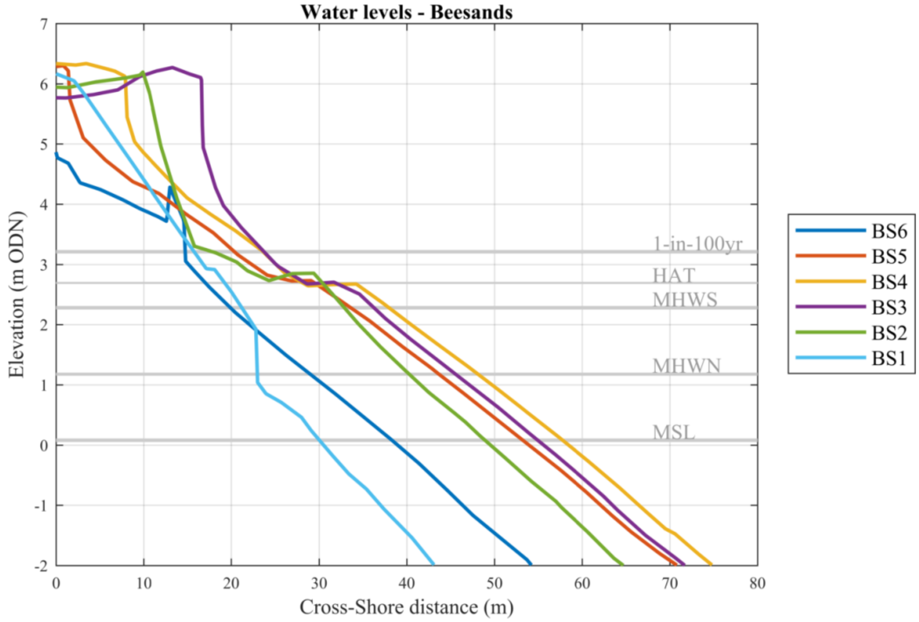

Figure 3-15. High water levels projected onto the latest beach profiles (as measured on 16/11/16) at Beesands. The geographic location of each profile is shown in Figure 2-3. The water levels are (from top to bottom): 1-in-100 year water level including storm surge and wind set-up (from Table 3-4), Highest Astronomical Tide (HAT), Mean High Water Springs (MHWS), Mean High Water Neaps (MHWN), Mean Sea Level (MSL).

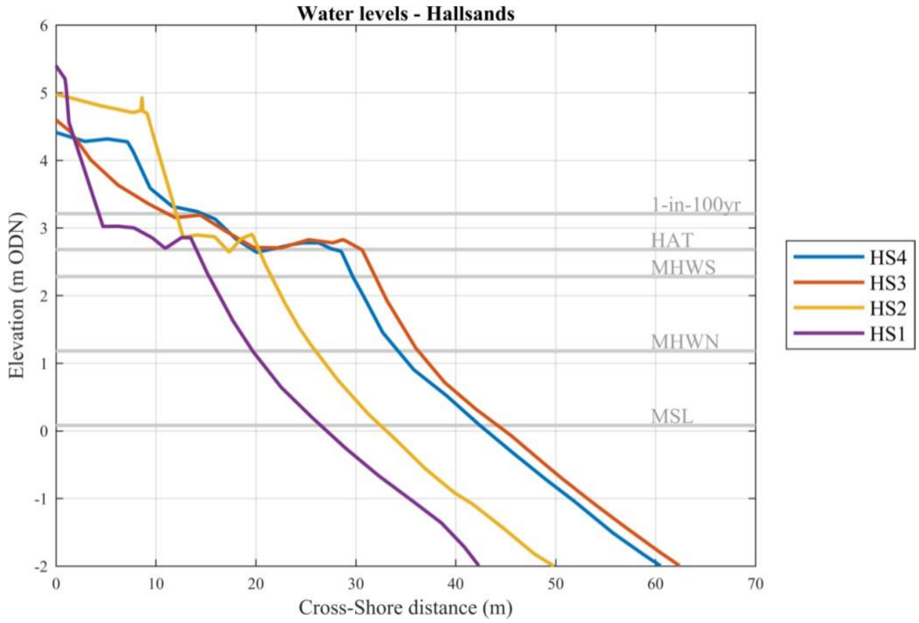

Figure 3-16. High water levels projected onto the latest beach profiles (as measured on 16/11/16) at Hallsands. The geographic location of each profile is shown in Figure 2-3. The water levels are (from top to bottom): 1-in-100 year water level including storm surge and wind set-up (from Table 3-4), Highest Astronomical Tide (HAT), Mean High Water Springs (MHWS), Mean High Water Neaps (MHWN), Mean Sea Level (MSL).

3.6. Joint Probability of Extreme Wave and Water Levels

With the combination of an extreme water level and extreme wave conditions, it is possible that any of the profiles along Start Bay could be overtopped, as wave run-up can add many meters of elevation to the still water level. For that reason, it is important to consider the combined probability of an extreme wave and water level event. Figure 3-17 shows extreme wave and water level scenarios modelled in Start Bay at 5 m depth for the Environment Agency's 'State of the Nation' project (model node 921, HR Wallingford, 2015). Contour lines are shown on the figure, representing events with different wave heights and water levels, but the same joint probability of occurrence. For each wave and water level event, the joint probability was calculated by 'counting back' the number of events with a larger wave or water level than that event, indicating how many times each event would be exceeded in a 10,000 year period (the 'length' of the State of the Nation simulations).

Figure 3-17 demonstrates that large wave conditions combined with an average water level, can have the same probability of occurrence as small wave conditions combined with a very high water level. For example, a 100-year event could consist of 5 m high waves, combined with water levels only 1 m above MSL (~1 m ODN), or it could consist of 1 m high waves, combined with water levels more than 3 m above MSL. The chance of overtopping from these two different events could be very different, given that there would be a substantial difference in the wave run-up. This highlights the need to model wave run-up for many different scenarios, in order to adequately predict coastal flooding (see Section 7.2).

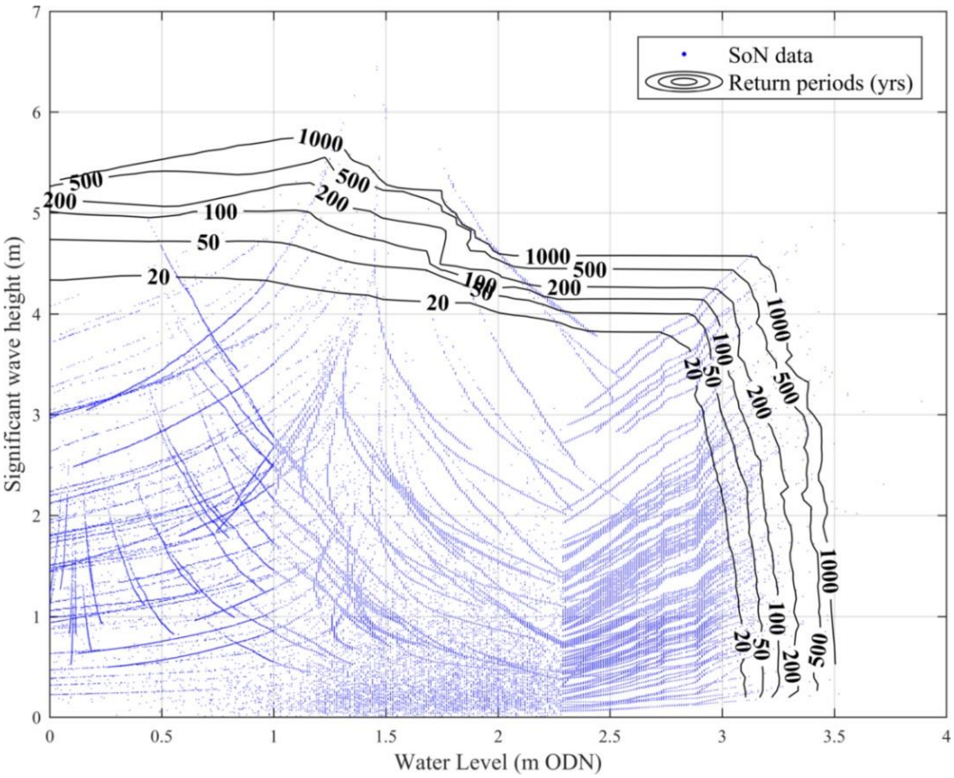

Figure 3-17. State of the Nation modelled extreme wave and water level events, showing possible combinations with return periods of up to 1-in-10,000 years. Each contour line shows different events with the same joint return period (1-in-20 to 1-in-1000 years).

3.7. Climate Change and Risk

Climate change poses two major risks to the coastal environment. The first is the gradual raising of sea levels, which increases the chances of coastal flooding, and elevates the action of erosive and energetic waves higher up the coastal profile, which consequently causes the shore and coastline to migrate landwards (Nicholls and Cazenave, 2010). Relative sea level in southwest England is controlled by both sea-level rise and large-scale subsidence of the land in southern England caused by isostatic rebound following de-glaciation. From local sediment cores (including two from Slapton barrier itself), Massey *et al*. (2008) determined that relative sea level along the south Devon coastline has risen by 21 +/- 4 m during the past 9000 years. Sea-level rise slowed during the middle and late Holocene and they estimate that 8 +/- 1 m of relative sea-level rise has occurred in the last 7000 years. It can therefore be estimated that the average historic rate of relative sea-level rise in South Devon is on the order of 1.1 mm/year, but the contemporary rate is likely to be higher (Nicholls and Cazenave, 2010).

Projections of future relative sea-level rise are provided by the United Kingdom Climate projections 2009 (UKCP09) database[1], and are dependent on global greenhouse gas emissions occurring now and in the future. UKCP09 provide projections based on three scenarios: low, medium, and high emissions. From these projections, the rate of relative sea-level rise around Start Bay since 1990 is expected to have been between 2.9 and 3.9 mm/year (Figure 3-18, 50th percentile projections), depending on the actual emissions scenario that has occurred up to this point in time, which is not indicated by UKCP09. The sea level projections in Figure 3-18 indicate that, under all emissions scenarios, the rate of sea-level rise will increase in the future, and local sea levels are likely to be 42 – 59 cm higher than their 1990 levels by the year 2100. However, uncertainty in the projections increases through time (as indicated by the 5th and 95th percentile projections), and sea level could be between 22 – 92 cm higher when model uncertainties are considered.

The second climate-induced risk to the coastal environment is an increase in storminess caused by global warming, which may increase the magnitude and frequency of storms arriving at our coast (Harley *et al.*, 2006). UKCP09 does not directly project the magnitude and frequency of storms or storm wave conditions in the future, so their effect on coastal processes is harder to quantify. Even if some

[1] In 2018, the UKCP18 project will revise the climate change projections made by UKCP09, and the updated projections should therefore be considered in future beach management decisions where possible (http://ukclimateprojections.metoffice.gov.uk/2412).

projection were available, predicting their effects on the coast would carry extreme uncertainties, as it is impossible to predict the sequence and timing of future storms. This factor is therefore not explicitly considered in this report; however, historic trends in storminess are implicitly considered within the barrier retreat model of Orford *et al*. (1995b), used in Section 4 to predict barrier retreat in the future.

UKCP09 does make projections of future skew surge, however (Figure 3-19), which is a storm-related phenomenon and, like sea-level rise, has implications for coastal flooding. Their projections indicate that each year, the magnitude of an extreme skew surge event of a given return period will increase. It is expected that skew surge events with 20 and 50 year return periods (the highest available from UKCP09), will increase in magnitude by 0.3 and 0.4 mm/year, respectively, under a medium emissions scenario. These increases are small compared to the predicted change in sea level – over the next 100 years, a 1-in-20 year and 1-in-50 year skew surge event will only increase in magnitude by 3 cm and 4 cm, respectively. However, at present, skew surge can elevate the height of the still water level during a storm by 85 cm, 96 cm, and 104 cm during 20-year 50-year, and 100-year return period events, respectively, and it is therefore already a major potential contributor to coastal flooding, regardless of the magnitude of increase in the future.

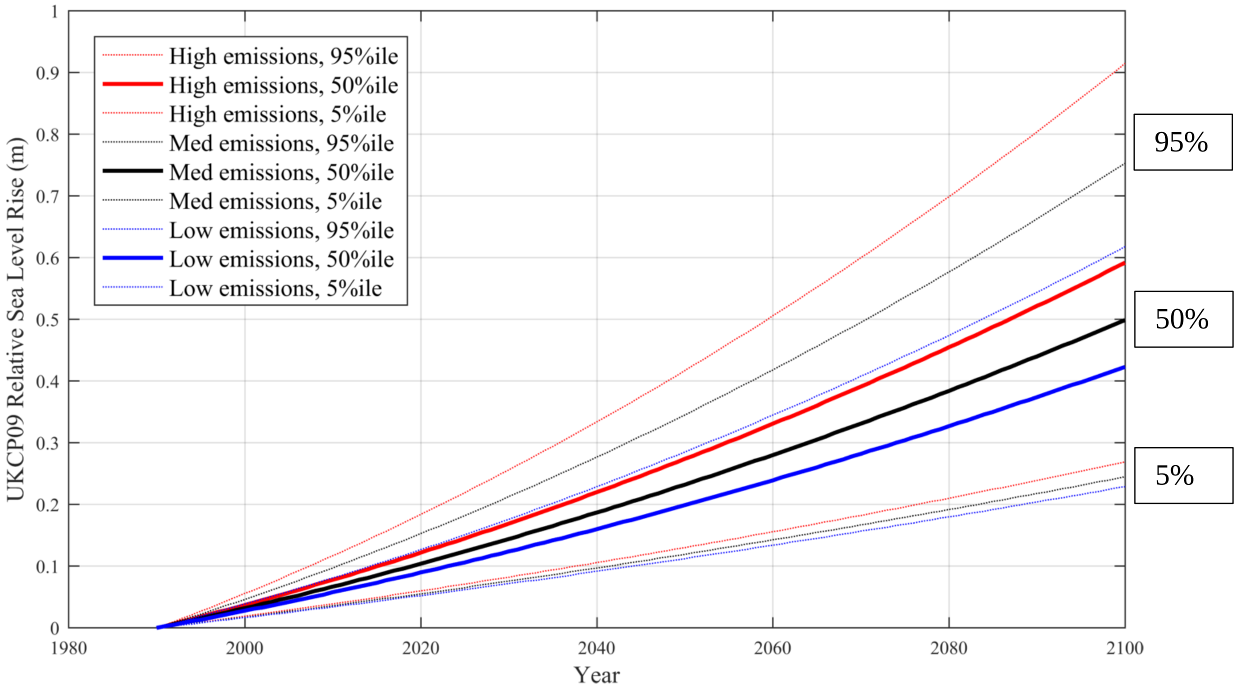

Figure 3-18. UKCP09 predictions of relative sea-level rise at Start Bay, under high, medium, and low emissions scenarios (from http://ukclimateprojections.metoffice.gov.uk). Lower (5th percentile), median (50th percentile), and upper (95th percentile) predictions are shown for each scenario, indicating the magnitude of uncertainty, determined from an ensemble of UKCP09 model predictions.

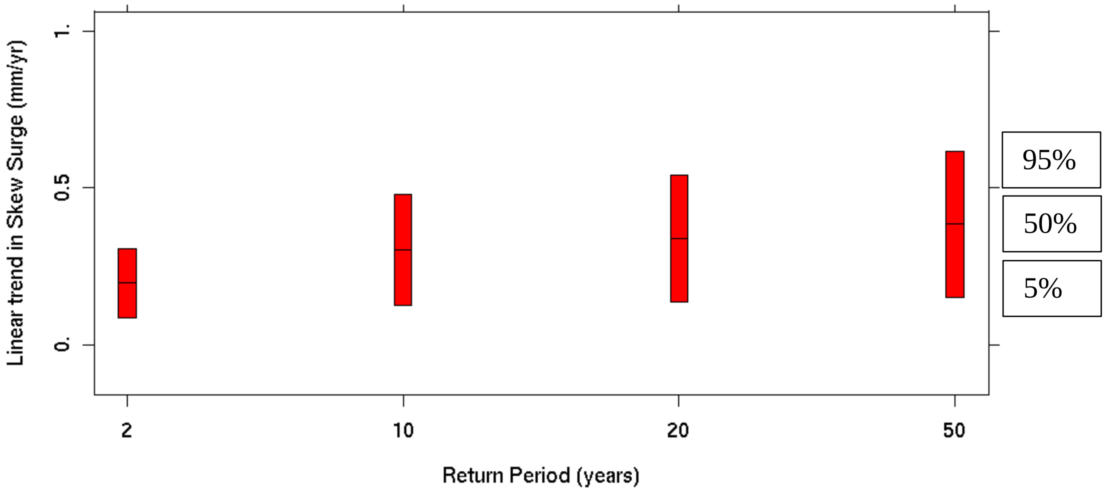

Figure 3-19. UKCP09 predictions of the linear trend in skew surge magnitude for different return periods under a medium emissions scenario at Start Bay (figure adapted from http://ukclimateprojections.metoffice.gov.uk). The bottom, middle, and top of each box indicates the 5th, 50th, and 95th percentiles of each prediction, indicating the magnitude of uncertainty, determined from an ensemble of UKCP09 model predictions. Although small, the trends are all significant at the 5% confidence level.

COASTAL MARINE APPLIED RESEARCH WITH PLYMOUTH UNIVERSITY

4. Long-Term Morphological Processes: Barrier Retreat

4.1. Introduction

This section of the report provides an overview of the coastal processes affecting the shoreline and beach morphology of Blackpool Sands, Slapton Sands, Beesands and Hallsands over the long-term (years – centuries). The information presented provides a new analysis of potential barrier retreat rates at Slapton Sands over the next century using UKCP09 projections of sea-level rise, providing revised and more comprehensive projections than those in Chapter 5 of the SCZM (Scott Wilson, 2006).

4.2. Methods for Predicting Beach and Barrier Retreat

Over time scales of years to centuries, the effects of sea-level rise drive shoreline and barrier retreat. Barrier beaches respond to sea-level rise by 'roll-over' and by increasing the crest height of the beach (Orford *et al.*, 1991). This process involves overwashing – the transferring of sediment from the shore-face to the back barrier area – which is an episodic rather than continuous process.

On sandy coasts, the most widely used method for predicting shoreline response to rising sea-level is the 'Bruun rule' (Bruun, 1962), which works on the hypothesis that as sea level rises, the shoreface adjusts by moving landward as a result of shoreline erosion, whilst maintaining its equilibrium shape. The Bruun rule assumes that shoreface erosion on the upper beach is balanced by shoreface accretion on the lower beach, and the resulting change in shoreline position, δy, is predicted with equation (1):

$$\delta y = -S\frac{W}{h+B} \tag{1}$$

where S is the rise in sea-level, W is the cross-shore width of the active shoreface, h is the height of the active shoreface (here taken as the depth of closure), and B is the height of the subaerial beach. Because of its widespread use on sandy coastlines, the Bruun rule will be applied in this section as a preliminary model to estimate the future retreat of Slapton barrier. However, its intended use is on sandy beaches not gravel barriers, and it has been argued that the Bruun rule should be abandoned altogether because its scientific assumptions are invalid and other more sophisticated models have superseded it (Cooper and Pilkey, 2004). The future retreat of Slapton barrier will therefore primarily be predicted here using a more recent model, specifically developed for gravel barriers (Orford *et al*. (1995b), Section 4.3), and the Bruun rule is only applied in Section 4.3 to provide a comparison.

Over meso-term time-scales (1 – 100 years), the rate at which a gravel barrier will naturally retreat landward has been found to relate to the rate of local sea-level rise, as well as the characteristic size, or ‘intertia’, of the barrier (Orford *et al.*, 1995b). A comparison of barrier retreat rates in Europe and Canada by Orford *et al*. (1995b) suggests that the retreat efficiency (the change in retreat rate per unit increase in the rate of sea-level rise) is related to the barrier size or barrier inertia (cross sectional area multiplied by crest height above mean sea-level). Increasing rates of sea-level rise therefore increase the rate at which a gravel barrier will migrate landward, and additionally, smaller barriers will migrate faster than larger barriers (Figure 4-1).

Figure 4-1 (right panel) presents the relationship between retreat efficiency and barrier inertia observed by Orford *et al*. (1995b). From this relationship, the Slapton barrier (characteristic cross sectional area of around 450 m^2 and crest height of 6 m, inertia = 2700 m^3/m) would be expected to have a retreat efficiency of around 0.2. Using this efficiency value, and assuming a contemporary rate of sea-level rise of 1.7 mm/year, Scott Wilson (2006) estimated the rate of barrier retreat at the time of the previous Slapton Sands beach management plan to be 0.34 m/year, increasing to 0.4 m/year due to increases in sea-level rise. As these previously determined rates only considered *absolute* values of sea-level rise rate and barrier retreat rate, they are considered erroneous, as the relationship in Figure 4-1 (right panel) predicts *changes* in these values. The formula therefore requires the predicted changes in retreat rate and sea-level rise to be added to estimates of current retreat rate and sea-level rise in order to make a prediction of future retreat, and it is understood this was not correctly accounted for in the SCZMS (Chadwick *et al.*, 2005; Scott Wilson, 2006).

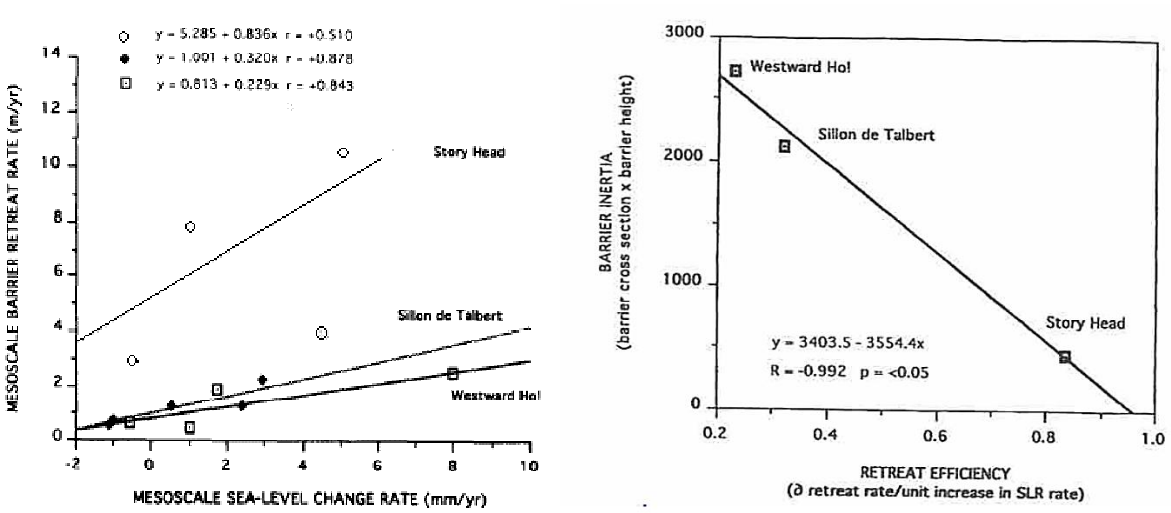

Figure 4-1. Left panel: relationship between barrier retreat rate and sea-level rise (SLR) rate determined from three gravel barriers in Europe and Canada by Orford *et al*. (1995b). Right panel: relationship between the gradient of each line in the left panel (barrier 'retreat efficiency'), versus the geometry of the barrier ('barrier inertia').

To correctly predict the rate of retreat of Slapton barrier using Orford *et al*.'s (1995b) formula (Figure 4-1), a contemporary retreat rate of 0.1 m/year has been assumed. This value was estimated as the average rate of beach crest retreat from an analysis of historic maps and aerial photographs of Slapton barrier, over a number of epochs between 1880 and 2003 (Scott Wilson, 2006), and represents a reasonable estimate of historic barrier retreat given the lack of measured data available. It should be noted that the barrier crest is thought to have moved by as much as 0.4 – 0.6 m during short-term erosion events (Scott Wilson, 2006), and Pethick (2001) estimated that between 1972 and 1995 the rate of barrier retreat was 0.8 m/year. However, this value is significantly higher than the longer-term rate derived from historic maps and photographs, and the retreat rate of 0.1 m/year will be used here as it represents a spatially and temporally averaged value over the last century. The contemporary rate of relative sea-level rise will be estimated using the UKCP09 predictions of sea-level rise between 1990 and 2017 (Figure 3-18 and Section 3.7).

Using the UKCP09 predictions of local relative sea level from Figure 3-18, future increases in sea-level rise rate can be applied to Orford *et al*.'s formula in order to predict the change in barrier retreat rate from the estimated contemporary value of 0.1 m/year, to increased rates due to the effects of accelerating sea-level rise. Following guidance for Shoreline Management Plans, sea-level rise rate over three epochs has been considered:

- Epoch 1: 0 - 20 years (2017 to 2036)
- Epoch 2: 20 - 50 years (2036 to 2065)
- Epoch 3: 50 - 100 years[2] (2065 to 2117)

4.3. Results

Figure 4-2 shows the retreat of the barrier crest under different sea-level rise scenarios, as predicted by Orford *et al*.'s formula, relative to its current position in 2017. These data are summarised in Table 4-1, Table 4-2, and Table 4-3 for the low, medium, and high UKCP09 emissions scenarios, respectively. Barrier retreat predicted using the Bruun rule is also presented in the tables and in Figure 4-3, for comparison. The predictions from Orford *et al*.'s formula indicate that accelerating sea-level rise will increase the rate of landward barrier migration in each epoch, and that the historic rate of barrier retreat will, in future, be exceeded under any of the future emissions scenarios. In comparison, the Bruun rule predicts that under a medium emissions scenario the estimated rate of barrier retreat over the past century will continue for the next century, while low emissions or high emissions scenarios would result in slower retreat and faster retreat over the next century, respectively, compared to the estimated historic rate of retreat. It should be stressed that the Bruun rule predictions are used here only to provide a comparative model, and it is expected that in reality the barrier will respond as per the predictions of Orford *et al*.'s formula, which are based on observations of real gravel barriers.

Depending on which emissions scenario is considered, Orford *et al*.'s formula predicts that the Slapton barrier will have migrated landward 3.4 – 4.5 m by the year 2036, 9.6 – 12 m by the year 2065, and 22 – 28 m by the year 2117. These retreat rates are 20 – 40% lower than those predicted in the SCZMS (Scott Wilson, 2006) as it is understood that the model was applied incorrectly during that study (refer to Section 4.2), and, until UKCP18 climate predictions are made available, these new predictions represent the best estimates of barrier retreat possible using current methods and climate projections. However, it should be noted that there is a great deal of uncertainty in the UKCP09 sea-level rise predictions (as demonstrated by the spread in the confidence bounds in Figure 3-18), and the level of uncertainty increases with time. The predicted retreat rates share this uncertainty (as demonstrated by the spread in the confidence bounds in Figure 4-2), and should therefore be treated cautiously. They are also subject to a number of other uncertainties:

[2] As UKCP09 projections (Figure 3-18) stop at year 2100, it has been assumed for the present analysis that sea level will rise at the same rate over the whole of epoch 3.

1. The estimated historic retreat rate of 0.1 m/year (on which the predictions are based) cannot be considered a natural retreat rate, as it incorporates the effects of engineered structures and beach recharge following overtopping events, which may have influenced the observed retreat rate.
2. The projections will only become a reality if the expected number of severe storm events occur within a given time period, as it is severe storm events which drive the retreat of the barrier. Increasing storminess due to climate change is not accounted for within the formula used to predict the barrier retreat. With increasing storm frequency and magnitude, it is likely that barrier retreat rate will increase, as overwash events become more frequent.
3. It was previously postulated that as the barrier retreats into the curved embayment, it is likely that the length of the shoreline will increase (Scott Wilson, 2006). As a result, the barrier's width is expected to reduce, due to the relatively fixed sediment volume, by 15 m per century (Pethick, 2001), which would increase the barrier's retreat efficiency. The rate of barrier retreat may therefore increase further in future, due to the smaller barrier size and increasing retreat efficiency.
4. The retreat rate is likely to vary along the length of the barrier, given that the cross-sectional area, height, and level of engineering vary along the barrier's length. The projections made here do not attempt to account for such spatial variation in the retreat.

Despite these uncertainties, the predictions provide an indication of the potential mobility of the barrier crest over the next 100 years, and it can be concluded that the relatively stable barrier position of the last century cannot be assumed to continue into the future. The projected future position of Slapton barrier under low, medium, and high emissions scenarios (as predicted by Orford *et al*.'s formula) has been superimposed onto aerial imagery in Appendix A, Appendix B, and Appendix C, respectively. These figures further demonstrate that under all emissions scenarios the barriers position is likely to migrate inland over the next 100 years, and that the majority of the road and southwest coast path will be affected within this period, regardless of the emissions scenario considered. These projections are only provided for indicative purposes however, due to the uncertainties described above.

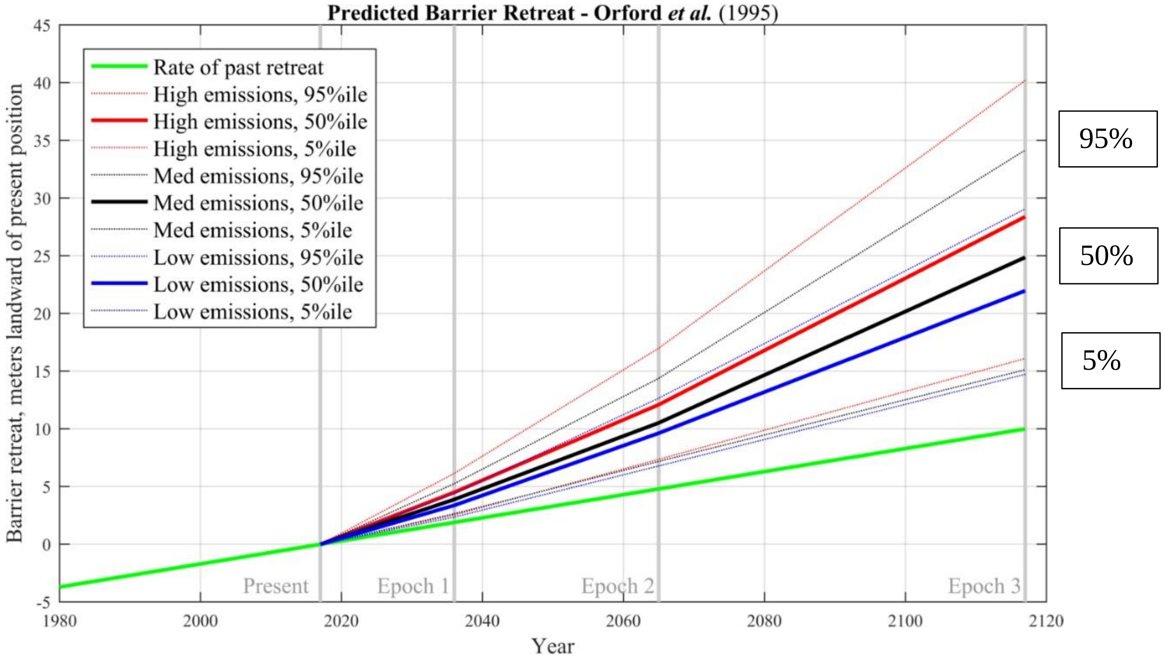

Figure 4-2. Retreat of Slapton barrier due to sea-level rise predicted using Orford *et al*.'s (1995b) model (Figure 4-1) for different UKCP09 emissions scenarios. Epoch 1 is years 2017 to 2036 (0 - 20 years), epoch 2 is years 2036 – 2065 (20 – 50 years), and epoch 3 is years 2065 – 2117 (50 – 100 years). Lower (5th percentile), median (50th percentile), and upper (95th percentile) predictions are shown for each scenario, indicating the magnitude of uncertainty in the UKCP09 sea-level rise predictions (Figure 3-18).

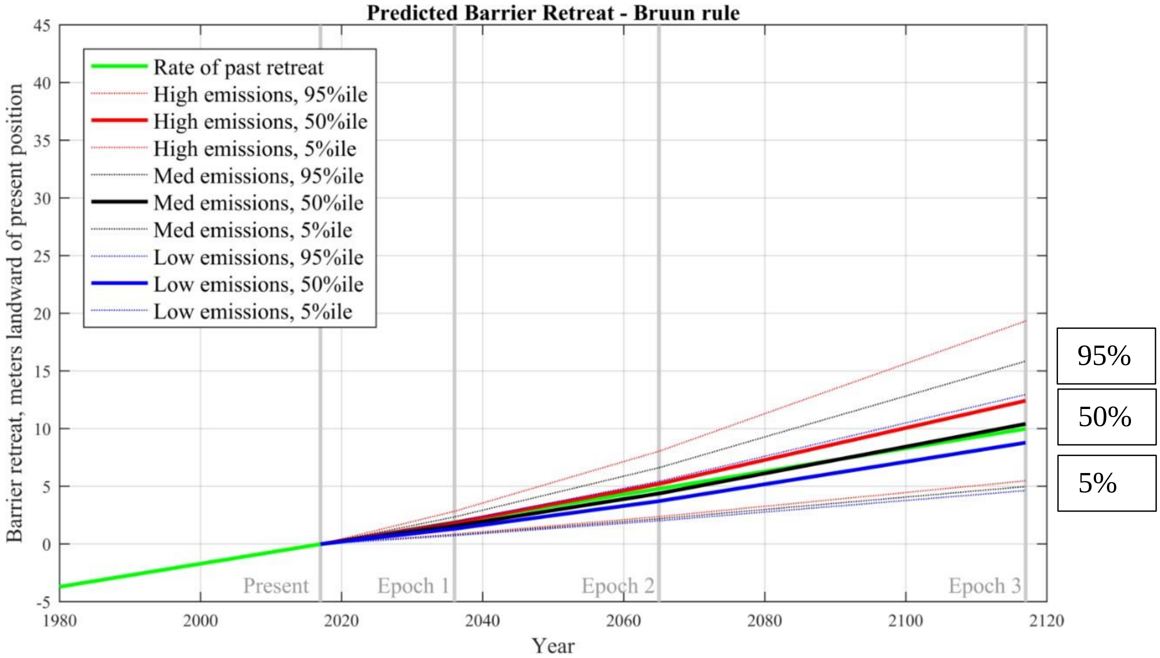

Figure 4-3. Retreat of Slapton barrier due to sea-level rise predicted using the Bruun rule (Bruun, 1962) for different UKCP09 emissions scenarios. Epoch 1 is years 2017 to 2036 (0 - 20 years), epoch 2 is years 2036 – 2065 (20 – 50 years), and epoch 3 is years 2065 – 2117 (50 – 100 years). Lower (5th percentile), median (50th percentile), and upper (95th percentile) predictions are shown for each scenario, indicating the magnitude of uncertainty in the UKCP09 sea-level rise predictions (Figure 3-18).

Table 4-1. Predicted retreat rate and retreat distance of Slapton barrier under varying sea-level rise from a low emissions scenario (50th percentile prediction). Values are given to 2 significant figures. The retreat distances predicted by the model of Orford *et al*. (1995b) are overlaid onto aerial imagery in Appendix A.

Timeframe	UKCP09 rate of sea-level rise (mm/year)	Orford *et al.* (1995)		Bruun rule	
		Retreat rate (m/year)	Retreat distance (m landward)	Retreat rate (m/year)	Retreat distance (m landward)
0 – 20 years	3.3	0.18	3.4	0.07	1.3
20 – 50 years	3.8	0.22	9.6	0.08	3.7
50 – 100 years	4.5	0.24	22	0.10	8.8

Table 4-2. Predicted retreat rate and retreat distance of Slapton barrier under varying sea-level rise from a medium emissions scenario (50th percentile prediction). Values are given to 2 significant figures. The retreat distances predicted by the model of Orford *et al*. (1995b) are overlaid onto aerial imagery in Appendix B.

Timeframe	UKCP09 rate of sea-level rise (mm/year)	Orford *et al.* (1995)		Bruun rule	
		Retreat rate (m/year)	Retreat distance (m landward)	Retreat rate (m/year)	Retreat distance (m landward)
0 – 20 years	3.9	0.20	3.9	0.08	1.6
20 – 50 years	4.5	0.23	11	0.10	4.4
50 – 100 years	5.4	0.28	25	0.12	10

Table 4-3. Predicted retreat rate and retreat distance of Slapton barrier under varying sea-level rise from a high emissions scenario (50th percentile prediction). Values are given to 2 significant figures. The retreat distances predicted by the model of Orford *et al*. (1995b) are overlaid onto aerial imagery in Appendix C.

Timeframe	UKCP09 rate of sea-level rise (mm/year)	Orford *et al.* (1995)		Bruun rule	
		Retreat rate (m/year)	Retreat distance (m landward)	Retreat rate (m/year)	Retreat distance (m landward)
0 – 20 years	4.6	0.24	4.5	0.10	1.9
20 – 50 years	5.4	0.26	12	0.12	5.2
50 – 100 years	6.4	0.31	28	0.14	12

5. Medium-Term Morphological Processes: Alongshore Transport

5.1. Introduction

This section provides an overview of the coastal processes affecting the shoreline and beach morphology of Blackpool Sands, Slapton Sands, Beesands, and Hallsands over the medium-term (weeks – years). The information presented draws from existing literature as well as new analyses of wave and beach profile data, including:

- Analysis of beach profiles to assess cross-sectional area and sediment volume change (refer to Section 5.3);
- Investigation of dominant morphological changes and wave-beach forcing using Empirical Orthogonal Function (EOF) analysis (refer to Section 5.4);
- Analysis of maximum alongshore sediment transport rates (refer to Section 5.6); and
- Discussion of large-scale climate 'cycles' responsible for medium-term processes (refer to Section 5.7).

These analyses have been undertaken to provide new understanding of the beach dynamics and trends in Start Bay, and thereby provide an update to Chapter 11 of the SCZMS (Scott Wilson, 2006).

5.2. Alongshore Sediment Transport

Over time-scales of weeks to years, the key morphological process shaping the beaches in Start Bay is alongshore transport of sediment (Chadwick *et al.*, 2005), which is primarily a function of the sediment characteristics, the level of incident wave energy, and the angle of wave approach (US Army Corps Of Engineers, 1984). The net sediment transport direction in Start Bay is from south to north (Scott Wilson, 2006), however, as illustrated in Section 3.2, the beaches in Start Bay experience a bi-directional wave climate, with waves arriving at oblique angles from the south and from the east. These wave approaches drive opposing alongshore transport (Figure 5-1), which intermittently redistributes the gravel along the beaches of Start Bay (Chadwick *et al.*, 2005; Scott Wilson, 2006; de Alegria-Arzaburu and Masselink, 2010; de Alegría-Arzaburu *et al.*, 2010; Wiggins *et al.*, 2017). The natural response of the shoreline to such alongshore transport, is to rotate around the bay in a clockwise (during southerly wave events) or anti-clockwise (during easterly wave events) direction. As a result, shoreline position along Slapton Sands has been seen to vary horizontally by up to 10 m in a single month (Chadwick *et al.*, 2005), and the shoreline of the other beaches in Start Bay also exhibits significant rotation in response to energetic wave events because of this process (Scott *et al.*, 2016; Wiggins *et al.*, 2017).

Figure 5-1. Images of southerly (left panel) and easterly (right panel) storm waves arriving at the Strete Gate end of Slapton Sands in March and April of 2008, respectively (modified from de Alegria-Arzaburu and Masselink, 2010). Note the oblique opposing angles of the breaking waves (indicated by red arrows and dashed lines), and associated opposing alongshore transport potential (indicated by blue arrows).

The morphodynamic response of Slapton Sands to easterly and southerly wave events is primarily a switching of alongshore transport direction (Chadwick *et al.*, 2005; de Alegria-Arzaburu and Masselink, 2010) from southward (easterly wave event) to northward (southerly wave event). However, some cross-shore redistribution of sediment does occur, and southerly and easterly wave events incur opposing responses in the profile shape of the beach (de Alegria-Arzaburu and Masselink, 2010), which is discussed further in Section 6. As a result of trends in the alongshore transport in Start Bay, profiles at the south end of the bay show a long term (> 10 years) erosion trend, caused by the recent predominance of southerly winter storms (Scott *et al.*, 2016; Wiggins *et al.*, 2017). In contrast, the north end of Slapton Sands has experienced long-term accretion, with erosion only occurring during relatively infrequent easterly storms. This response is considered a direct reflection of the imbalance in total hours of easterly and southerly waves with sufficient energy to cause significant alongshore sediment transport (i.e. > 2.5 m H_s) over the last 10 years (Scott *et al.*, 2016).

5.3. Beach Profile Analysis

5.3.1. Source Data and Methodology

For the purpose of the present study, new analysis of beach profile data has been undertaken to assess how the beaches at Blackpool Sands, Slapton Sands, Beesands, and Hallsands have changed over time.

A series of profile data, dating from August 1972 to March 2017, has been collated from the Slapton Field Studies Centre (FSC), Plymouth University (PU) and Plymouth Coastal Observatory (PCO), and is analysed here to determine changes in profile cross-sectional area and height (refer to Section 5.3.2), and beach volume (refer to Section 5.3.3).

More than 10 years of profile data from Blackpool Sands, Slapton Sands, Beesands, and Hallsands has been sourced from PU and PCO. An additional older data set from the Slapton FSC will also be used to examine the behaviour of the beach over a longer period. Beach profiles at Slapton Sands (P0 – P20 in Figure 2-3) have been monitored monthly by PU from Nov 2006 to the present day. At Blackpool Sands, Slapton Sands, Beesands, and Hallsands, profiles have been monitored bi-annually in spring and autumn by PCO (www.channelcoast.org/southwest) since May 2007. The profile data collected by PU and PCO were measured using pole-mounted RTK-GPS, which has a nominal positional accuracy of +/- 3 cm.

From the 21 profiles monitored by PU at Slapton Sands since 2006, a continuous data set was created from the 11 most consistently surveyed profiles (p1, p5, p7, p9, p10, p11, p12, p13, p15, p17, and p18), which are well spread along the 5 km length of Slapton Sands (Figure 2-3). These profiles were surveyed approximately monthly, and the available data run between November 2006 and March 2017. PCO Profiles at Hallsands (HS1, HS2, HS3, and HS4 on Figure 2-3), Beesands (BS1, BS2, BS3, BS4, BS5, and BS6 on Figure 2-3), and Blackpool Sands (BK1, BK2, BK3, and BK4 on Figure 2-3) were monitored twice yearly, with data available between May 2007, and Nov 2016.

5.3.2. Beach Profile Cross-Sectional Change

The evolution of the profiles at the four beaches in Start Bay over the last 10 years is shown in Figure 5-2 to Figure 5-5. From these figures, the following conclusions about net profile changes at each beach can be drawn:

- **At Blackpool Sands**, all four profiles gained sediment over the last 10 years, with profiles gaining up to 6 m of elevation in places. At profiles BK1 – BK3, the first and last measurements represent approximately the least and most accreted profiles measured, respectively. This indicates a steady net increase in sediment at the northern most part of Start Bay over the last 10 years, although it is possible that fluctuations occurred between interim surveys. At the most northerly profile at Blackpool Sands (BK 4), sediment appears to have been gained and lost over the last 10 years.

- **At Slapton Sands**, profiles P1 – P13 situated along the southern half of the beach (Figure 2-3), all lost sediment over the last 10 years. At profile P15 there is little change in position between the first and last measurements and it has been the most stable profile at Slapton Sands, although some cross-shore redistribution of sediment is apparent. Profiles P17 and P19, at the northern end of the beach gained sediment over the last 10 years.
- **At Beesands**, there has been relatively little net profile change at profiles BS4 – BS6 at the north end of the beach over the last 10 years. In contrast, profiles BS1 – BS3 at the southern half of the beach have all shown a decrease in profile elevation, with parts of those profiles losing more than 2 m of elevation.
- **At Hallsands** all four of the monitored profiles show a net decrease in profile elevation of up to 2 m, indicating net erosion at this beach over the last 10 years.

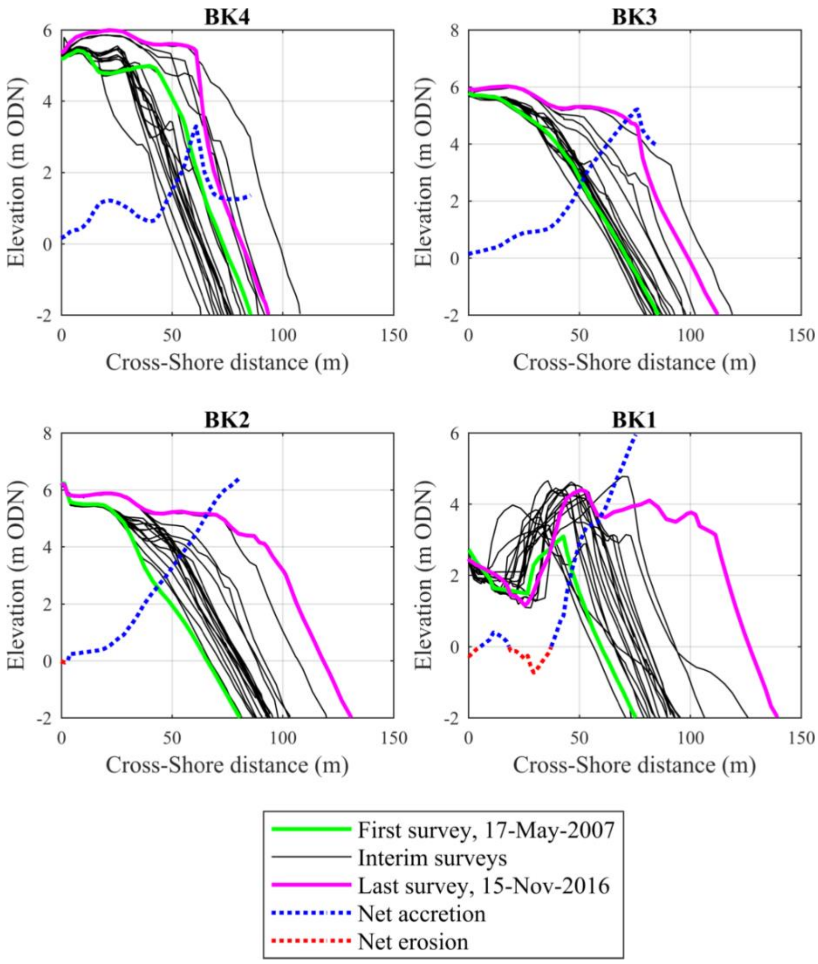

Figure 5-2. Evolution of Blackpool Sand's profiles over the last 10 years. The difference in profile elevation between the latest survey and the first survey is shown as a dashed line in each panel. The location of each profile is shown in Figure 2-3.

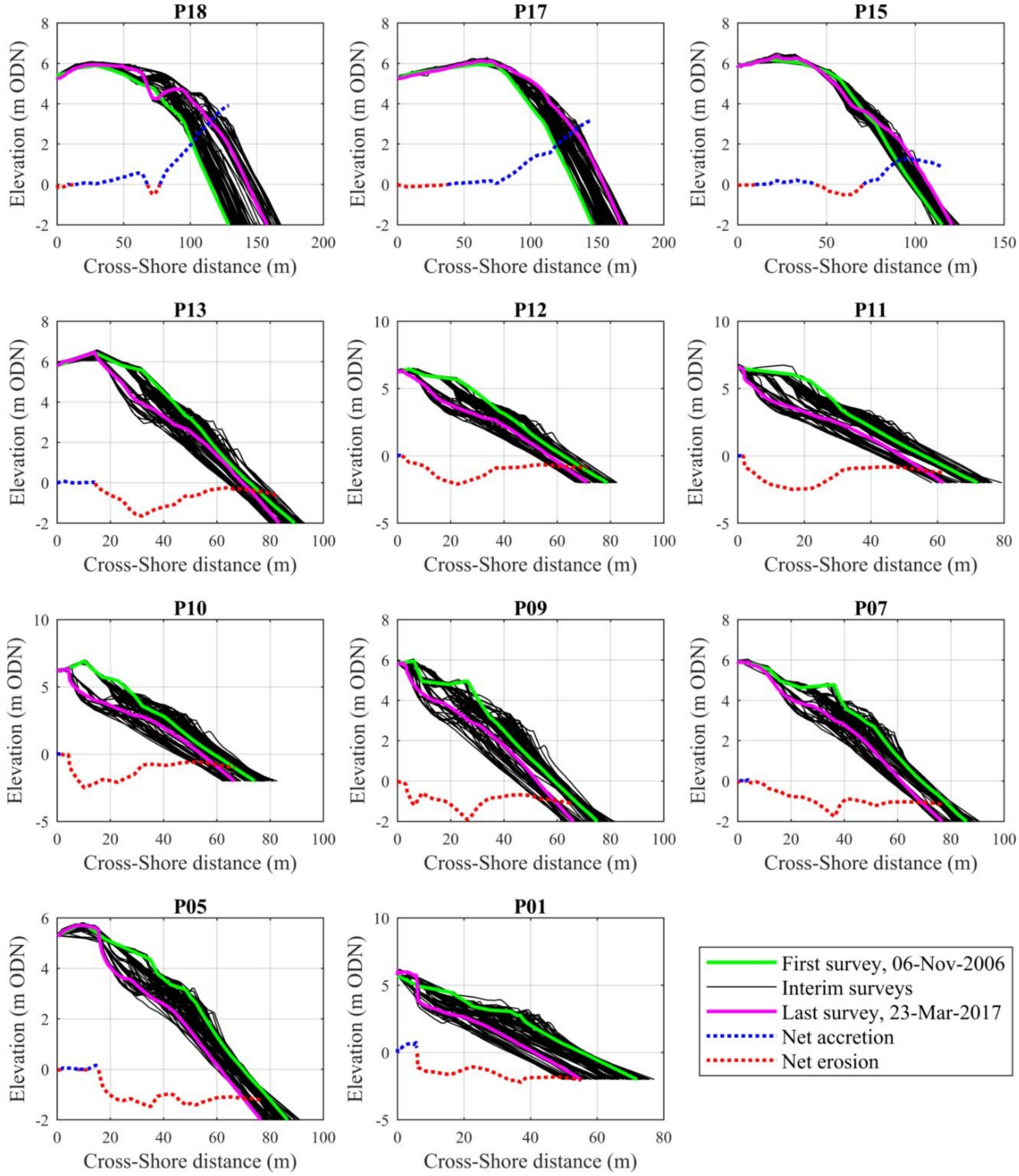

Figure 5-3. Evolution of Slapton Sand's profiles over the last 10 years. The difference in profile elevation between the latest survey and the first survey is shown as a dashed line in each panel. The location of each profile is shown in Figure 2-3.

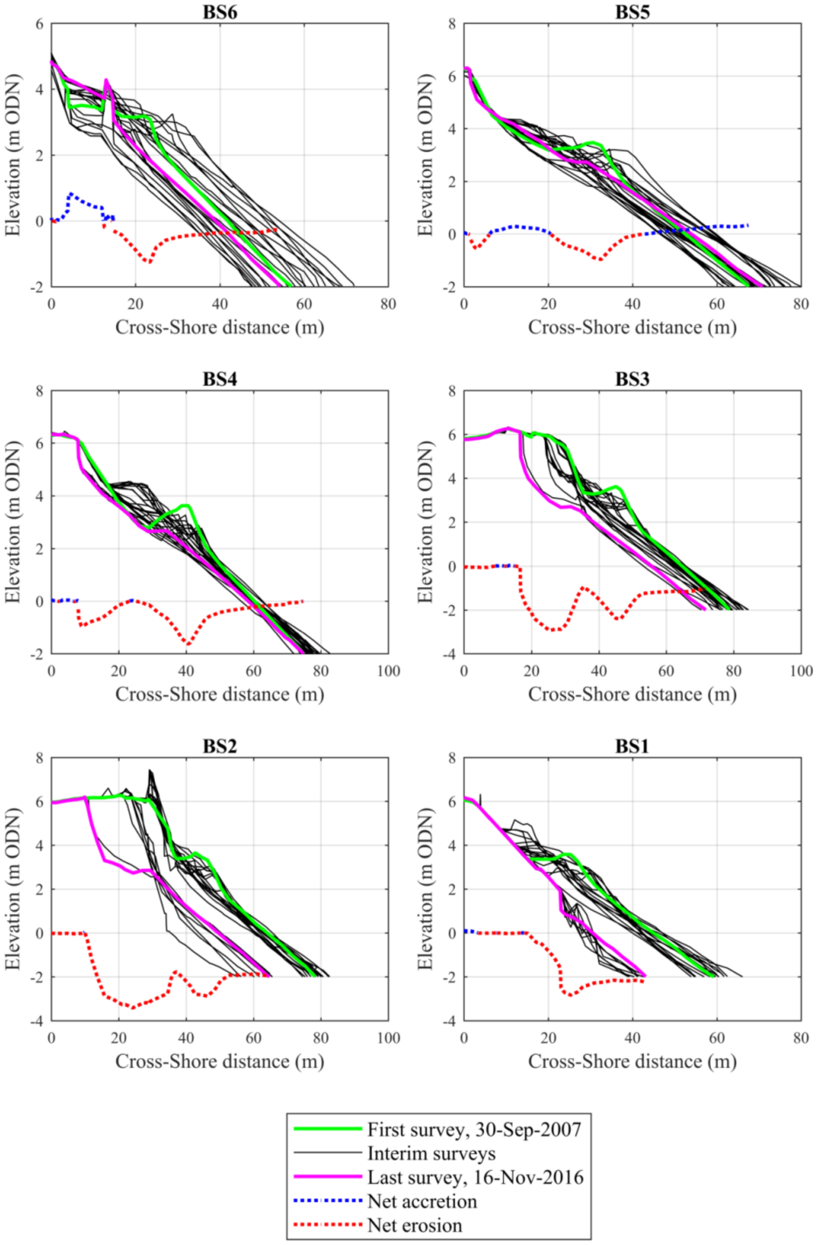

Figure 5-4. Evolution of Beesand's profiles over the last 10 years. The difference in profile elevation between the latest survey and the first survey is shown as a dashed line in each panel. The location of each profile is shown in Figure 2-3.

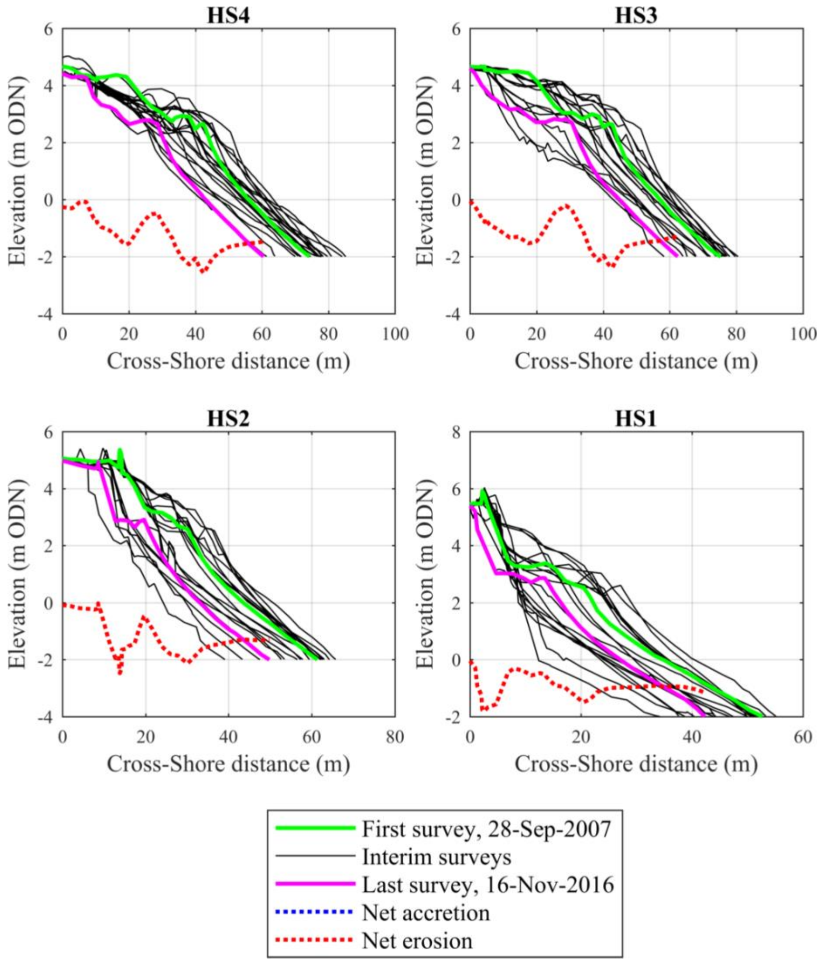

Figure 5-5. Evolution of Hallsand's profiles over the last 10 years. The difference in profile elevation between the latest survey and the first survey is shown as a dashed line in each panel. The location of each profile is shown in Figure 2-3.

5.3.3. Beach Volume Change

Changes in sediment volume indicate the relative health of a beach, with increasing beach volumes representing accretion and progradation of the shoreline. Beaches with greater sediment volumes therefore have greater capacity to provide resilience against storm impacts and coastal flooding, whereas beaches with diminishing volume are susceptible to cut-back, overtopping, overwashing, and eventually to breaching, in the case of a barrier beach. In this section, intertidal beach profiles are used to investigate the volume of sediment available at each beach in Start Bay. The volume of sediment per metre of shoreline was calculated from the profile area between -1 m ODN (approximately MLWN) and the top of the beach, going as far landward as the benchmark for each profile (usually the location of a road, cliff, or engineered structure at the top of the profile).

Figure 5-6 to Figure 5-9 (right panels) collectively illustrate the overall trend in Start Bay: profiles north of P16 (Figure 2-3), up to BK4, gained 25 – 350 m^3 of sediment per meter of shoreline over the last 10 years, while profiles south of P15, down to HS1, lost up to 130 m^3/m volume over the last 10 years. The individual gains in sediment volume at the north end of Start Bay are much larger than the losses anywhere else along the length of the bay, but the losses occurred over a much greater length of the shoreline. The volume statistics shown in Figure 5-6 to Figure 5-9 (left panels) reveal that the area with the greatest overall beach volume in Start Bay is the Strete (north) end of Slapton Sands, with mean volumes of gravel in excess of 800 m^3 per meter of shoreline. Blackpool Sands also has a large sediment volume, with around 300 – 400 m^3 per meter of shoreline. The areas with the lowest sediment volumes, and therefore those that are most vulnerable to storm impacts and coastal flooding, are the middle and south of Slapton Sands (~75 – 300 m^3/m), the entirety of Beesands (~150 – 300 m^3/m), and Hallsands (~100 – 200 m^3/m).

Changes in beach volume through time along the length of Start Bay are shown in Figure 5-11 (Wiggins *et al.*, 2017), using the bi-annual data set collected by PCO over the last 10 years. This further demonstrates that there has been an overall net loss of volume at all profiles in Start Bay south of Strete since 2007, with net gains seen at the Strete end of Slapton Sands, and at Blackpool Sands. The exception to this rule is at the north end of Beesands (profiles BS5 and BS6) and in the middle of Slapton Sands (profiles P15 and P16), where sediment has been both gained and lost, and little net volume change occured over the last 10 years.

Over the longer term, a net trend of sediment loss at the middle and south of Slapton, and net gains at the north end of Slapton, has been occuring since at least 1972, as demonstrated by older topographic data collected by the Slapton Field Studies Centre (FSC, Figure 5-10) between August 1972 and May 2003. Although the beach area values in Figure 5-10 are not directly comparable to the beach volumes presented in Figure 5-6 to Figure 5-9 because of the profile area over which they were calculated, they are equivalent to profile volume above the mean water level (MWL, approximately 0 m ODN) and the mean high water level (MHWL, approximately 1.7 m ODN) (m^3 per meter of shoreline), and show the same overall trend as the more recent beach volumes collected between 2006 and 2017. Unfortunately, there are no data available to show the behaviour of Slapton Sands (or the other beaches of Start Bay) between May 2003 and November 2006.

In addition to the conspicuous north/south trend in accretion/erosion, sediment volume has also fluctuated over time at different parts of Start Bay, and a number of key periods over the last 10 years have been identified (shown as boxes A – F on Figure 5-10 and Figure 5-11):

A. **1972 – 2003: northward transport.** Over this period, surveys were only sporadically conducted at Slapton Sands, but net increases in beach volume were observed at the north end of Slapton Sands, with decreases at the middle and south end.
B. **2003 – 2006: no survey data available.**
C. **2007 – 2012: variable north/south transport.** Over this period beach volumes fluctuated, with alternating north-south sediment transport indicated by the alternating increases and decreases in volume. North to south sediment transport and beach rotation appears to have occurred at Blackpool Sands, but obvious trends at the other beaches are not apparent over this period.
D. **2012 – 2013: southward transport.** Over this period quite significant north-south transport of sediment occurred, and sediment was gained in all areas apart from the northern most section of Beesands, Slapton Sands, and Blackpool Sands at the downdrift side of each headland.
E. **Winter of 2013/2014: significant northward transport.** During this winter very large volumes of sediment were transported northwards, as is evident by the decreasing volumes in the south of the bay and increasing volumes north of P18. The opposing erosion/accretion at the south/north ends of Beesands, Slapton Sands, and Blackpool Sands indicates that beach rotation occured at those beaches.
F. **2014 – 2017: variable north/south transport.** The period since 2014 has seen some minor recovery of sediment following the the 2013/2014 winter, and Hallsands almost returned to its 2007 volume by the middle of 2015, but subsequent northward transport has meant that, overall, the profiles in the south of Start Bay have not recovered to their 2013 levels and have in fact eroded further, while Blackpool Sands has continued to gain sediment.

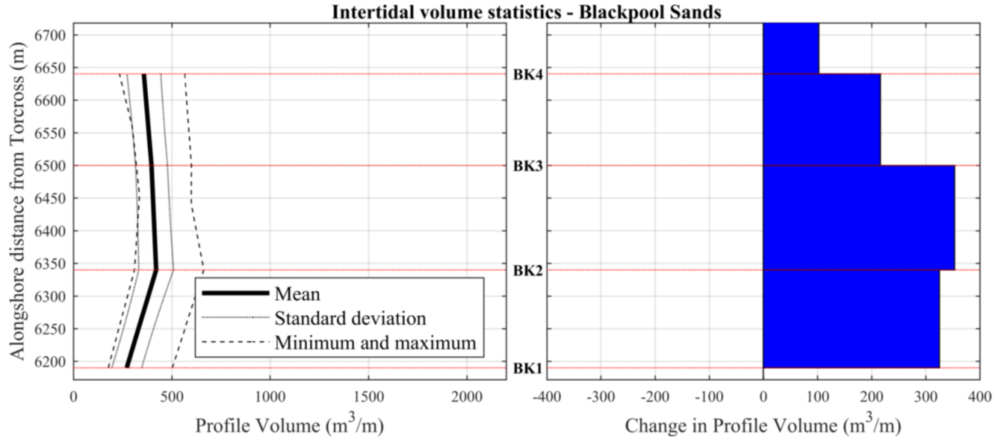

Figure 5-6. Intertidal beach volume statistics (left panel) and net change in intertidal beach volume (right panel), interpolated from profiles BK1 – BK4 (red dotted lines) at Blackpool Sands between May 2007 and November 2016. Net erosion and accretion are shown in red and blue, respectively, in the right panel (where applicable).

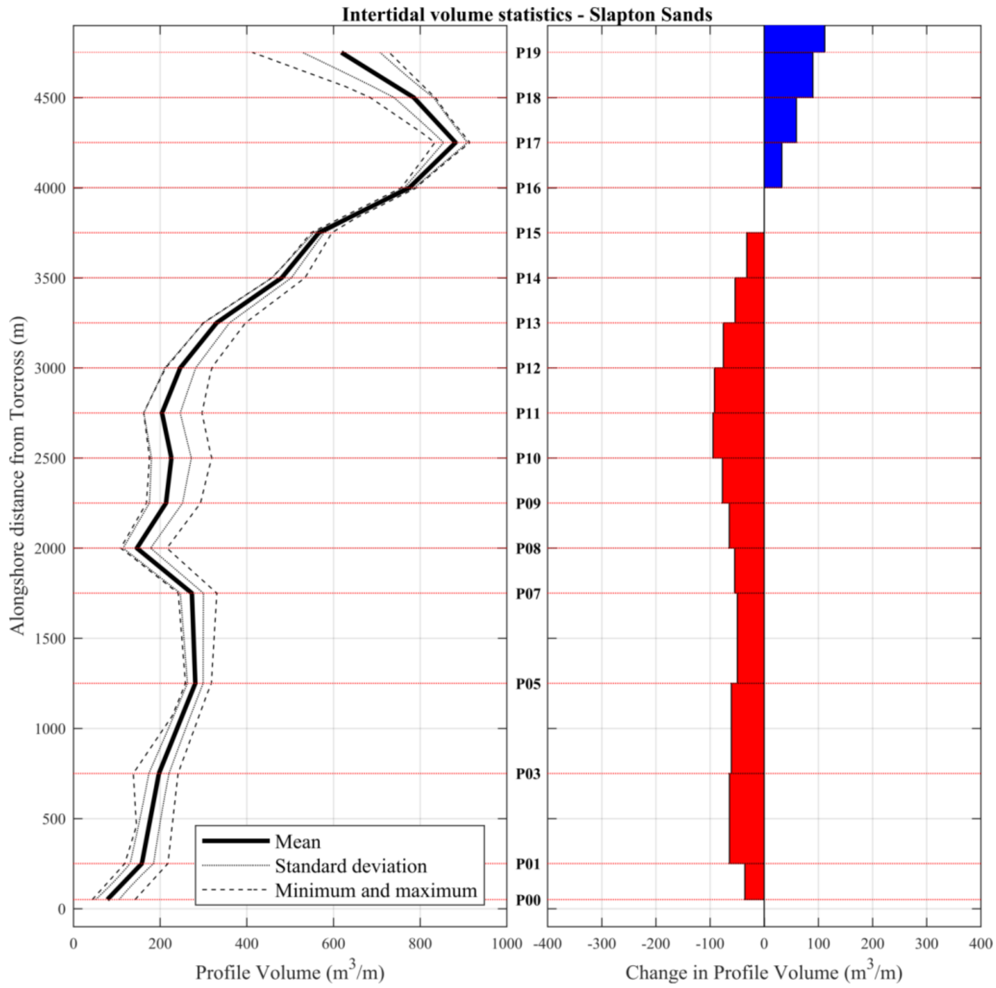

Figure 5-7. Intertidal beach volume statistics (left panel) and net change in intertidal beach volume (right panel), interpolated from profiles P00 – P19 (red dotted lines) at Slapton Sands between May 2007 and March 2017. Net erosion and accretion are shown in red and blue, respectively, in the right panel (where applicable).

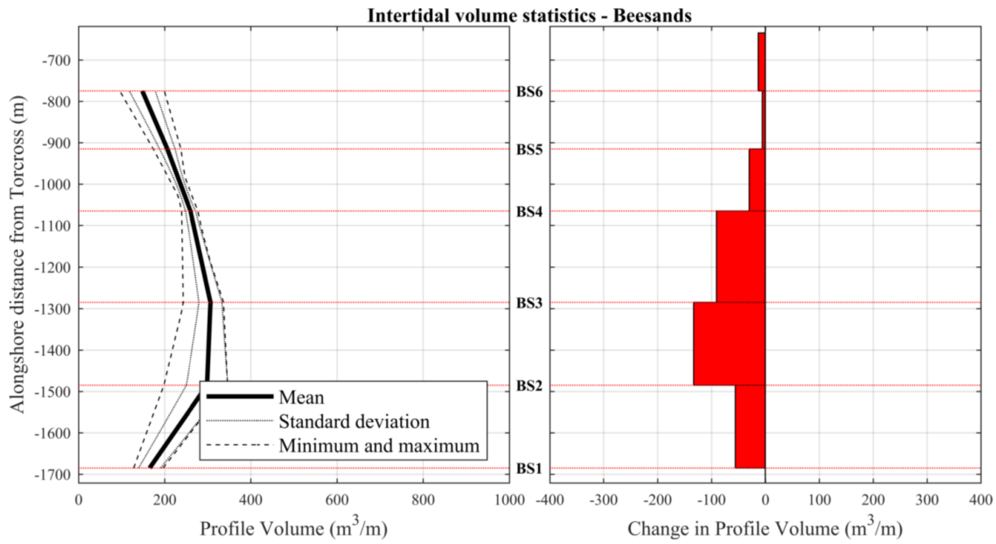

Figure 5-8. Intertidal beach volume statistics (left panel) and net change in intertidal beach volume (right panel), interpolated from profiles BS1 – BS6 (red dotted lines) at Beesands between May 2007 and November 2016. Net erosion and accretion are shown in red and blue, respectively, in the right panel (where applicable).

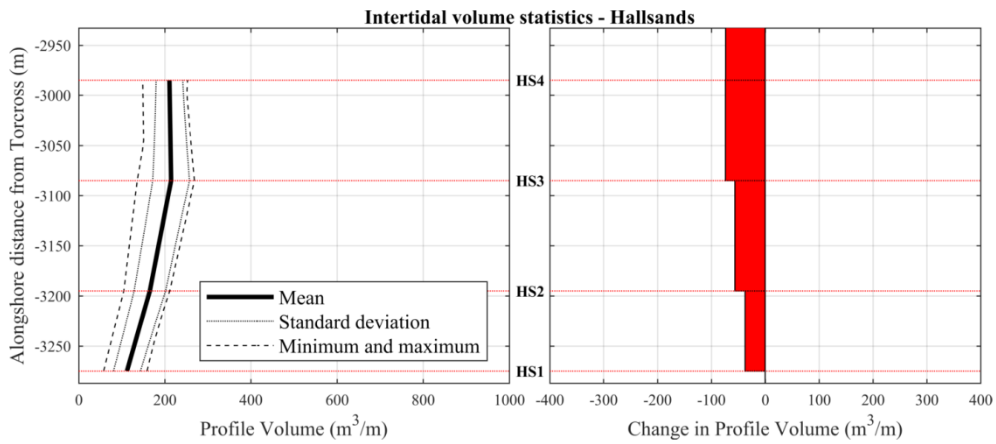

Figure 5-9. Intertidal beach volume statistics (left panel) and net change in intertidal beach volume (right panel), interpolated from profiles HS1 – HS4 (red dotted lines) at Hallsands between May 2007 and November 2016. Net erosion and accretion are shown in red and blue, respectively, in the right panel (where applicable).

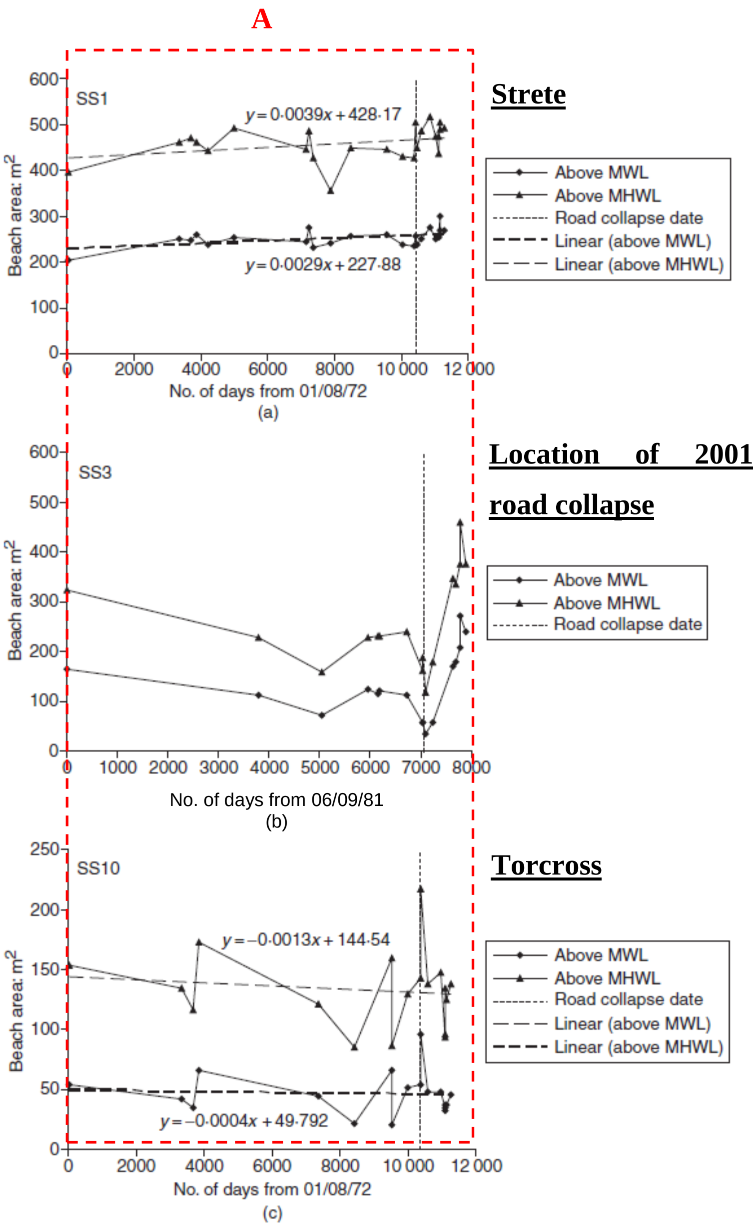

Figure 5-10. Beach area above mean water level (MWL) and mean high water level (MHWL), collected by the Slapton Field Studies Centre (FSC) between August 1972 (0 days on the figure) and May 2003 (12,000 days). FSC Profiles SS1 (Strete, top panel), SS3 (location of 2001 road collapse, middle panel), and SS10 (Torcross, lower panel) are approximately equivalent to profiles P17, P12, and P0 in Figure 2-3. The increase at SS3 after 7000 days is due to beach nourishment following the 2001 road collapse. Red dashed box 'A' is a key period described in the text. Figure modified from Chadwick *et al.* (2005).

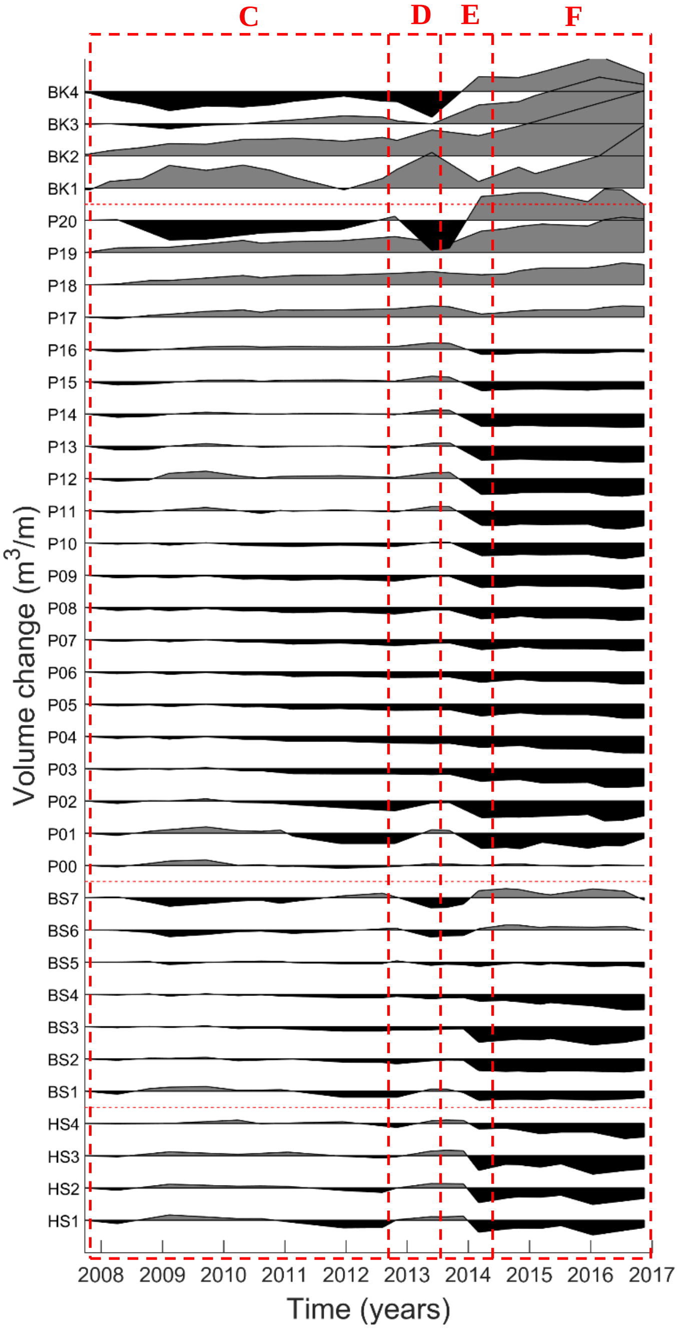

Figure 5-11. Volume change time series for surveyed profiles along Start Bay, collected between 2007 and 2016 by PCO. Profiles are displayed from north to south (top to bottom), with Blackpool Sands at the top of the figure, and Hallsands at the bottom. The location of each profile is shown in Figure 2-3. The red dashed line indicates the separation of sub-embayments. Volume change at each profile is shown relative to the first survey in 2007, and represents volume change as a unit of beach width (m^3/m). Areas of black below the line indicate periods of negative volume change, whilst the grey areas above the horizontal lines indicate positive change. Red dashed boxes C to F indicate key periods described in the text. Figure modified from Wiggins *et al.* (2017).

5.4. Erosional Hot-Spots

Erosional hot-spots in Start Bay can be identified as areas of beach that have the combination of a low mean sediment volume, and a large variance in sediment volume. This combination indicates that regular erosion of the profile occurs, and that there is limited sediment available to provide resilience against such erosion. From examination of the volume statistics in Figure 5-6 to Figure 5-9, a number of erosional hot-spots (listed from north to south) have been identified within Start Bay:

1. **Middle of Slapton Sands (profiles P8 – P11).** These profiles have, on average, 150 – 200 m^3/m of sediment, and have had as little as 100 m^3/m in the last 10 years.
2. **South end of Slapton Sands (profile P0 – P3).** These profiles have, on average, 75 – 200 m^3/m of sediment, and P0 in front of Torcross village has had as little as 50 m^3/m in the last 10 years.
3. **North end of Beesands (profile BS6).** This profile has, on average, around 150 m^3/m of sediment, and has had as little as 100 m^3/m in the last 10 years.
4. **South end of Beesands (profile BS1).** This profile has, on average, around 180 m^3/m of sediment, and has had as little as 150 m^3/m in the last 10 years.
5. **All of Hallsands (profiles HS1 – HS4).** Profile HS4 at the north of Hallsands has had, on average, around 200 m^3/m of sediment, and has had as little as 150 m^3/m in the last 10 years. Profile HS1 at the south of Hallsands has had, on average, around 100 m^3/m of sediment, and has had as little as 50 m^3/m in the last 10 years.

The vulnerability of these sections of Start Bay to storm impacts is discussed further in Section 6.4 of this report.

5.5. Empirical Orthogonal Function Analysis

One approach to studying beach morphodynamics is to adopt a statistical method that can concisely summarise the complex natural variability in the beach topography in a small number of dominant patterns of change. The method of Empirical Orthogonal Function (EOF) analysis, has been applied widely to achieve such a purpose (Winant, 1975; Aubrey, 1979; Clarke and Eliot, 1982; Hsu *et al.*, 1986; Larson *et al.*, 1999; Miller and Dean, 2007a; Fairley *et al.*, 2009; Gómez-Pujol *et al.*, 2011; Loureiro *et al.*, 2012; Stokes *et al.*, 2013), and is adopted in this study to better understand the relationship between the key morphological changes at Slapton Sands, and the forcing wave conditions that lead to those changes. For the EOF analysis, a complete and consistent data set is required, therefore only the monthly topographic data from Slapton Sands could be analysed in this way, as Blackpool Sands, Beesands, and Hallsands were surveyed less frequently.

EOF analysis determines the most dominant spatial signals (the spatial eigenvectors) in the topographic data, and quantifies how those spatial patterns vary through time (the temporal coefficients). The EOF patterns can be thought of as standing oscillations whose amplitude varies over time, and can be used to show which areas of the beach co-vary about their mean position at a given moment in time. Additionally, each EOF describes an orthogonal, and therefore independent, mode of change. The method is an effective data reduction tool, as normally the first few EOF patterns can explain a large majority of the total beach variability. Lower EOF modes explaining a small amount of the total variance can be considered noise, and are usually disregarded.

The continuous data set of 11 profiles at Slapton Sands yielded 96 individual observations of beach volume at each profile over the the last 10 years of monitoring. These were used to interpolate the intertidal beach volume every 1 m along the length of Slapton beach, on each survey date. The mean volume at every alongshore position was removed from the timeseries, as otherwise the mean of the data can dominate the EOF patterns, reducing the usefulness of the results. The resulting patterns therefore represent the dominant changes about the mean beach volume. The analysis was performed on the beach volume time series, rather than the time series of shoreline position, as beach volume is more representative of beach health and resilience to storm impacts, whereas shoreline position fluctuates rapidly in the presence of transitionary morphological features.

5.5.1. EOF Results

Only one statistically significant EOF mode was revealed by the analysis (Figure 5-12), which captures 90% of the morphological change that occurred over the last 10 years. This pattern therefore conscisely describes the vast majority of the changes in beach volume, and the other EOF modes were disregarded as noise in the signal.

The eigenvector of the dominant EOF depicts a rotational mode of beach change: the spatial pattern (Figure 5-12, upper panel) is positive at the northern end of Slapton Sands (3800 – 4500 m north of Torcross) while the rest of the beach is negative. There is a ‘hinge-point’ around profile P15, where little change has occurred over the last 10 years (Figure 5-7), and the EOF shows this as a nodal point around which the beach pivots as it rotates. This means that at times when the north of the beach has had higher than average volume, i.e. when the temporal coefficient (Figure 5-12, lower panel) was positive, the middle and south of the beach have simultaneously had lower than average volumes (for instance, since 2014). Conversely, when the temporal coefficient has been negative (for instance, prior to 2013), the middle and southern part of the Slapton Sands had higher than average volumes, while the northern end of the beach had a lower than average volume. Upwards gradients in the temporal pattern indicate northward sediment transport (even when the coefficient itself is negative), and downwards gradients indicate southward sediment transport (even when the coefficient is positive).

From the temporal pattern in Figure 5-12 (lower panel), the beach was predominantly rotated towards the middle and south prior to 2013 (relative to the average shoreline position), but the temporal coefficient was gradually increasing over this period indicating that, overall, more sediment was being transported northward than southward. In 2013 there was a notable downward gradient, where southward transport of sediment rotated the beach temporarily back towards the south. Shortly after this, the exceptional winter of 2013/2014 caused the largest upward gradient (northward rotation) in the time series, and further rotation to the north occurred in 2016, with some subsequent recovery.

A number of conclusions can be drawn from the EOF signal:

- The dominant EOF describes a rotational mode of beach change: at times when the north end of Slapton Sands has been acreting, the middle and south of the beach has eroded, and vice versa.
- Overall, a net upward trend in the EOF is seen, indicating increasing beach volume at the north of Slapton Sands, and decreasing volume at the middle and south, over the last 10 years.
- Periods of rapid northward (clockwise) beach rotation occured every few years over winter, interspersed by more gradual southward (anti-clockwise) beach rotation in between, except during early 2013 when a rapid southward rotation occurred.
- As the northward rotation events have been stronger than the intervening southward rotation, the net effect has been a bias towards northward sediment transport and rotation in a clockwise direction.

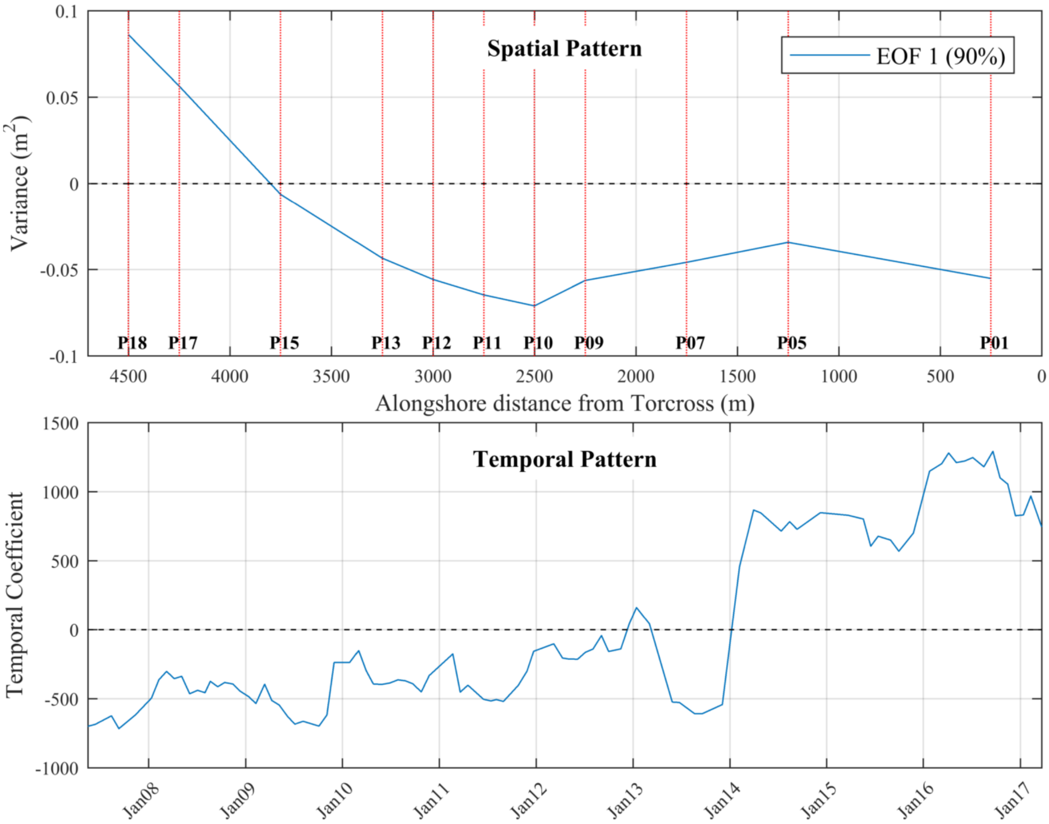

Figure 5-12. Results of Empirical Orthogonal Function (EOF) analysis on the 10-year time series of PU monitored profile volumes along Slapton Sands beach. The upper and lower panels show the spatial and temporal patterns, respectively, of the single dominant mode of morphological change, which accounts for 90% of all changes in the profile volumes along the beach. The alongshore position of the monitored profiles are shown as red dotted lines in the upper panel, and their geographic location is shown in Figure 2-3.

5.5.2. Relation to Wave Forcing

In this section of the report, the dominant mode of beach change determined through the EOF analysis in Section 5.5.1 was compared to the time series of a variety of wave parameters from the Met Office WWIII data, to explore which wave conditions were responsible for forcing the observed changes. Alongshore sediment transport and beach rotation is shown to be strongly related to the magnitude and direction of the incident wave power, and that the cumulative effects of powerful waves arriving obliquely from the south drives the net sediment transport to the north in Start Bay.

To conduct this analysis, deepwater, nearshore (35 m depth), and breaking wave parameters were computed from the WWIII data, including wave height, period, and direction, wave energy and power, the alongshore component of wave power, the alongshore and cross-shore components of wave energy flux, wave length, and the dimensionless fall velocity (Gourlay, 1968; Dean, 1973) and surf-similarity (Bauer and Greenwood, 1988) parameters. The time series of each parameter was tested for correlation against the temporal signal of the EOF in Figure 5-12 (lower panel).

The strongest correlation to the dominant EOF came from the alongshore component of wave power, P_y, derived from breaking wave heights and directions (Loureiro *et al.*, 2012) computed using the formulae of Larson *et al*. (2010), assuming a shoreline orientation of 100° from north. The instantaneous values of alongshore wave power themselves did not yield a strong correlation, but when the cumulative integral of the de-meaned signal was tested, a highly significant and strong correlation, R = 0.94, was achieved (Figure 5-13, left panel). This manifestation of the alongshore wave power assumes that the beach volume is in a state of equilibrium when alongshore wave power is at its mean value (Fairley *et al.*, 2009). Deviations from the mean alongshore wave power are therefore assumed to promote deviations from the equilibrium (mean) beach condition. To reflect that wave conditions have a cumulative rather than instantaneous effect on the beach, the cumulative integral is used:

$$P_{y,CI}(n) = \int_{t_0}^{t_n} \left(\overline{P_y} - P_y\right) dt \qquad (2)$$

where t_0 is the start of the time series, and $P_{y,CI}(n)$ denotes the cumulative integral up to time-step t_n.

Upwards (downwards) gradients in $P_{y,CI}$ (Figure 5-13, left panel) result from extended periods of waves arriving obliquely from the south (north), and steeper gradients result from greater incident wave power. The same pattern is seen in both the EOF temporal coefficient and the time series of $P_{y,CI}$, and the significant morphological changes that occurred during the 2013/2014 winter are well captured by the time series of $P_{y,CI}$. The strong relationship between the dominant EOF and $P_{y,CI}$ confirms that alongshore sediment transport and beach rotation are highly related to the magnitude and direction of the incident wave power, and that it is the cumulative effects of powerful waves arriving obliquely from the south (north) that drives sediment transport and beach rotation to the north (south) at Slapton Sands. As the beaches in Start Bay act as an interconnected sediment system, it is likely that this relationship is relevant to Hallsands, Beesands, and Blackpool Sands, as well as Slapton Sands.

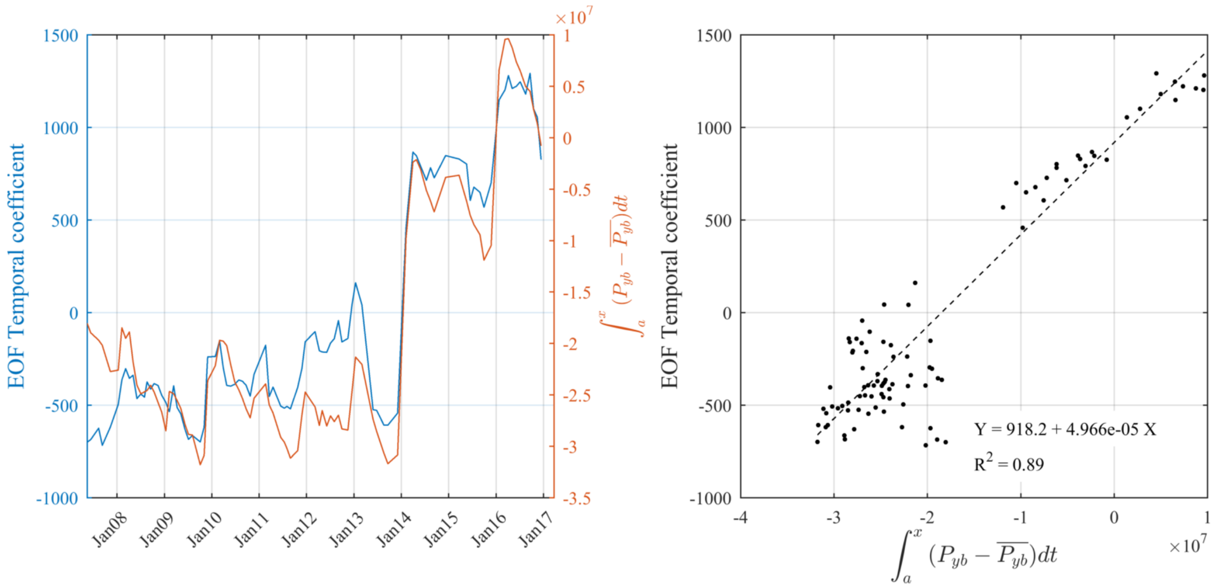

Figure 5-13. Left panel: Comparison between the dominant EOF mode temporal signal (left y-axis) and the time series of the cumulative integral of the de-meaned alongshore wave power (right y-axis). Right panel: comparison of respective data points from the two time-series, fitted with a robust linear model (dashed line).

5.5.3. Hindcasting Beach Morphology

A linear model was fitted to the forcing relationship described in Section 5.5.2, which is capable of explaining approximately 90% of the variance in the EOF signal (Figure 5-13, left panel). This model was then applied to the entire time series of alongshore wave power from the 37-year Met Office WWIII wave hindcast, allowing for changes in beach volume over the last 37 years to be hindcast (Figure 5-14). This provides a novel insight into the state of Slapton Sands over a longer time period, even in the absence of measured topographic data[3]. The hindcast time series in Figure 5-14 reveals a number of interesting events that have occurred since 1980:

1. For a significant period, between 1980 and 2004, it is suggested that Slapton Sands was rotated towards the north, similar to the present beach configuration. Over this period, the north end of Slapton Sands had a higher than average volume of sediment, while the middle and south of the beach had a lower than average volume of sediment.
2. Between 2003 and 2007 there were very few significant southerly wave events, and the dominance of easterly waves would have rotated the beach back towards the south.
3. Between 2007 and 2014 the south end of the beach had more sediment than average, while the north of the beach had less sediment than average. During this time, powerful southerly wave events intermittently returned the beach back to its mean position, but overall southerly rotation dominated this period.
4. Powerful southerly waves over the 2013/2014 winter rotated the beach strongly back towards the north, and further southerly waves in 2016 caused further northward rotation.
5. Despite some subsequent recovery, since 2016 the beach has had more sediment in the north, and less sediment in the middle and south, than at any other time since 1980.

The reconstruction of historic beach volumes in Figure 5-15 from the product of the spatial and temporal EOF signal indicates that, on average, during a winter of southerly waves around 50 m^3/m of gravel is gained (lost) in the north (middle and south). Intervening easterly waves move approximately the same volume of sediment, but over longer time spans. During more extreme events, greater volumes of sediment are gained or lost; for instance, during the dominant period of easterly waves in 2003 – 2007, around 150 m^3/m of gravel was gained (lost) at the profiles in the middle and south (north), and during the 2013/2014 winter, 150 m^3/m of gravel was gained (lost) at the profiles in the north (middle and south). However, even when the beach was rotated southward between 2007 and 2014, the middle and south of the beach had, at most, only 50 m^3/m of gravel more than the average volume. In comparison, the north of the beach had almost 150 m^3/m of gravel more than average by 2016.

[3] This model could also be used to forecast beach volumes along the length of Slapton Sands up to a week into the future, using operational wave forecast data. Such a model could provide a real-time warning if parts of Slapton Sands were to reach critically low levels of sediment, which could help coastal managers to mitigate against storm impacts. However, development of such an operational tool is beyond the scope of the present study.

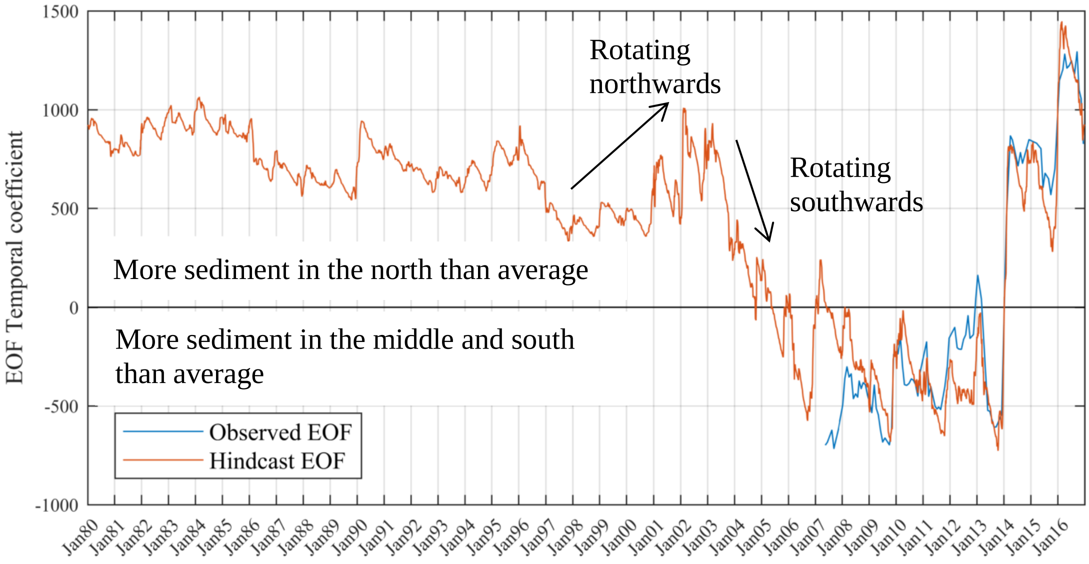

Figure 5-14. Hindcast prediction of the dominant EOF mode temporal signal since 1980. The hindcast was generated using the robust linear model in Figure 5-13, fitted to the cumulative integral of the de-meaned alongshore wave power from the 37-year Met Office WWIII hindcast.

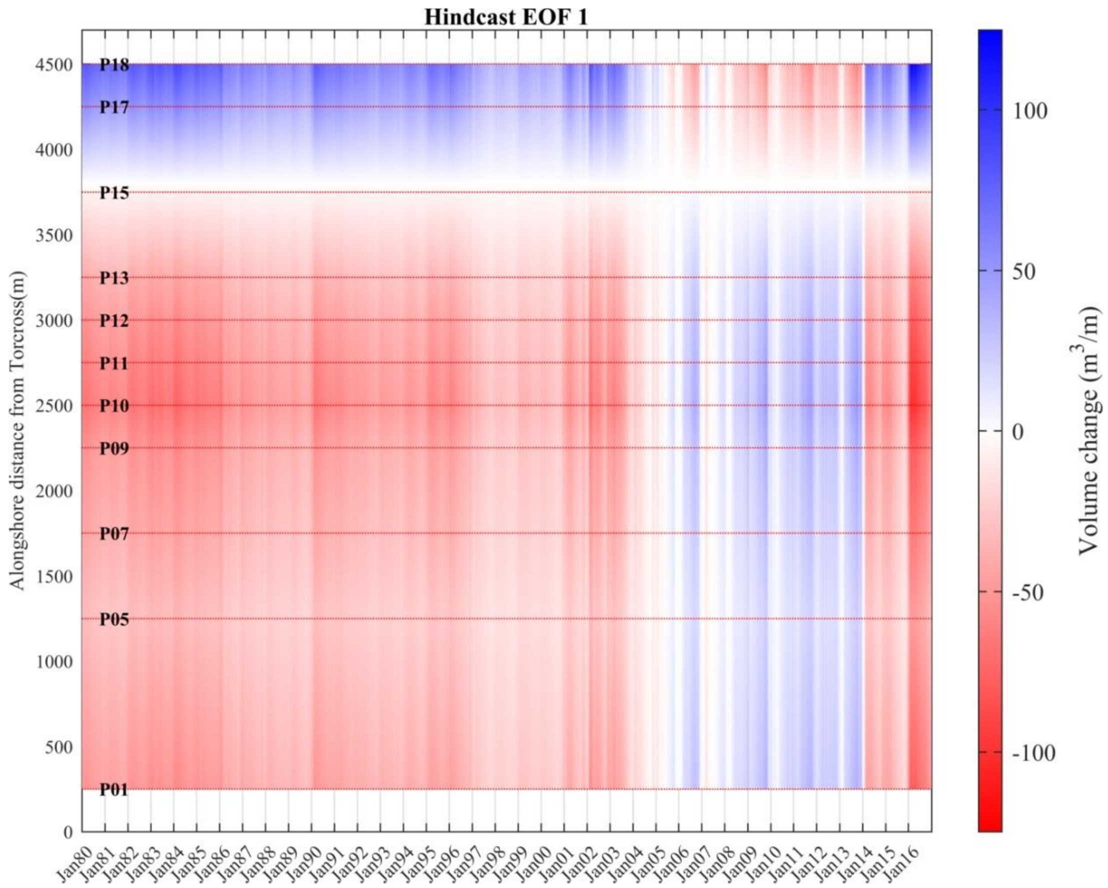

Figure 5-15. Reconstruction of the dominant changes in beach volume along Slapton Sands since 1980, from the product of the spatial EOF pattern shown in Figure 5-12 and the hindcast temporal EOF signal shown in Figure 5-14. Areas of red and blue show lesser and greater volumes of sediment, respectively, compared to the mean volume at that position along the beach. The alongshore position of the monitored profiles are shown as red dotted lines, and their geographic location is shown in Figure 2-3.

5.6. Alongshore Transport Rates

Previous assessments of alongshore transport rates in Start Bay (including the Shoreline Management Plan of 1998, and the Slapton Coastal Zone Management Study of 2004) have suffered from a lack of subtidal (i.e. bathymetric) information, as they only considered the intertidal changes that occurred. Net alongshore sediment transport within Start Bay was recently assessed by Wiggins *et al.* (2017) over the summer 2013 to summer 2016 period, including the contribution from intertidal changes (from topographic surveys) and subtidal changes (from bathymetric surveys). Figure 5-16 and Figure 5-17 show the results of this assessment.

The embayment-wide beach rotation described in Section 5.3.3 is clearly visible from the plot of elevation difference between the 2013 survey and the 2016 survey (Figure 5-16). The vast majority of the sediment re-distribution over this period occurred between -5 m ODN and + 5 m ODN, with very little change in the profiles occurring below -5 m ODN depth (approximately 100 – 200 m offshore). Additionally, very little opposing cross-shore erosion/accretion is visible in Figure 5-16, indicating that nearly all of the sediment redistribution that occurred within Start Bay was due to alongshore, rather than cross-shore, sediment transport.

The extreme winter of 2013/2014 provided the most energetic sequence of wave conditions to have occurred in at least the last 65 years (Masselink *et al.*, 2015), and the sediment fluxes that occurred over that period, shown in Figure 5-17, provide some proxy for the net transport rate that resulted from that sequence of storms. Figure 5-17 indicates that, between 2013 and 2014, 741,500 m^3 of erosion occurred along Start Bay, while 747,600 m^3 of accretion was observed. As the difference between these two values is within the error bounds of the estimates, it can be concluded that the amount of sediment eroded was perfectly balanced by the amount of sediment deposited elsewhere within the bay, indicating that no sediment was lost from the system during that time. Start Bay can therefore be considered a closed sediment cell.

The survey data from which these values were calculated were collected in the summer of 2013 and the summer of 2014, but it is expected that the vast majority of the total sediment transport occurred over the 5-month period between 25/10/2013 and 31/03/2014, when 22 significant storm events with deepwater H_s > 4.5 m occurred (Masselink *et al.*, 2016). Therefore, over this 5-month period, the total volume of sediment transported northward can be estimated as approximately 745,000 m^3. This observed transport rate is far greater than the average alongshore transport rate of 150,000 m^3 per annum estimated by Chadwick *et al*. (2005) prior to the winter of 2013/2014.

Assuming that all the observed change was due to alongshore processes and occurred during the 22 storms (approximately 26 days in total), the average alongshore transport rate equates to 28,654 m^3 per day, equivalent to around 48,000 metric tonnes of gravel per day. Although the transport rate would have differed during individual storms, this provides some estimate of the maximum alongshore transport rate likely to occur in Start Bay, given the magnitude and return period of the storms experienced during that time. We therefore conclude that, for all practical purposes, Start Bay can be considered a closed sediment cell, with maximum alongshore transport rates on the order of 28,654 m^3 of gravel per day during extreme storm events.

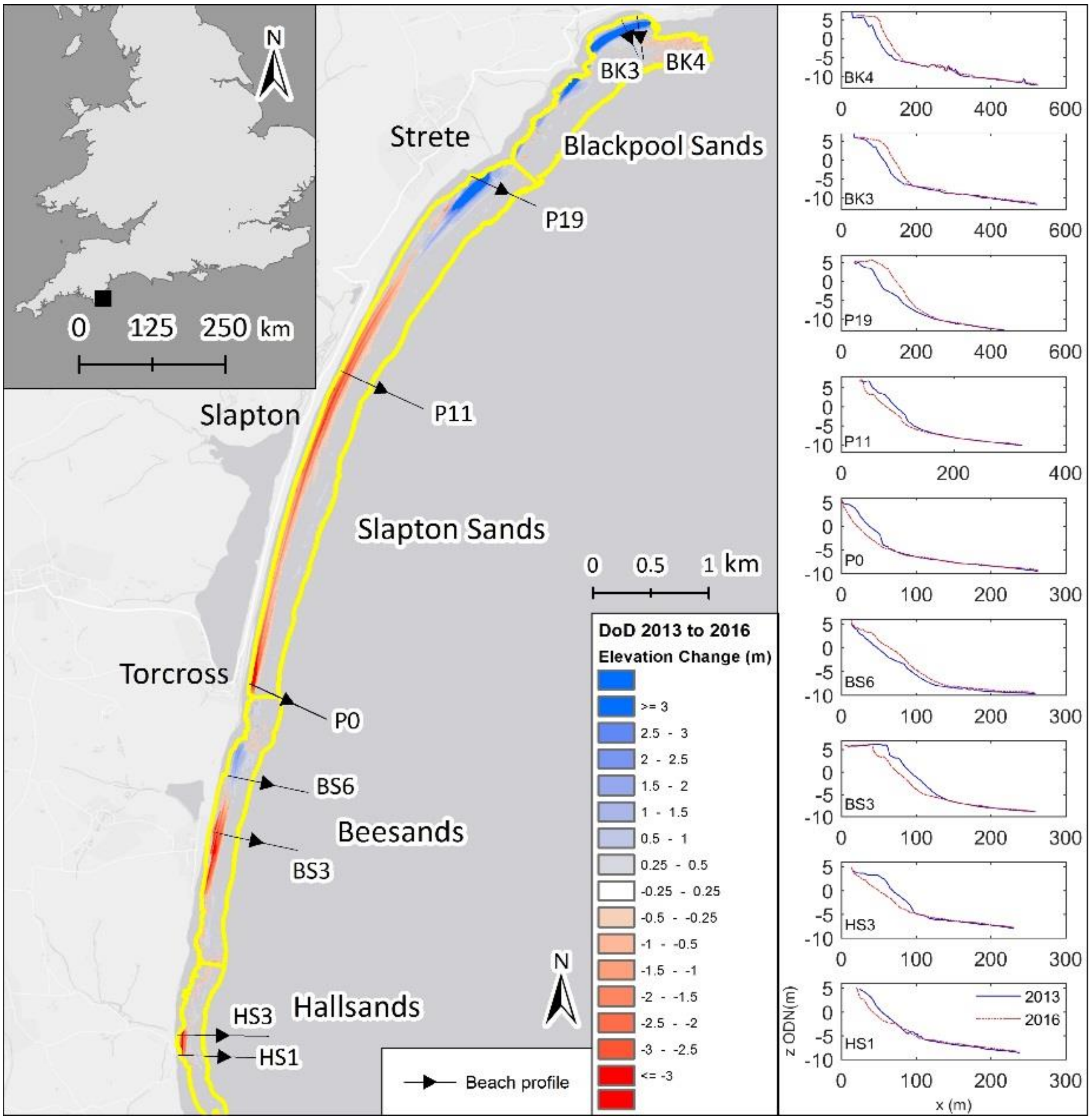

Figure 5-16. Left: Digital elevation model of difference of Start Bay from 2013 to 2016, including subaerial and subtidal extents. Right: Subaerial to subtidal Profiles extracted from digital elevation models, from 2013 (red) and 2016 (blue). Figure from Wiggins *et al.* (2017).

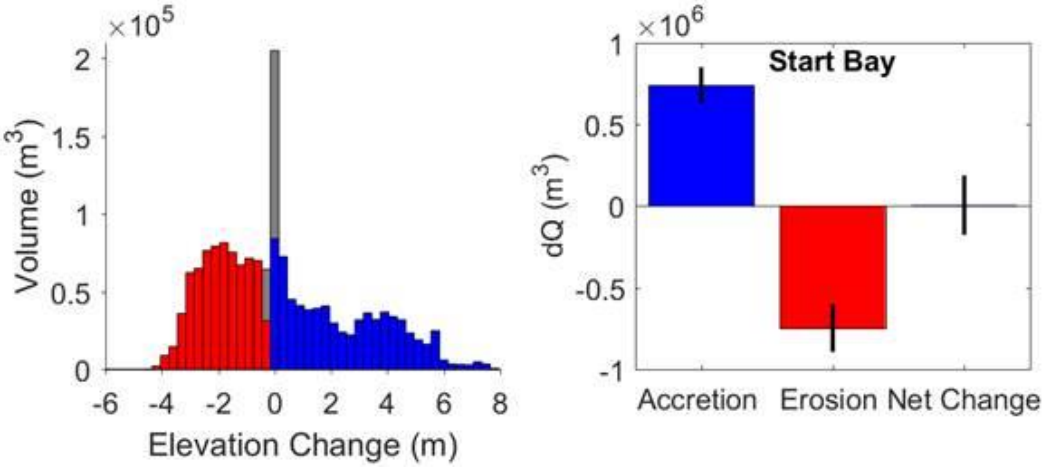

Figure 5-17. Total observed sediment gains and losses in Start Bay between summer 2013 and summer 2014 (From Wiggins *et al*. (in preparation)). 741,500 m^3 of erosion was observed Vs 747,600 m^3 of accretion along the length of Start Bay. The net amount of change is within the error bars (black lines in the right panel) of the estimates, indicating that no sediment was lost from Start Bay over this period. The grey bar in the left panel represents the observed changes that are considered to be within the error bounds of the instruments used to collect the data.

5.7. Medium-Term Climate 'Cycles'

The importance of medium-term beach rotation in governing the coastal dynamics in Start Bay is evident, but this knowledge and understanding is of most use if we are able to predict the medium-term variability in the wave conditions, especially due to climate change. Although it has been possible in this report to hindcast beach morphology 37 years into the past, it is not currently possible to confidently predict wave conditions more than a few days into the future, so it is impossible to accurately forecast how Slapton Sands will change due to variations in alongshore wave power far into the future.

However, some advances have been made through cross-correlating offshore wave conditions at Start Bay, in particular southwesterly and easterly wave power, to climate indices such as NAO (North Atlantic Oscillation; Hurrell *et al.* (2001)) and WEPA (West Europe Pressure Anomaly; Castelle *et al.* (2017). These climate indices quantify the large-scale atmospheric pressure distribution across the eastern Atlantic (Figure 5-18), which in turn controls the strength of the westerly wind field and the latitudinal location of the extra-tropical storm tracks. Negative NAO, which blocks strong westerly Atlantic storm tracks, increases the occurrence of easterly winds and wind waves arriving at Start Bay. Conversely, positive WEPA is associated with an enhancement of westerly storm tracks directly approaching the western coast of Europe, and therefore relates to south-southwesterly waves arriving at Start Bay.

Winter (DJFM) average values of NAO and WEPA were compared with winter average values of wave power (computed from the Met Office WWIII data) from the east, and wave power from the south-southwest (referred to as west in Figure 5-19). Winter NAO is significantly and negatively correlated with wave power from the east (r = -0.64), but is not correlated with wave power from the south-southwest. Conversely, winter average values of WEPA are significantly and positively correlated with wave power from the south-southwest (r = 0.79), but not with wave power from the east (Figure 5-19).

In the last 30 years, there has been a 75% reduction in the 10-year averaged activity of easterly storms with H_s greater than 2.5 m arriving at Start Bay (Scott *et al.*, 2016). In contrast, southerly storm activity stayed relatively constant over that period (Figure 5-20). Easterlies contributed approximately 30% of the east/south balance of storm waves during the 1950s to 1980s, and then dropped to less than 10% after 1990. As previously indicated this is directly related to shifts in the distribution of atmospheric pressure and resulting storm tracks across the Atlantic Ocean, with easterly storm conditions only developing during periods of negative NAO (Figure 5-19), which have declined in the last 30 years.

Medium-term modulation of the balance between southwesterly and easterly storm waves, and the alongshore wave power that controls beach rotation at Slapton Sands, are therefore related to time series of NAO and WEPA (Figure 5-19), suggesting, perhaps, that these medium-term atmospheric cycles could be used to predict beach rotation cycles into the future (Wiggins *et al.*, 2017). However, as current understanding about NAO and WEPA cycles is limited, this would carry a large degree of uncertainty, and is not attempted in this report. It does, however, represent a step change in our understanding of medium-term morphological forcing, and may provide a potential avenue for predicting medium-term beach rotation in Start Bay in the future, as the Met Office now have the ability to forecast NAO up to a year ahead, with some level of skill (Dunstone *et al.*, 2016).

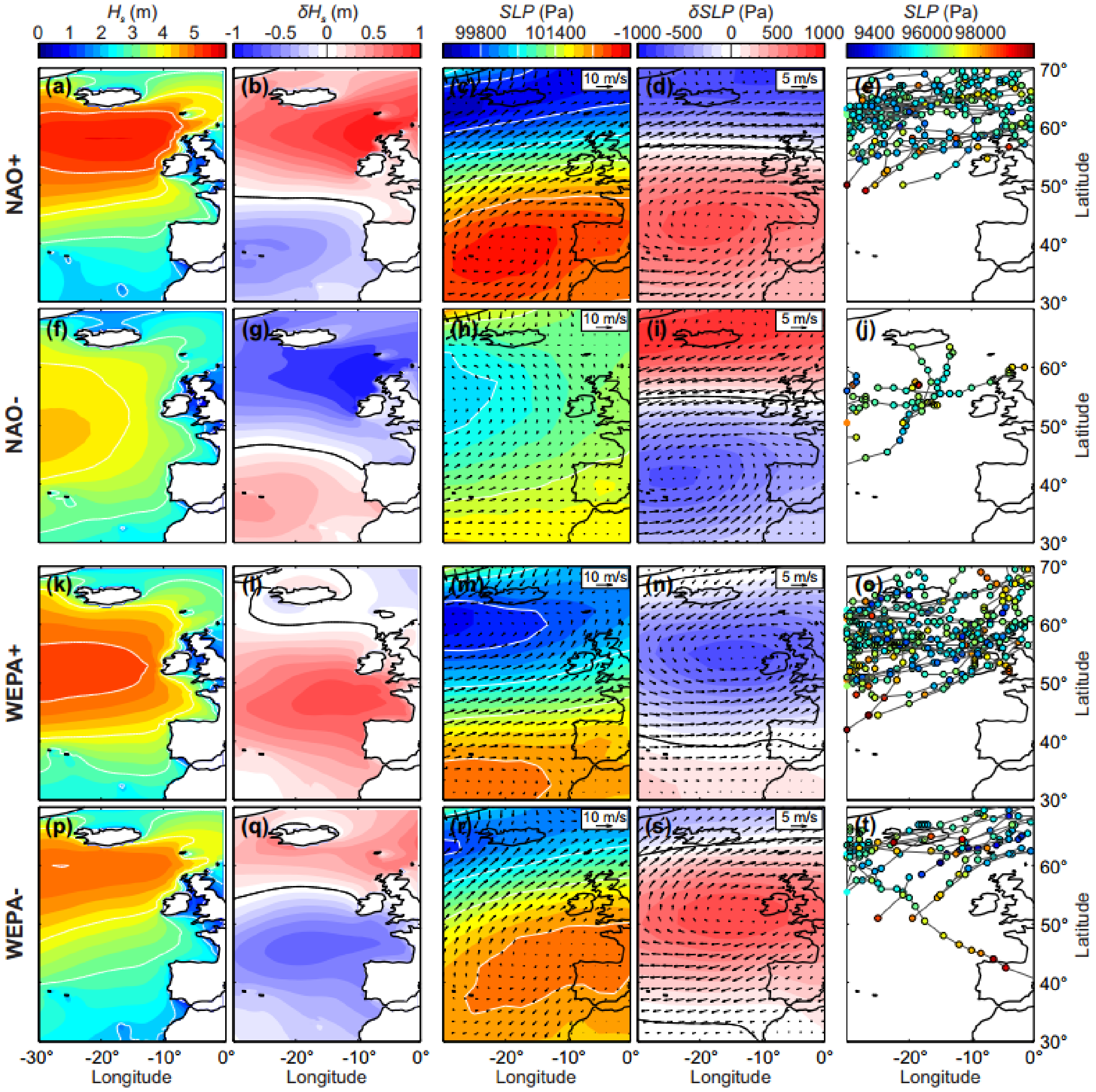

Figure 5-18. Influence of the NAO and WEPA indices on winter-averaged H_s, sea level pressure (SLP), and wind velocity at 10 m elevation ($\vec{u}10$), with positive phase and negative phase of each index addressed by averaging the 5 years with the largest and smallest index values over 1950–2016, respectively. (a, f, k, and p) winter-averaged Hs; (b, g, l, and q) corresponding anomaly; (c, h, m, and r) winter-averaged SLP with superimposed $\vec{u}10$ field; (d, i, n, and s) corresponding anomaly; (e, j, o, and t) superimposed storm tracks over the 5 years with the colored circles indicating the sea level pressure at the center of the low-pressure system every 6 h. Note that for clarity and to focus on the more severe storms, only identified storms that have a low-pressure center deeper than 96,000 Pa are plotted. By order of decreasing importance, the five winter years considered for each index phase are NAO+ (2015, 1989, 1995, 2012, and 2000); NAO− (2010, 1964, 1969, 1963, and 1977); WEPA+ (2014, 1994, 2001, 2016, and 1977); WEPA− (1992, 1953, 2005, 1976, and 1993), where, for instance, 1977 means the DJFM 1976/1977 winter. Figure modified from Castelle *et al*. (2017).

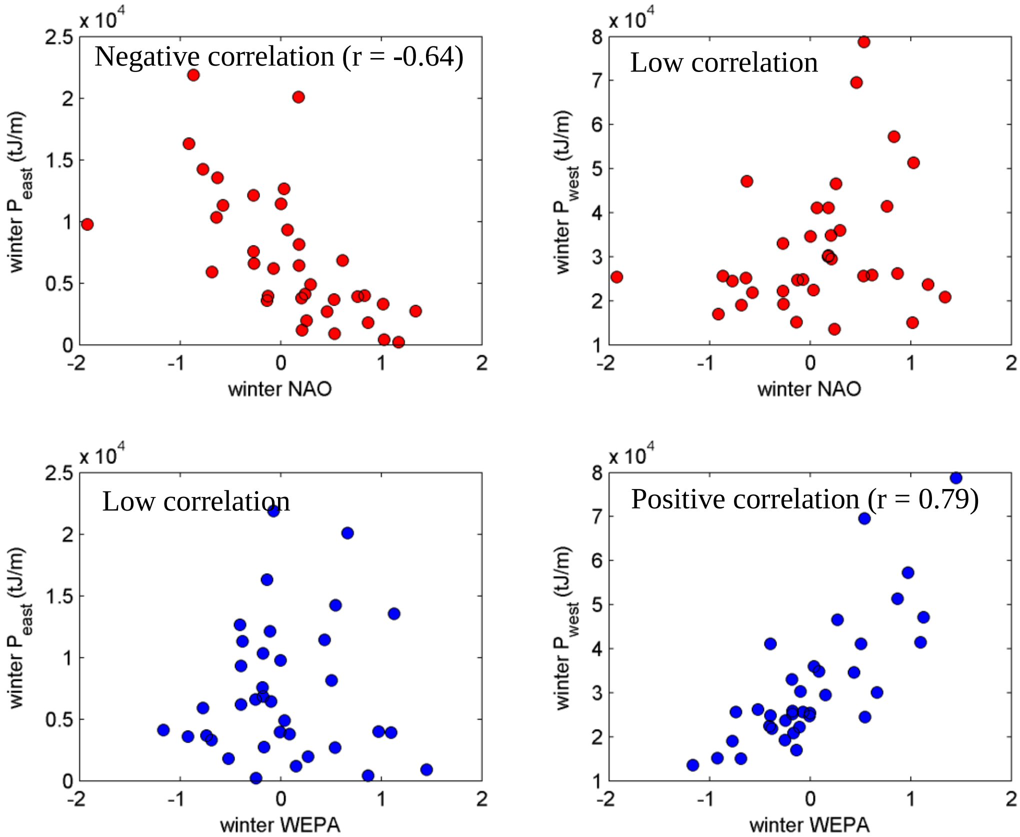

Figure 5-19. Upper panels: Scatter plots of winter (DJFM) average NAO versus deep water wave power from the east (upper-left) and from the south-southwest (upper-right). Lower panels: Scatter plots of winter average WEPA versus deep water wave power from the east (lower-left panel) and from the south-southwest (lower-right panel).

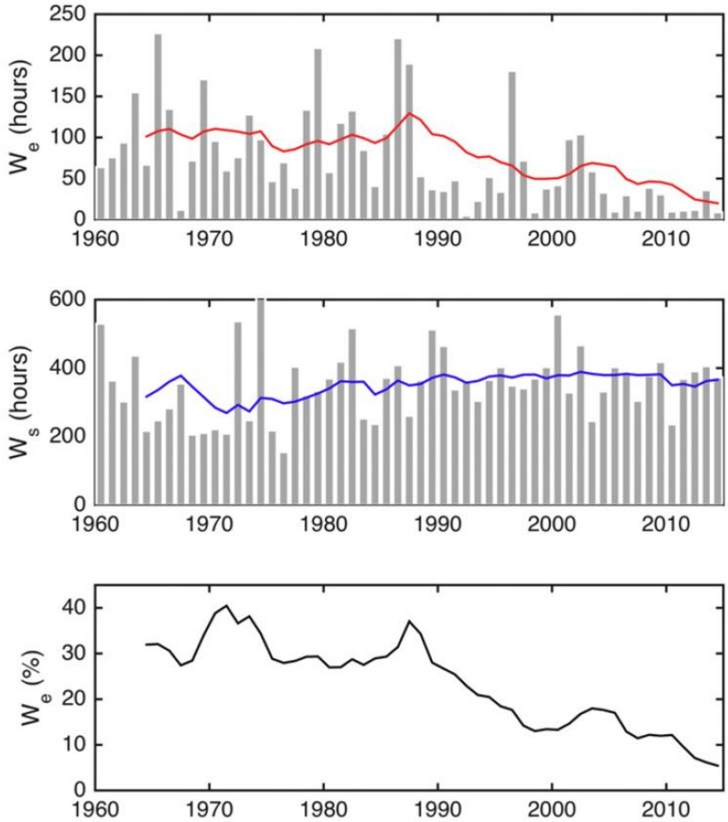

Figure 5-20. Long term contribution of east and south storms at Start bay (from Scott *et al.*, 2016). Upper panels show histograms of hourly frequency of easterly (W_e) and southerly (W_s) wave events with $H_s > 2.5$ m in grey with the red and blue lines indicting the 10-year moving average (backwards-looking) for easterly and southerly events, respectively. Wave heights are calculated from local wind records using the SMB method (US Army Corps Of Engineers, 1984). The lower panel shows the percentage contribution of 10-year average W_e to the W_s/W_e balance.

6. Short-Term Morphological Processes: Storm Response

6.1. Introduction

This section provides an overview of the coastal processes affecting the shoreline and beach morphology of Blackpool Sands, Slapton Sands, Beesands, and Hallsands over short time-scales (hours – days). The information presented draws from existing literature as well as the new analyses of beach volumes undertaken in Sections 5.3 to 5.5 of this report, to provide comment on the vulnerability of beaches in Start Bay to storm impacts. This provides an update to Chapter 11 of the SCZMS (Scott Wilson, 2006), which identified areas of Slapton Sands vulnerable to storm erosion, and additionally identifies vulnerable areas at Blackpool Sands, Hallsands, and Beesands.

6.2. Alongshore and Cross-Shore Processes

Over short time-scales (hours – days), the key coastal processes affecting Start Bay relate to storms. Storms incur coastal changes through the action of energetic waves eroding and transporting sediment within the bay, and/or causing wave run-up and overwashing. Locally generated storms can additionally super-elevate sea-levels through storm surge.

The cumulative effects of alongshore sediment transport, especially during sequences of energetic storm conditions, drives the medium-term net clockwise beach rotation described in Section 5. Therefore, the medium-term alongshore redistribution of sediment in Start Bay is, for a large part, related to a number of short-term alongshore contributions from energetic storm waves. However, cross-shore sediment transport during storms also occurs (de Alegria-Arzaburu and Masselink, 2010), with onshore transport across the top of the beach driven by overwash, and offshore sediment transport across the lower part of the beach due to bed return flow and/or powerful backwashes. Offshore transport is lower than the amount of onshore transport, as the energy of the wave backwash is absorbed as water infiltrates into the barrier (seepage); the net effect means that onshore migration of the barrier through overwashing is an inevitable response to storm waves (Carter and Orford, 1984), and drives the long-term barrier roll-back described in Section 4 when overwash occurs.

Overwash is perhaps the most important cross-shore sediment transport process occurring at gravel barriers like Slapton Sands. When overwash occurs as a result of wave run-up, there is no mechanism to return sediment that has been washed over to the leeward side of the barrier back to the seaward side of the barrier, and post-storm recovery is therefore impossible (Scott *et al.*, 2016). Powerful storm waves arriving perpendicular to the coast at Start Bay therefore have the greatest potential to influence the long-term development of Slapton barrier, as they can incur irreversible changes to the barrier through overwashing of sediment (Carter and Orford, 1984). Oblique waves can also result in overwash, however, as significant volumes of gravel were washed over Slapton Barrier and across the A379 road during powerful southerly waves of the 2013/2014 winter (Figure 6-2).

6.3. Response to Southerly Vs Easterly Storms

Scott *et al*. (2016) identified that, in southwest England, the response of beaches to the extremely energetic storms of the 2013/2014 winter differed greatly at sites exposed to the westerly Atlantic wave approach, compared to sites that were semi-sheltered from it. Exposed sandy beaches (for example Perranporth, north Cornwall coast) experienced cross-shore sediment transport, with significant losses of sediment offshore from the intertidal zone (> 200 m^3/m). Exposed gravel beaches (for example Loe Bar, south Cornwall coast) experienced significant overwashing and landward loss of sediment from the beach/barrier. In contrast, beaches that were semi-sheltered from the westerly storms, such as those in Start Bay, experienced a rotational response due to alongshore sediment redistribution. The powerful westerly storm waves were refracted to a southerly direction as they entered Start Bay, and promoted significant northward beach rotation (Section 5) which Scott *et al*. (2016) argue will require multiple years of energetic easterly wave conditions to recover from. Indeed, recovery has not yet occurred and the beach has been rotated further northward by subsequent southerly storm waves in 2016.

The occurrence of easterly and southerly storm events not only controls the short and medium-term alongshore transport of sediment in Start Bay, but also influences cross-shore sediment transport processes. Opposing modes of cross-shore sediment exchange from southerly and easterly wave events were observed at Slapton Sands (Figure 6-1) by de Alegria-Arzaburu and Masselink (2010), where southerly events were seen to promote accretion of the upper beach and erosion of the lower beach (beach steepening), while easterly events were seen to erode the upper beach and accrete the lower beach (beach flattening). These opposing responses are a result of steep, short period storm waves from the east eroding and flattening the beach profile, and lower energy, longer period waves from the south acting to steepen the profile (de Alegria-Arzaburu and Masselink, 2010).

The most significant erosion at the beaches in Start Bay is likely to occur due to the sequential action of southerly and easterly wave conditions. As was previously shown, southerly waves have the potential to drive significant alongshore sediment transport to the north (beach rotation), and while easterly waves can also drive alongshore transport (to the south), their greatest impact is likely to come from their ability to erode the beach profile due to their steep, short-period nature (Section 3.1).

The combination of these two processes can have a significant effect on the vulnerability of the coastline in Start Bay. An example of this is the storm of 2001, during which part of the A379 road around the location of P10 to P13 (Figure 2-3) was undermined by powerful, but not exceptional, storm waves from the east. Chadwick *et al*. (2005) propose that the undermining of the road was not due to the magnitude of the storm waves alone, or even the combined effect of the waves and water level (which had a joint return period of around 1-in-25 years), but was in fact due to shoreline recession caused by alongshore transport from southerly waves over the preceding autumn (Figure 5-10). This created a vulnerable stretch of the beach and made it possible for the easterly storm waves in 2001, which lasted four days, to cut the crest of the profile back to the location of the road. The barrier was not breached (Chadwick *et al.*, 2005), but the barrier would have been highly vulnerable to overwashing, and potentially to breaching, following that series of events.

6.4. Vulnerability to Storm Impacts

From the erosional hot-spots identified in Section 5.4 it can be concluded that the most vulnerable/ least resilient sections of coast in Start Bay to storm impacts are at the south of Hallsands beach and at the south of Slapton Sands in front of Torcross village, due to their low sediment volumes and long term erosional trend. However, all of the hot-spots listed in Section 5.4 are severely vulnerable to coastal erosion and storm impacts. In contrast, profiles at the north of Slapton Sands (P15 – P19) are the least vulnerable to coastal erosion, having had at least 400 m^3/m, and at most 900 m^3/m, of sediment at any moment over the last 10 years, and are therefore, currently, the most resilient to storm impacts.

The middle of Slapton Sands (P8 – P11) has experienced greater net erosion than any other part of the beach over the last 10 years (Figure 5-7), it experienced the most significant overwash and erosion during the 2013/2014 winter (Figure 6-2 and Figure 6-3), and is adjacent to the location of the 2001 road collapse. This is likely to be a result of the highly dynamic nature of that section of Slapton Sands. The EOF results in Figure 5-12 show that, during rotational events, the greatest variance along Slapton Sands occurred around P10, meaning that when the beach is rotated towards the north, as it presently is, the middle of the beach has less sediment volume than any other part of the beach, compared to average profile volumes. This section of the beach, where the road was realigned following the 2001 storm, has previously been demonstrated to have the highest variance in the shoreline (de Alegría-Arzaburu *et al.*, 2010), and was identified as an erosional hot-spot based on the assessment of sediment volumes (Section 5.4). It can be concluded that this section of the Slapton Barrier (and the A379 road) is the most vulnerable to overwashing of sediment, and to potential future undermining of the road, or even breaching of the barrier.

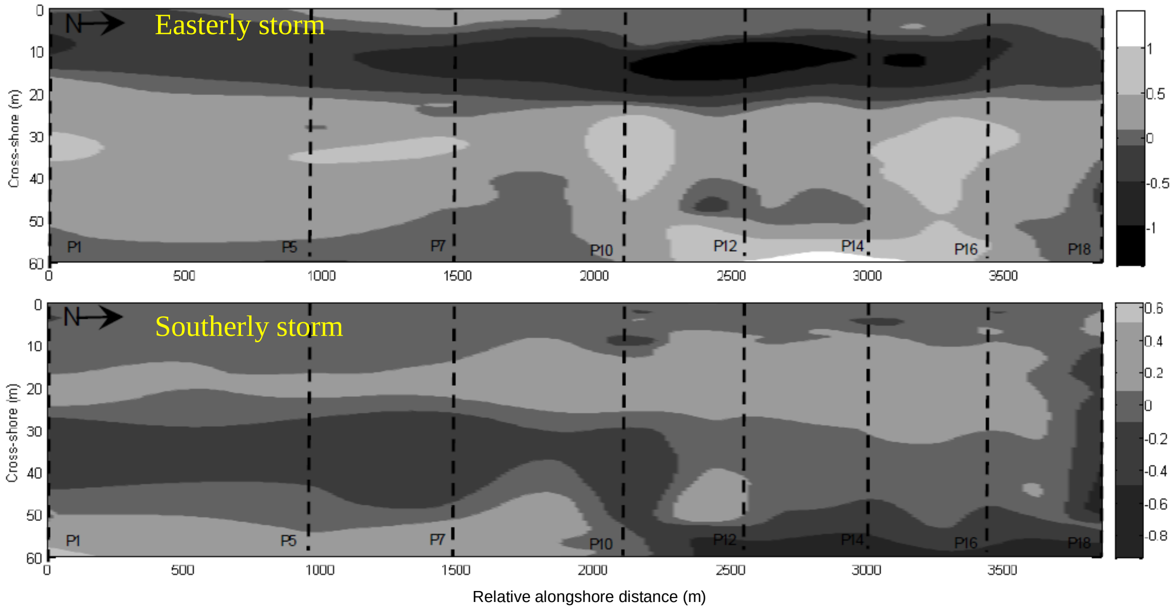

Figure 6-1. Opposing cross-shore morphological response at Slapton Sands to an easterly storm in April 2008 (upper panel) and a southerly storm in January 2009 (lower panel). Elevation change is shown in meters, with darker and lighter colours representing erosion and accretion, respectively. Figure modified from de Alegria-Arzaburu et al. (2010).

Figure 6-2. Example of overwash at Slapton Sands (from Scott *et al.*, 2016). The A379 road became covered with gravel due to overwash occurring during the significant storm 'Petra' on 5 February 2014, and the 'Valentine's Day' storm on 14 February 2014 (http://www.bbc.co.uk/news/uk-26064424).

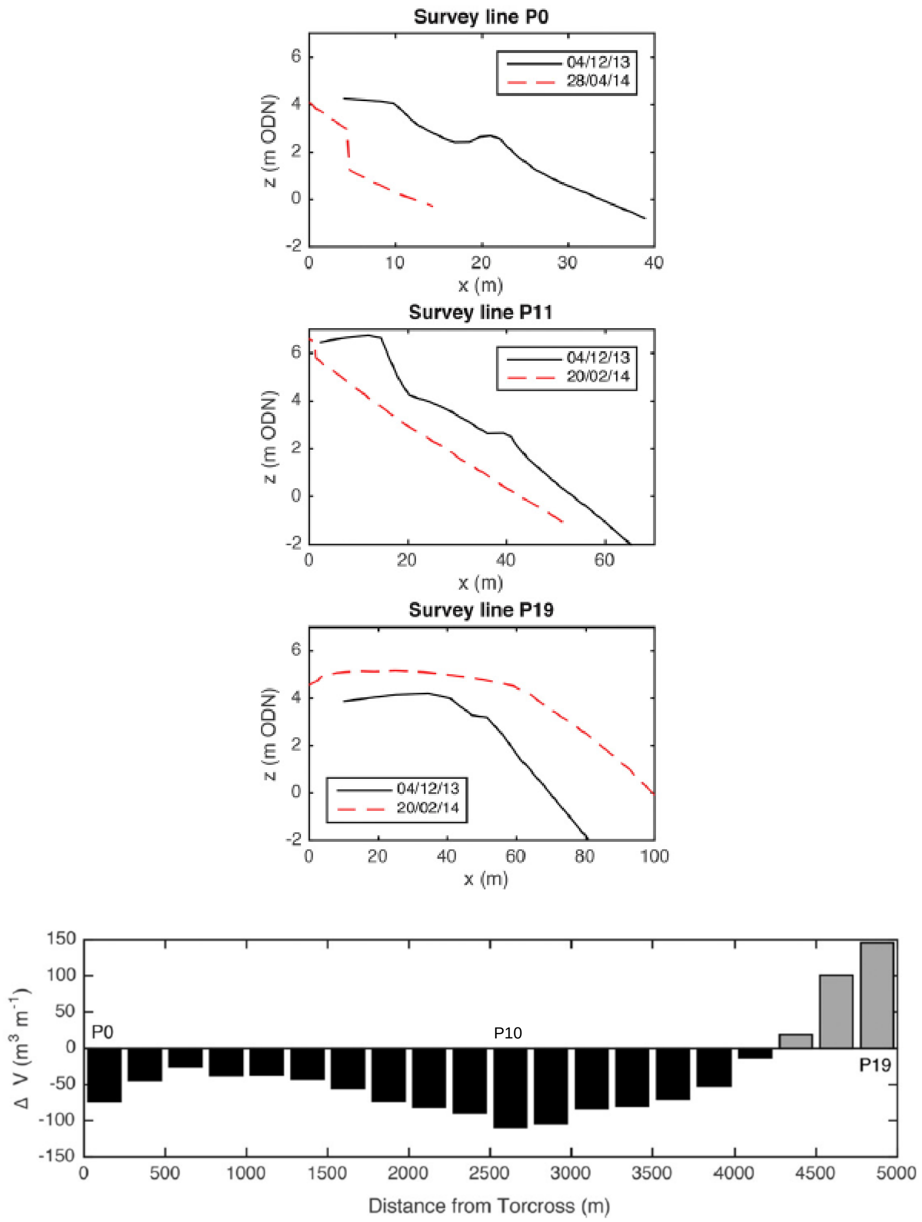

Figure 6-3. Storm impacts on Slapton Sands during the 2013/2014 winter season (modified from Scott *et al*., 2016). The upper panel shows the cross-shore morphological response for selected locations along the beach. The lower panel shows the alongshore distribution of the intertidal beach volumetric change ΔV, above -2 m ODN.

7. Conceptual Model

In this report, coastal processes and morphological change acting over three key time-scales (long-term, medium-term, and short-term) in Start Bay have been examined, with a detailed focus on Slapton Sands. In this section of the report, the findings from the previous sections are synthesised to provide a coherent conceptual model of the key coastal processes occurring. This provides an update to the conceptual beach process model developed in Chapter 11 of the SCZM (Scott Wilson, 2006). Table 7-1 presents the complex interactions occurring between these processes, which can be summarised as follows:

- Over long time-scales, relative sea-level rise gradually increases the vertical reach of waves; this increasingly allows for short-term events (storm waves) to cut-back the upper beach profile and for wave run-up to overtop/overwash the crest of the beach.
- Meanwhile, alongshore-oriented waves cause beach rotation over medium time-scales, which intermittently reduces the sediment volume along certain stretches of Start Bay. Those sections are then vulnerable to short-term wave attack and overwashing.
- Short-term storm wave attack results in vulnerable sections of Start Bay being cut-back even further, and allows wave run-up to overtop and overwash sections of the beaches.
- These episodic, short time-scale overwashing events are the mechanism for long-term barrier roll-back, and allow the barrier to retreat in response to sea level rise.
- Eventually, the decreasing cross-sectional area of Slapton barrier, caused by the lengthening of the shoreline as it retreats, will make the barrier increasingly vulnerable to breaching. Once significant breaching occurs, the barrier could begin to break down into a series of tidal inlets.

Because of the decreasing trend in easterly storm waves over the last 30 years or more, alongshore sediment transport to the south is becoming less prevalent. This means that the southern part of Start Bay (between Hallsands and Strete) is suffering from a gradually decreasing sediment supply from the north, and is increasingly vulnerable to storm wave attack, overtopping, and barrier retreat.

These interacting coastal processes cause a number of coastal management challenges. In the short-term, storm wave attack is the main concern to coastal management, as this can cause coastal flooding and undermining of the A379 road, storm defences, and other engineered structures. Over medium time-scales, the alongshore supply of sediment and resulting vulnerability of the different sections of Start Bay is a concern for coastal management. Over the long-term, the retreat of Slapton barrier will potentially expose Torcross village to the sea, and will require consideration to be given to the future of the Slapton line section of the A379 road. This may involve gradual realignment, to maintain the roads position on the barrier, or eventually to complete re-routing or re-engineering of the road in the extreme case of barrier breakdown.

Table 7-1. Conceptual model of key coastal processes and related management challenges in Start Bay

Time-scale		Forcing	Beach response	Coastal management challenges
Increasing time-scale	**Long term (decades-centuries)**	Relative sea-level rise	Barrier breaching and breakdown Barrier roll-back/shoreline recession	• Realignment/ re-engineering of Slapton line • Exposure of Torcross
	Medium term (weeks-years)	Alongshore-oriented wave power	Beach rotation	• Spatially and temporally varying sediment supply along Start Bay • Temporally varying vulnerability of different sections of Start Bay
	Short term (hours-days)	Storm wave run-up	Profile cut-back/ wave overwashing	• Gravel deposition on A379 • Undermining of A379 and other engineered structures • Wave overtopping and coastal flooding

7.1. Uncertainties in Coastal Process Understanding

Conceptually, short-term, medium-term, and long-term coastal processes in Start Bay are relatively well understood. There is little uncertainty about which are the key processes acting on the beaches and barrier, where these processes are having the greatest effect, or, conceptually, how the processes will interact over the long-term to shape the future coastline. Since the SCZMS (Scott Wilson, 2006), there is now far better understanding of the mechanisms leading to rotation of Slapton Sands in response to the bi-directional wave climate (Section 5.5.2), and the large scale atmospheric causes of the net trend in northward sediment transport (Section 5.7). Since the Environment Agency's State of the Nation project (HR Wallingford, 2015), the joint distribution of extreme wave and water level events in Start Bay is also now far better quantified than ever before (Section 3.6).

There is, however, uncertainty in the effect that different wave and water level combinations would have on beach/barrier morphology and coastal flooding. This uncertainty can now largely be circumvented through computer modelling, as there have been recent advances in modelling hydro- and morphodynamics on gravel beaches with the development of the model XBeach-G (McCall *et al.*, 2014), and such modelling is described in Section 7.2 of this report. There is even greater uncertainty in predicting when significant events will occur, or what magnitude and sequence of hydrodynamic forcing would be required to cause significant coastal change. These uncertainties originate from a number of sources:

- Future emission levels are unknown, and there is therefore uncertainty in predicting the future rate of sea level rise (Section 3.7) and barrier retreat (Section 4).
- The timing and sequencing of future storm wave events is unknown, and therefore the resulting beach configuration cannot yet be predicted into the future.
- Increasing storminess due to climate change is not well understood, and the effect that this will have on the probability (return period) of extreme storm waves is presently unclear.
- It is very unclear how climate change will affect Atlantic weather system and thus NAO and WEPA, which we now understand to be critically important in driving storms in Start Bay.

There is a need to understand the vulnerability of different sections of Start Bay, and the impact that would arise from certain combined events. For instance, there is a need to quantify the probability of overtopping (some gravel on the road), overwashing (a lot of gravel on the road), and breaching (catastrophic failure of road/breaching of the lagoon) of the Slapton barrier under different future wave events, levels of beach depletion, and sea level.

7.2. Recommendations for Further Monitoring, Study, or Investigations

For the past 10 years, there has been a comprehensive level of beach monitoring in Start Bay, in the form of regular topographic surveys, and collection of inshore wave data. In addition to this, it is recommended that real-time monitoring of beach levels (especially those in front of sea defences at Torcross, Beesands, and Hallsands) using either semi-permanent video cameras or laser scanners installed at each beach, would provide coastal managers with some warning about beach levels and imminent undermining of the engineered structures in Start Bay.

In addition to reactive management through such beach monitoring, some proactive investigations are also recommended: from the uncertainties identified in Section 7.1, two linked modelling exercises are recommended:

1. Detailed modelling is required in order to better understand the inshore wave conditions along the length of Start Bay under different scenarios[4]. This can then feed into detailed alongshore transport modelling which will enable the quantification of alongshore transport rates and sediment gains/losses along the bay under different wave scenarios.
2. To fully assess the vulnerability of the barrier system, and hence the A379 road, to overwash and breaching under different wave and sea-level scenarios, process-based morphodynamic modelling is required.

In addition to well established wave transformation and alongshore transport models for modelling exercise 1 above, one-dimensional profile models are now available for exercise 2, to determine the morphodynamic response of gravel beaches as a function of waves and water levels, as well as beach morphology and sediment type. XBeach-G (https://oss.deltares.nl/web/xbeach/xbeach-og) is an example of such a model, and has the advantages of being able to account for incident and infragravity (low-frequency) wave run-up, and the influence of water infiltration and coastal structures on wave run-up. The value of such models is not only in determining the vulnerability of certain barrier sections to certain wave and water level conditions, but also in their ability to help design a suitable barrier profile to inform coastal management. Such a modelling approach (for example, as previously undertaken by Prime *et al.* (2016) at the Dungeness power station) is beyond the scope of this coastal processes

[4] To some extent, this has been achieved in the State of the Nation data, but as these data were output at 5 m depth, wave breaking prior to 5 m depth may limit their use. Additionally, the State of the Nation data are event based, and could not be used to examine sequences of wave and water levels occurring consecutively.

baseline, but is highly recommended for future assessments of coastal vulnerability to storm impacts and barrier breaching in Start Bay.

The following outline methodology is suggested as a suitable approach for future modelling in Start Bay:

- Conduct alongshore transport modelling under long time-sequences of wave conditions, to determine possible future shoreline positions.
- In addition to these predicted future profiles, create synthetic beach profiles with different levels of denudation/nourishment.
- Determine a selection of extreme (low probability) wave and water level events (State of the Nation data could be used for this).
- Apply the effects of sea-level rise to these conditions.
- Use the process-based morphodynamic model XBeach-G (developed specifically for modelling gravel beaches) to simulate wave overtopping, overwashing, and breaching during extreme events over the previously determined profiles.
- Assess the predicted morphological change and overwash rates during the selected events.

Because the timing and sequencing of future storm wave events is unknown, a probabilistic approach is required in order to understand the future vulnerability of the beaches in Start Bay. Multiple scenarios based on historic wave statistics need to be modelled in order to provide some insight into the range of possible outcomes (a Monte-Carlo approach, for instance). This could be used, for instance, to predict beach volumes into the future based on the statistical characteristics of the wave climate, with the uncertainty in the future wave conditions dealt with via a distribution of possible outcomes.

8. Conclusions

The purpose of this report is to provide an up-to-date understanding of the coastal processes operating along the coastline at Slapton Sands and to the north at Blackpool Sands and to the south at Hallsands and Beesands. In this report, coastal processes and morphological change acting over three key time-scales (long-term, medium-term, and short-term) in Start Bay have been examined, with a detailed focus on Slapton Sands. Table 7-1 presents the complex interactions occurring between these processes, which can be summarised as follows:

- Over long time-scales, relative sea level rise gradually increases the vertical reach of waves; this increasingly allows for short-term events (storm waves) to cut-back the upper beach profile and for wave run-up to overtop/overwash the crest of the beach.
- Meanwhile, alongshore-oriented waves cause beach rotation (a natural response of the shoreline to rotate around the bay in a clockwise or anti-clockwise direction due to alongshore sediment transport) over medium time-scales, which reduces the sediment volume along certain stretches of Start Bay. Those sections are then vulnerable to short-term wave attack and overwashing.
- Short-term storm wave attack results in vulnerable sections of Start Bay being cut-back even further, and allows wave run-up to overtop and overwash sections of the beaches.
- These episodic, short time-scale overwashing events are the mechanism for long-term barrier roll-back, and allow the barrier to retreat in response to sea level rise.
- As Slapton Barrier retreats, its overall length is expected to increase as a result of the barrier conforming to the embayed shape of the Ley during its retreat.
- Eventually, the decreasing cross-sectional area of Slapton Barrier, caused by the lengthening of the shoreline as it retreats, will make the barrier increasingly vulnerable to breaching. Once significant breaching occurs, the barrier could begin to break down into a series of tidal inlets.

These interacting coastal processes cause a number of coastal management challenges. In the short-term, storm wave attack is the main concern to coastal management, as this can cause barrier erosion/cut-back in response to wave run-up, overtopping or overwashing, as well as coastal flooding and undermining of the A379 road, storm defences (seawalls and rip-rap), and other engineered structures. Over medium time-scales (weeks – years), the alongshore supply of sediment and resulting vulnerability of the different sections of Start Bay is a concern for coastal management as it will make certain sections of the barrier more vulnerable to short-term storm processes (barrier erosion and overwashing). Over the long-term (decades – centuries), without appropriate mitigation, the retreat of

Slapton barrier could potentially expose Torcross village to the sea, and will require consideration to be given to the future of the Slapton line section of the A379 road. This may involve gradual realignment, to maintain the roads position on the barrier, or eventually to complete re-routing or re-engineering of the road in the extreme case of barrier breaching/breakdown. In the long-term, barrier retreat and potential breaching of the barrier road may also have significant implications for the freshwater status of Slapton Ley.

8.1. Hydrodynamics

8.1.1. Wave Climate

- In Start Bay, wave conditions arrive from both a southerly direction and an easterly direction. The southerly waves originate in the Atlantic Ocean, and refract into Start Bay as they propagate up the English Channel, whereas the easterly waves originate from local storms occurring in the Channel itself.
- From the WWIII data shown in Figure 3-5 and Figure 3-6, around 70% of all wave conditions arriving at Start Bay have H_s = 0 – 1.5 m, and T_p = 2 – 10 s, with around 45% of these waves arriving from the southwest, and around 15% arriving from the east.
- There is little variation in the heights of extreme waves with return periods of 20, 50, and 100 years. However, extreme waves arriving from the south (H_s = 5.99, 6.36, and 6.60 m, respectively) are predicted to be larger than extreme waves arriving from the east (H_s = 4.28, 4.57, and 4.76 m, respectively).
- In the last 30 years, there has been a 75% reduction in the 10-year averaged activity of easterly storms with H_s greater than 2.5 m arriving at Start Bay (Scott *et al.*, 2016). In contrast, southerly storm activity stayed relatively constant over that period (Figure 5-20).
- This is directly related to shifts in the distribution of atmospheric pressure and resulting storm tracks across the Atlantic Ocean, with easterly storm conditions only developing during periods of negative NAO, which have declined in the last 30 years (Wiggins *et al.*, 2017).

8.1.2. Water Levels

- Mean spring and neap tide ranges in Start Bay are 4.70 m and 2.20 m, respectively.
- Water levels could reach 3.2 m above ODN during a 100-year event, and storm surge could super-elevate the water level more than 1 m above the predicted highest tide level once in a 100 year period.

- A 100-year water level would not be sufficient alone to cause coastal flooding in Start Bay, as the water surface would not exceed the height of the beach berm at any of the profiles in Start Bay. However, with some level of wave run-up occurring at the same time as this water level, it is very likely that overtopping or overwashing of the beach profiles would occur, which could cause flooding and damage to the properties, infrastructure, and ecology along the beaches of Start Bay.
- In the last 7000 years the average historic rate of relative sea-level rise in South Devon is on the order of 1.1 mm/year, but from UKCP09 projections the rate of relative sea-level rise around Start Bay since 1990 is expected to have been between 2.9 and 3.9 mm/year.
- Under all UKCP09 emissions scenarios, the rate of sea-level rise will increase in the future, and local sea levels are likely to be 42 – 59 cm higher than their 1990 levels by the year 2100. Coastal flooding in Start Bay will therefore become more likely in the future, and in the first instance is most likely to affect parts of Hallsands and Beesands, which have the lowest profiles in Start Bay (Figure 3-15 and Figure 3-16).
- At present, skew surge can super-elevate the height of the still water level during a storm by 85 – 104 cm during 20-year to 100-year return period events, and is therefore a major potential contributor to coastal flooding. Over the next 100 years, a 1-in-20 year and 1-in-50 year skew surge event is expected to increase by 3 cm and 4 cm, respectively (under a medium UKCP09 emissions scenario).

8.1.3. Joint Probability of Extreme Wave and Water Levels

- Large wave conditions combined with an average water level can have the same probability of occurrence as small wave conditions combined with a very high water level.
- The chance of overtopping from these two different events could be very different, given that there would be a substantial difference in the wave run-up. This highlights the need to model wave run-up for many different scenarios, in order to adequately predict coastal flooding.

8.2. Long-Term Morphological Processes

- Over time scales of years to centuries, the effects of sea-level rise drive shoreline and barrier retreat. Barrier beaches respond to sea-level rise by ‘roll-over’ and by increasing the crest height of the beach (Orford *et al.*, 1991). This process involves overwashing – the transferring of sediment from the shore-face to the back barrier area – which is an episodic rather than continuous process.

- Orford *et al*.'s (1995b) formula indicates that accelerating sea-level rise will increase the rate of landward migration of Slapton barrier in the next 100 years, and that the historic rate of barrier retreat will, in future, be exceeded under any future UKCP09 emissions scenarios.
- In comparison, the Bruun rule predicts that under a medium emissions scenario the estimated rate of barrier retreat over the past century will continue for the next century, while low emissions or high emissions scenarios would result in slower retreat and faster retreat over the next century, respectively, compared to the estimated historic rate of retreat.
- Accounting for uncertainty in future emissions levels, Orford *et al*.'s formula predicts that the Slapton barrier could have migrated landward 3.4 – 4.5 m by the year 2036, 9.6 – 12 m by the year 2065, and 22 – 28 m by the year 2117.
- These projections will only become a reality if the expected number of severe storm events occur within a given time period, as it is severe storm events which drive the retreat of the barrier. Increasing storminess due to climate change is not accounted for within the formula used to predict barrier retreat. With increasing storm frequency and magnitude, it is likely that barrier retreat rate will increase, as overwash events become more frequent.
- It was previously postulated that as Slapton Barrier retreats into the curved embayment of the Ley, it is possible that the length of the shoreline will increase (Scott Wilson, 2006). As a result, the barrier's width is expected to reduce, due to the relatively fixed sediment volume, by 15 m per century (Pethick, 2001), which would increase the barrier's retreat efficiency. The rate of barrier retreat may therefore increase further in future, due to the smaller barrier size and increasing retreat efficiency.
- Despite a number of uncertainties inherent in the barrier roll-back predictions, the predictions provide an indication of the potential mobility of the barrier crest over the next 100 years, and it can be concluded that the relatively stable barrier position of the last century cannot be assumed to continue into the future. Under all UKCPP09 emissions scenarios, the barriers position is predicted to migrate inland over the next 100 years, and the majority of the road and southwest coast path will be affected within this period.

8.3. Medium-Term Morphological Processes

- Over time-scales of weeks to years, the key morphological process shaping the beaches in Start Bay is alongshore transport of sediment (Chadwick *et al.*, 2005), which is primarily a function of the sediment characteristics, the level of incident wave energy, and the angle of wave approach (US Army Corps Of Engineers, 1984).

- Net alongshore sediment transport in Start Bay is from south to north, driven by Atlantic waves arriving from the south of the bay. Drift reversals occur from north to south, when waves originating in the English Channel arrive from the east, usually under storm conditions.
- Alongshore sediment transport has lead to an overall net loss of volume at all profiles in Start Bay south of Strete since 2007, with net gains seen at the Strete end of Slapton Sands, and at Blackpool Sands. This erosion of the beaches to the south and accretion of the beaches to the north has effectively caused the shoreline in Start Bay to rotate in a clockwise direction.
- Over the longer term, a net trend of sediment loss at the middle and south of Slapton, and net gains at the north end of Slapton, has been occuring since at least 1972, as demonstrated by older topographic data collected by the Slapton Field Studies Centre (FSC, Figure 5-10) between August 1972 and May 2003.
- A number of erosional hot-spots (listed from north to south) have been identified within Start Bay:

    1. **Middle of Slapton Sands (profiles P8 – P11).** These profiles have, on average, 150 – 200 m^3/m of sediment, and have had as little as 100 m^3/m in the last 10 years.
    2. **South end of Slapton Sands (profile P0 – P3).** These profiles have, on average, 75 – 200 m^3/m of sediment, and P0 in front of Torcross village has had as little as 50 m^3/m in the last 10 years.
    3. **North end of Beesands (profile BS6).** This profile has, on average, around 150 m^3/m of sediment, and has had as little as 100 m^3/m in the last 10 years.
    4. **South end of Beesands (profile BS1).** This profile has, on average, around 180 m^3/m of sediment, and has had as little as 150 m^3/m in the last 10 years.
    5. **All of Hallsands (profiles HS1 – HS4).** Profile HS4 at the north of Hallsands has had, on average, around 200 m^3/m of sediment, and has had as little as 150 m^3/m in the last 10 years. Profile HS1 at the south of Hallsands has had, on average, around 100 m^3/m of sediment, and has had as little as 50 m^3/m in the last 10 years.

- An Empirical Orthogonal Function (EOF) analysis revealed that 90% of all the beach volume changes at Slapton Sands could be atributed to one dominant rotational mode of beach change. The spatial pattern (Figure 5-12, upper panel) of this mode is positive at the northern end of Slapton Sands (3800 – 4500 m north of Torcross) while the rest of the beach is negative. This means that at times when the north end of Slapton Sands has been acreting, the middle and south of the beach has eroded, and vice versa.

- Periods of rapid northward beach rotation occured every 1 – 2 years over winter, interspersed by more gradual southward beach rotation inbetween. As the northward rotation events have been stronger than the intervening southward rotation, the net effect has been a bias towards northward sediment transport and rotation.
- A correlation analysis showed that alongshore sediment transport and beach rotation is strongly related to the magnitude and direction of the incident wave power, and that it is the cumulative effects of powerful waves arriving obliquely from the south (north) that drives sediment transport and beach rotation to the north (south) at Slapton Sands.
- As the beaches in Start Bay act as an interconnected sediment system, it is likely that this relationship is relevant to Hallsands, Beesands, and Blackpool Sands, as well as Slapton Sands.
- The aformentioned relationship was used to hindcast beach volumes at Slapton Sands back to 1980. This revealed a number of interesting periods of beach change over the last 37 years, including northward beach rotation between 1980 and 2004, southward beach rotation between 2003 and 2014, and strong northward rotation since the 2013/2014 winter.
- This exercise revelealed that, despite some subsequent recovery, since 2016 the beach has had more sediment in the north, and less sediment in the middle and south, than at any other time since 1980.
- Analysis of both intertidal and subtidal survey data in Start Bay (Wiggins *et al.*, 2017) has revealed that the total volume of sediment transported northward during the extremely energetic winter of 2013/2014, was approximately 745,000 m^3. The average alongshore transport rate equates to around 28,654 m^3 per day, equivalent to around 48,000 metric tonnes of gravel per day, assuming all the transport occurred during the 26 days of storms within that period.
- Although the transport rate would have differed during individual storms, this provides some estimate of the maximum alongshore transport rate likely to occur in Start Bay, given the magnitude and return period of the storms experienced during that time.
- As no sediment volume appears to have been lost from Start Bay during the 2013/2014 winter, we conclude that, for all practical purposes, Start Bay can be considered a closed sediment cell, with maximum alongshore transport rates on the order of 28,654 m^3 of gravel per day during extreme storm events.
- Medium-term modulation of the balance between southwesterly and easterly storm waves (and therefore the alongshore wave power that controls beach rotation at Slapton Sands) is related to time series of NAO and WEPA (Figure 5-18), suggesting, perhaps, that these medium-term atmospheric cycles could be used to predict beach rotation cycles into the future. However, as

current understanding about NAO and WEPA cycles is limited, this would carry a large degree of uncertainty, and is not attempted in this report.

8.4. Short-Term Morphological Processes

- Over short time-scales (hours – days), the key coastal processes affecting Start Bay relate to storms. Storms incur coastal changes through the action of energetic waves eroding and transporting sediment within the bay, and/or causing wave run-up and overwashing. Locally generated storms can additionally super-elevate sea-levels through storm surge.
- The most significant erosion at the beaches in Start Bay is likely to occur due to the sequential action of southerly and easterly storm wave conditions.
- Southerly waves have the potential to drive significant alongshore sediment transport to the north, which results in beach narrowing to the south, widening to the north and resultant beach rotation in a clockwise direction. This leaves the coast to the south of Strete vulnerable to waves from the east, which can cause further profile cut-back and overwashing. This is believed to have been the cause of the 2001 road collapse.
- The most vulnerable sections of coast in Start Bay are at the south of Hallsands beach and at the south of Slapton Sands in front of Torcross village, but all of the sections listed are severely vulnerable to coastal erosion and storm impacts.
- In contrast, profiles at the north of Slapton Sands (P15 – P19) are the least vulnerable to coastal erosion, having had 400 – 900 m^3/m, of sediment at any moment over the last 10 years.
- The middle of Slapton Sands (P8 – P11) has experienced greater net erosion than any other part of the beach over the last 10 years (Figure 5-7), experienced the most significant overwash and erosion during the 2013/2014 winter (Figure 6-2 and Figure 6-3), and is adjacent to the location of the 2001 road collapse.
- It can be concluded that this section of the Slapton Barrier (and the A379 road) is the most vulnerable to overwashing of sediment, and to potential future undermining of the road, or even breaching of the barrier.

8.5. Knowledge Gaps and Reccomendations for Further Studies

- Detailed modelling is required in order to better understand the inshore wave conditions along the length of Start Bay under different scenarios. This can then feed into detailed alongshore transport modelling which will enable the quantification of alongshore transport rates and sediment gains/losses along the bay under different wave scenarios.

- To fully assess the vulnerability of the barrier system, and hence the A379 road, to overwash and breaching under different wave and sea-level scenarios, process-based morphodynamic modelling is required. An outline methodology for such a study is proposed in Section 7.2 of this report.
- Because the timing and sequencing of future storm wave events is unknown, a probabilistic approach is required in order to understand the future vulnerability of the beaches in Start Bay. Multiple scenarios based on historic wave statistics need to be modelled in order to provide some insight into the range of possible outcomes. This could be used, for instance, to predict beach volumes into the future based on the statistical characteristics of the wave climate, with the uncertainty in the future wave conditions dealt with via a distribution of possible outcomes.

References

Aubrey, D. G. 1979. Seasonal patterns of onshore/offshore sediment movement. *Journal of Geophysical Research*, **84**, (C10), 6347-6354.

Barne, J., Robson, C., Kaznowska, S., Doody, J., Davidson, N. and Buck, A. 1996. *Coasts and seas of the United Kingdom. Region 10. South-west England: Seaton to the Roseland Peninsula.* Joint Nature Conservation Committee (Great Britain).

Bauer, B. O. and Greenwood, B. 1988. Surf-zone similarity. *Geographical review*, **78**, (2), 137-147.

Bradbury, A. 2000. *Predicting breaching of shingle barrier beaches-recent advances to aid beach management*. Proceedings of 35th Annual MAFF Conference of River and Coastal Engineers. pp 1-5.

Bruun, P. 1962. Sea-level rise as a cause of shore erosion. *Journal of the Waterways and Harbors Division*, **88**, (1), 117-132.

Buscombe, D. D. 2008. *Morphodynamics, sedimentation and sediment dynamics of a gravel beach*. A Thesis submitted to the University of Plymouth in partial fulfilment for the degree of Doctor of Philosophy.

Caires, S. 2011. Extreme value analysis: wave data. *Joint WMO/IOC Technical Commission for Oceanography and Marine Meteorology (JCOMM) Technical Report*, (57), 33 pp.

Carter, R. and Orford, J. 1984. Coarse clastic barrier beaches: a discussion of the distinctive dynamic and morphosedimentary characteristics. *Marine Geology*, **60**, (1-4), 377-389.

Castelle, B., Dodet, G., Masselink, G. and Scott, T. 2017. A new climate index controlling winter wave activity along the Atlantic coast of Europe: The West Europe Pressure Anomaly. *Geophysical Research Letters*, **44**, (3), 1384-1392.

Castelle, B., Marieu, V., Bujan, S., Splinter, K. D., Robinet, A., Sénéchal, N. and Ferreira, S. 2015. Impact of the winter 2013–2014 series of severe Western Europe storms on a double-barred sandy coast: Beach and dune erosion and megacusp embayments. *Geomorphology*, **238**, 135-148.

Chadwick, A., Karunarathna, H., Gehrels, R., Massey, A., O Brien, D. and Dales, D. 2005. *A new analysis of the Slapton barrier beach system, UK*. Proceedings-Institution of Civil Engineers Maritime Engineering. pp 147.

Clarke, D. J. and Eliot, I. 1982. Description of littoral, alongshore sediment movement from empirical eigenfunction analysis. *Journal of the Geological Society of Australia*, **29**, (3-4), 327-341.

Cooper, J. A. G. and Pilkey, O. H. 2004. Sea-level rise and shoreline retreat: time to abandon the Bruun Rule. *Global and Planetary Change*, **43**, (3), 157-171.

de Alegria-Arzaburu, A. R. and Masselink, G. 2010. Storm response and beach rotation on a gravel beach, Slapton Sands, UK. *Marine Geology*, **278**, (1), 77-99.

de Alegría-Arzaburu, A. R., Pedrozo-Acuña, A., Horrillo-Caraballo, J. M., Masselink, G. and Reeve, D. E. 2010. Determination of wave–shoreline dynamics on a macrotidal gravel beach using Canonical Correlation Analysis. *Coastal Engineering*, **57**, (3), 290-303.

Dean, R. G. 1973. *Heuristic models of sand transport in the surf zone*. First Australian Conference on Coastal Engineering: Engineering Dynamics of the Coastal Zone. Institution of Engineers, Australia. pp 215.

Dunstone, N., Smith, D., Scaife, A., Hermanson, L., Eade, R., Robinson, N., Andrews, M. and Knight, J. 2016. Skilful predictions of the winter North Atlantic Oscillation one year ahead. *Nature Geosci*, **9**, (11), 809-814.

Fairley, I., Davidson, M., Kingston, K., Dolphin, T. and Phillips, R. 2009. Empirical orthogonal function analysis of shoreline changes behind two different designs of detached breakwaters. *Coastal Engineering*, **56**, (11–12), 1097-1108.

Futurecoast 2002. Halcrow Group, Swindon.

Gleason, R., Blackley, M. W. and Carr, A. P. 1975. Beach stability and particle size distribution, Start Bay. *Journal of the Geological Society*, **131**, (1), 83-101.

Gómez-Pujol, L., Orfila, A., Álvarez-Ellacuría, A. and Tintoré, J. 2011. Controls on sediment dynamics and medium-term morphological change in a barred microtidal beach (Cala Millor, Mallorca, Western Mediterranean). *Geomorphology*, **132**, (3–4), 87-98.

Gourlay, M. 1968. Beach and dune erosion tests (I). *Delft Hydraulics Laboratory*, Report MO935.

Hails, J. 1975. Offshore morphology and sediment distribution, Start Bay, Devon. *Philosophical Transactions of the Royal Society of London A: Mathematical, Physical and Engineering Sciences*, **279**, (1288), 221-228.

Halcrow Group 2011. *Durlston Head to Rame Head SMP2 Shoreline Management Plan.* Halcrow Group, Exeter.

Hamm, L., Mazas, F., Garcia, N. and Bailly, B. 2010. Assessment of extreme wave heights: an attempt to reconcile theory and practice. *European Journal of Environmental and Civil Engineering*, **14**, (2), 127-148.

Harley, C. D., Randall Hughes, A., Hultgren, K. M., Miner, B. G., Sorte, C. J., Thornber, C. S., Rodriguez, L. F., Tomanek, L. and Williams, S. L. 2006. The impacts of climate change in coastal marine systems. *Ecology letters*, **9**, (2), 228-241.

HR Wallingford 2015. *State of the Nation Flood Risk Analysis. Coastal Boundary Conditions.* Report No. MCR5289-RT025-R02-00. HR Wallingford, October 2015.

Hsu, T., Liaw, S., Wang, S. and Ou, S. 1986. *Two dimensional empirical eigenfunction model for the analysis and prediction of beach profile changes*. Edge, B. (Ed.). Twentieth Coastal Engineering Conference. New York, NY. pp 1180-1195.

Hurrell, J. W., Kushnir, Y. and Visbeck, M. 2001. The north Atlantic oscillation. *science*, **291**, (5504), 603-605.

Jonathan, P. and Ewans, K. 2013. Statistical modelling of extreme ocean environments for marine design: a review. *Ocean engineering*, **62**, 91-109.

Larson, M., Hanson, H., Kraus, N. C. and Newe, J. 1999. Short-and long-term responses of beach fills determined by EOF analysis. *Journal of waterway, port, coastal, and ocean engineering*, **125**, (6), 285-293.

Larson, M., Hoan, L. X. and Hanson, H. 2010. Direct formula to compute wave height and angle at incipient breaking. *Journal of waterway, port, coastal, and ocean engineering*, **136**, (2), 119-122.

Loureiro, C., Ferreira, Ó. and Cooper, J. A. G. 2012. Geologically constrained morphological variability and boundary effects on embayed beaches. *Marine Geology*, **329–331**, 1-15.

Masselink, G., Scott, T., Conley, D. C., Davidson, M. and Russell, P. 2015. *Regional Variability in Atlantic Storm Response Along the SouthWest Coast of England*. Coastal Sediments 2015. San Diego, CA, USA.

Masselink, G., Scott, T., Poate, T., Russell, P., Davidson, M. and Conley, D. 2016. The extreme 2013/2014 winter storms: hydrodynamic forcing and coastal response along the southwest coast of England. *Earth Surface Processes and Landforms*, **41**, (3), 378-391.

Massey, A. C. 2004. *Holocene sea-level changes along the Channel coast of south-west England*. University of Plymouth.

Massey, A. C., Gehrels, W. R., Charman, D. J., Milne, G. A., Peltier, W. R., Lambeck, K. and Selby, K. A. 2008. Relative sea-level change and postglacial isostatic adjustment along the coast of south Devon, United Kingdom. *Journal of Quaternary Science*, **23**, (5), 415-433.

McCall, R., Masselink, G., Poate, T., Roelvink, J., Almeida, L., Davidson, M. and Russell, P. 2014. Modelling storm hydrodynamics on gravel beaches with XBeach-G. *Coastal Engineering*, **91**, 231-250.

McMillan, A., Batstone, C., Worth, D., Tawn, J., Horsburgh, K. and Lawless, M. 2011. *Coastal flood boundary conditions for UK mainland and islands. Design sea levels.* Report No. SC060064/TR2: Design sea levels. Environment Agency and Defra, February 2011.

Miller, J. K. and Dean, R. G. 2007a. Shoreline variability via empirical orthogonal function analysis: Part I temporal and spatial characteristics. *Coastal Engineering*, **54**, (2), 111-131.

Morey, C. 1976. The Natural History of Slapton Ley Nature Reserve. IX—The morphology and history of the lake basins. *Field Studies*, **4**, (3), 353-368.

Morey, C. 1983. The evolution of a barrier-lagoon system—a case study from Start Bay. *Proceedings of the Ussher Society*, **5**, 454-459.

Nicholls, R. J. and Cazenave, A. 2010. Sea-level rise and its impact on coastal zones. *science*, **328**, (5985), 1517-1520.

Orford, J. 2001. *Slapton Sands: Implications of Rock Armouring.* Report to English Nature.

Orford, J., Carter, R. and Forbes, D. 1991. Gravel barrier migration and sea level rise: some observations from Story Head, Nova Scotia, Canada. *Journal of Coastal Research*, 477-489.

Orford, J., Carter, R. and Jennings, S. 1996. Control domains and morphological phases in gravel-dominated coastal barriers of Nova Scotia. *Journal of Coastal Research*, 589-604.

Orford, J., Carter, R., Jennings, S. and Hinton, A. 1995a. Processes and timescales by which a coastal gravel-dominated barrier responds geomorphologically to sea-level rise: Story head barrier, Nova Scotia. *Earth Surface Processes and Landforms*, **20**, (1), 21-37.

Orford, J., Carter, R., McKenna, J. and Jennings, S. 1995b. The relationship between the rate of mesoscale sea-level rise and the rate of retreat of swash-aligned gravel-dominated barriers. *Marine Geology*, **124**, (1-4), 177-186.

Pethick, J. 2001. *Slapton Sands: Proposed Road Realignment. Assessment of Geomorphological Impacts in Relation to Management of the Road.* Report to English Nature.

Prime, T., Brown, J. M. and Plater, A. J. 2016. Flood inundation uncertainty: The case of a 0.5% annual probability flood event. *Environmental Science & Policy*, **59**, 1-9.

Pullen, T., Allsop, N., Bruce, T., Kortenhaus, A., Schuttrumpf, H. and van der Meer, J. 2007. EurOtop: European Overtopping Manual. *Available at: www. overtopping-manual. com*,

Robinson, A. 1961. The hydrography of Start Bay and its relationship to beach changes at Hallsands. *The Geographical Journal*, **127**, (1), 63-77.

Scott, T., Masselink, G., O'Hare, T., Saulter, A., Poate, T., Russell, P., Davidson, M. and Conley, D. 2016. The extreme 2013/2014 winter storms: Beach recovery along the southwest coast of England. *Marine Geology*, **382**, 224-241.

Scott Wilson 2006. *Slapton Coastal Zone Management Main Study. Iteration 1: Determining the Shoreline Management Approach.* Basingstoke.

Stokes, C., Russell, P., Conley, D., Beaumont, E. and Greaves, D. 2013. Exploring Monthly To Seasonal Beach Morphodynamics Using Empirical Orthogonal Functions. *Journal of Coastal Research, 12th International Coastal Symposium* (Special Issue No. 65), 1868-1873.

US Army Corps Of Engineers 1984. Shore protection manual. *Army Engineer Waterways Experiment Station, Vicksburg, MS. 2v*, 37-53.

Wiggins, M., Scott, T., Masselink, G., Russell, P., Castelle, B. and Dodet, G. 2017. The role of multi-decadal climate variability in controlling coastal dynamics: re-interpretation of the 'lost village of hallsands'. Coastal Dynamics. Helsingør, Denmark.

Winant, C. D., Inman, D.L., Nordstrom, C.E. 1975. Description of seasonal beach changes using empirical eigenfunctions. *Journal of Geophysical Research*, **80**, (15), 1979-1986.

Zhang, K., Douglas, B. and Leatherman, S. 2002. Do storms cause long-term beach erosion along the US East Barrier Coast? *The Journal of Geology*, **110**, (4), 493-502.

Appendix A. Predicted Barrier Retreat Under UKCP09 Low Emissions Scenario

Figure A-1. Predicted retreat distance of Slapton barrier under rising sea-level rise from a low emissions scenario (50th percentile prediction). Barrier section 1 of 5 is shown, where 1 = Strete, and 5 = Torcross.

Figure A-2. Predicted retreat distance of Slapton barrier under rising sea-level rise from a low emissions scenario (50th percentile prediction). Barrier section 2 of 5 is shown, where 1 = Strete, and 5 = Torcross.

COASTAL MARINE APPLIED RESEARCH WITH PLYMOUTH UNIVERSITY

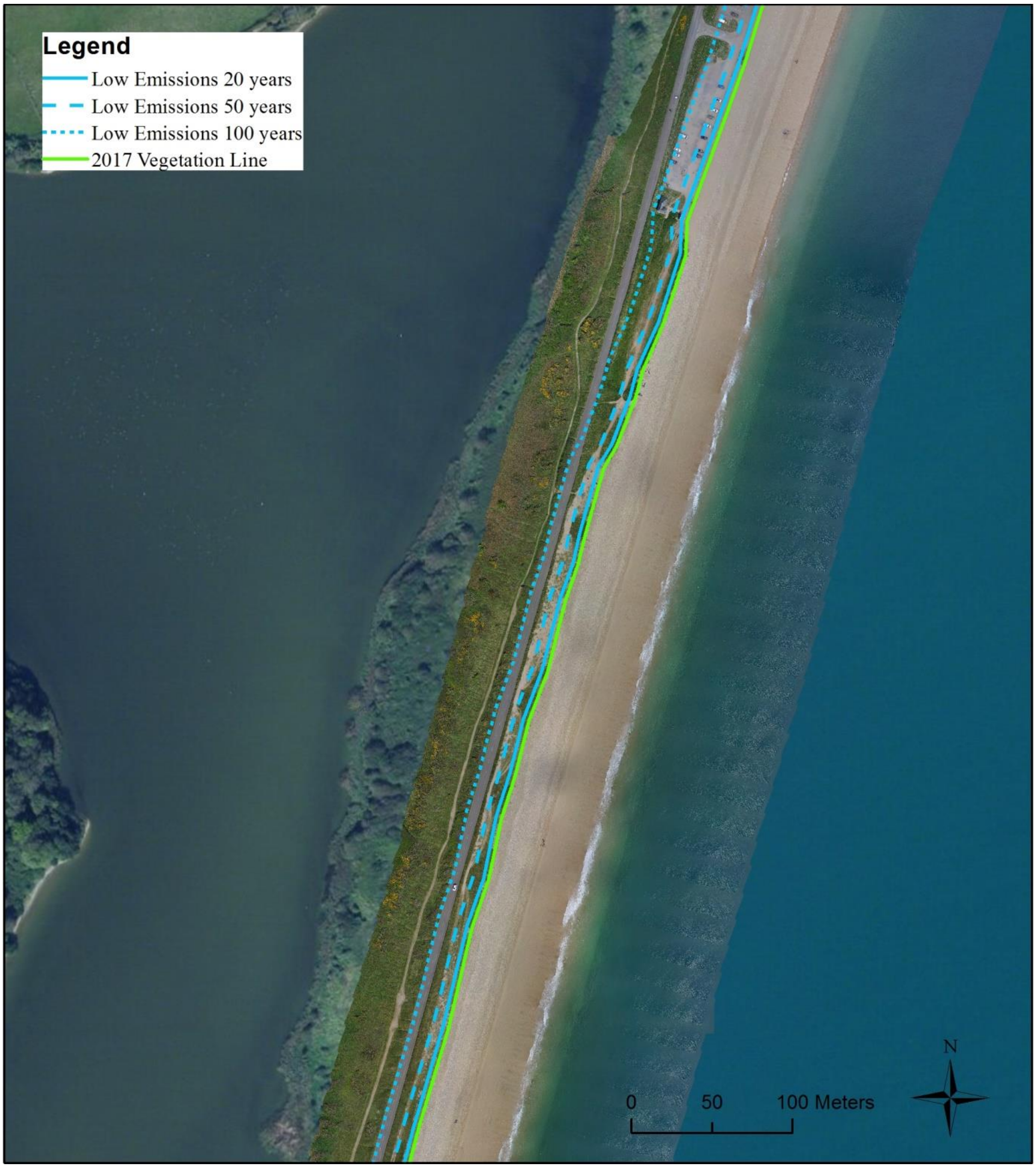

Figure A-3. Predicted retreat distance of Slapton barrier under rising sea-level rise from a low emissions scenario (50th percentile prediction). Barrier section 3 of 5 is shown, where 1 = Strete, and 5 = Torcross.

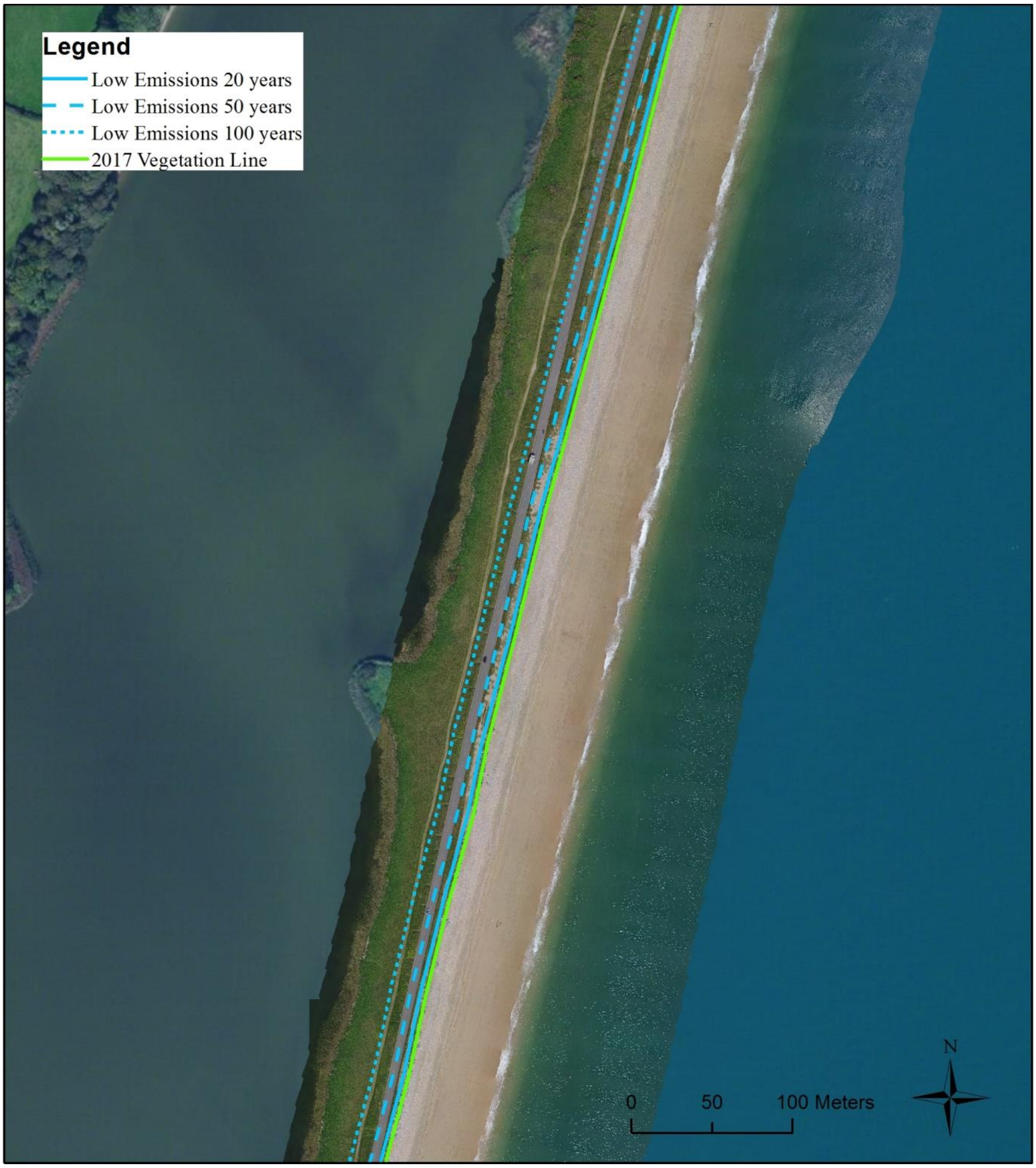

Figure A-4. Predicted retreat distance of Slapton barrier under rising sea-level rise from a low emissions scenario (50th percentile prediction). Barrier section 4 of 5 is shown, where 1 = Strete, and 5 = Torcross.

Figure A-5. Predicted retreat distance of Slapton barrier under rising sea-level rise from a low emissions scenario (50th percentile prediction). Barrier section 5 of 5 is shown, where 1 = Strete, and 5 = Torcross.

Appendix B. Predicted Barrier Retreat Under UKCP09 Medium Emissions Scenario

Figure B-1. Predicted retreat distance of Slapton barrier under rising sea-level rise from a medium emissions scenario (50th percentile prediction). Barrier section 1 of 5 is shown, where 1 = Strete, and 5 = Torcross.

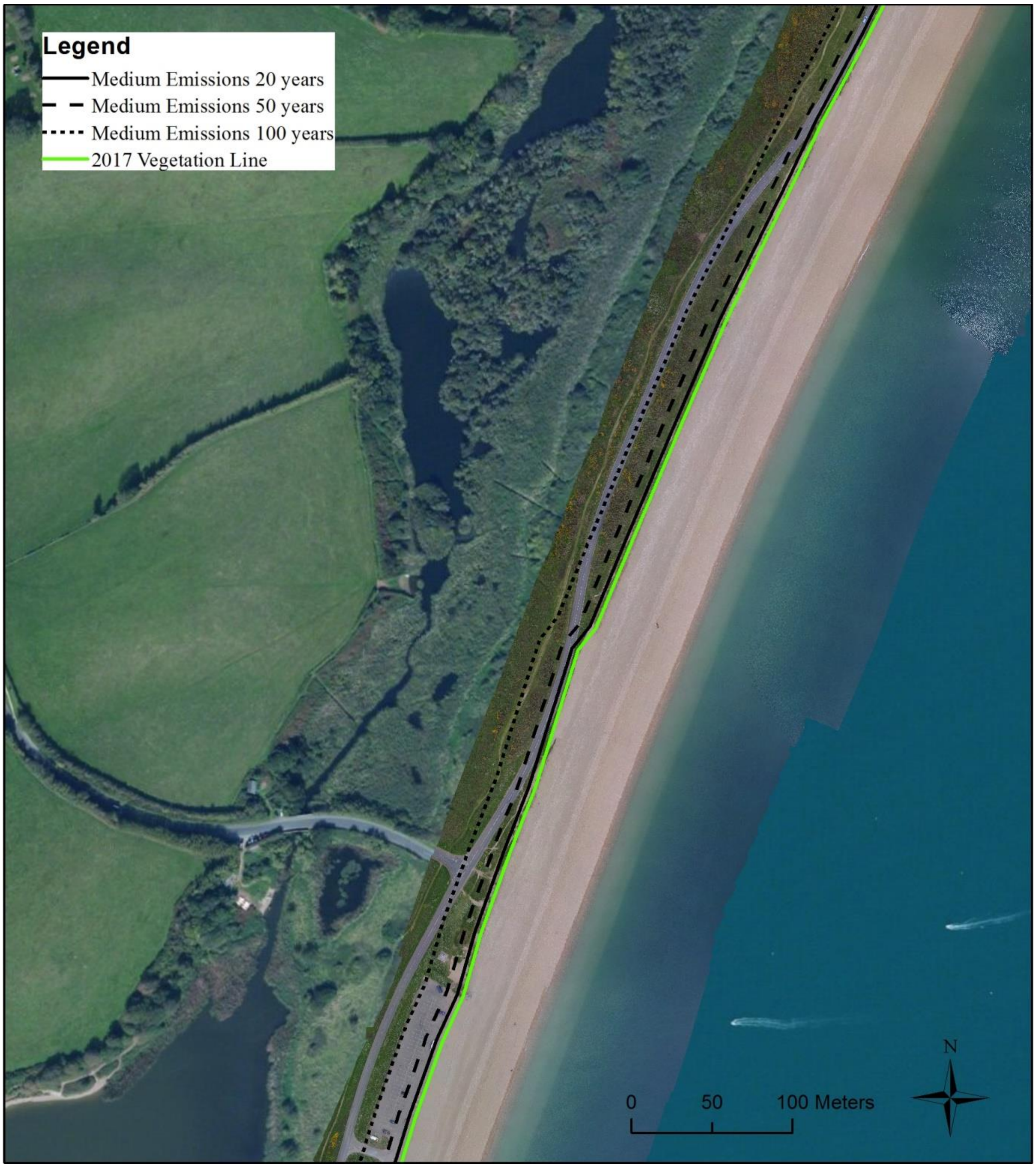

Figure B-2. Predicted retreat distance of Slapton barrier under rising sea-level rise from a medium emissions scenario (50th percentile prediction). Barrier section 2 of 5 is shown, where 1 = Strete, and 5 = Torcross.

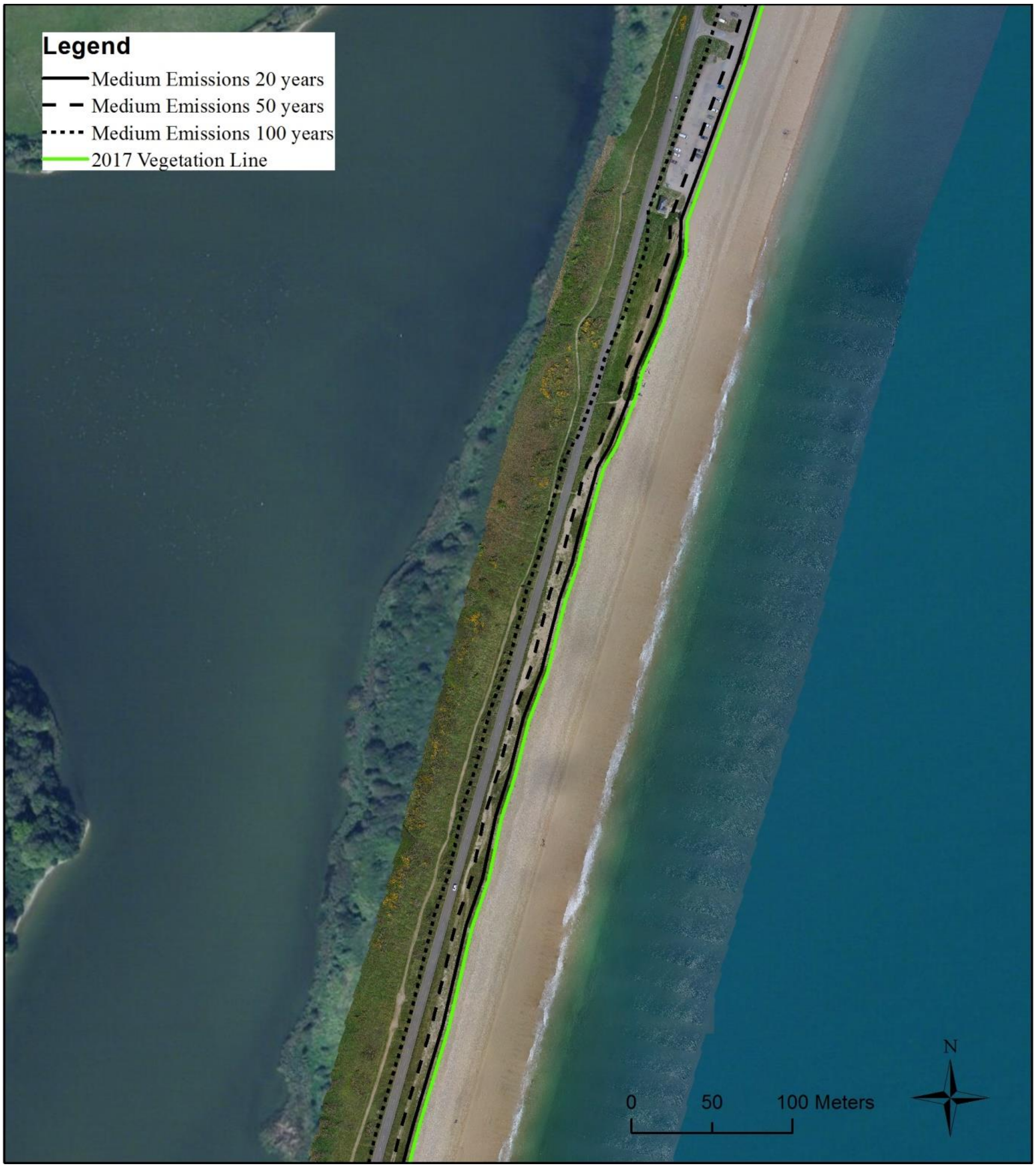

Figure B-3. Predicted retreat distance of Slapton barrier under rising sea-level rise from a medium emissions scenario (50th percentile prediction). Barrier section 3 of 5 is shown, where 1 = Strete, and 5 = Torcross.

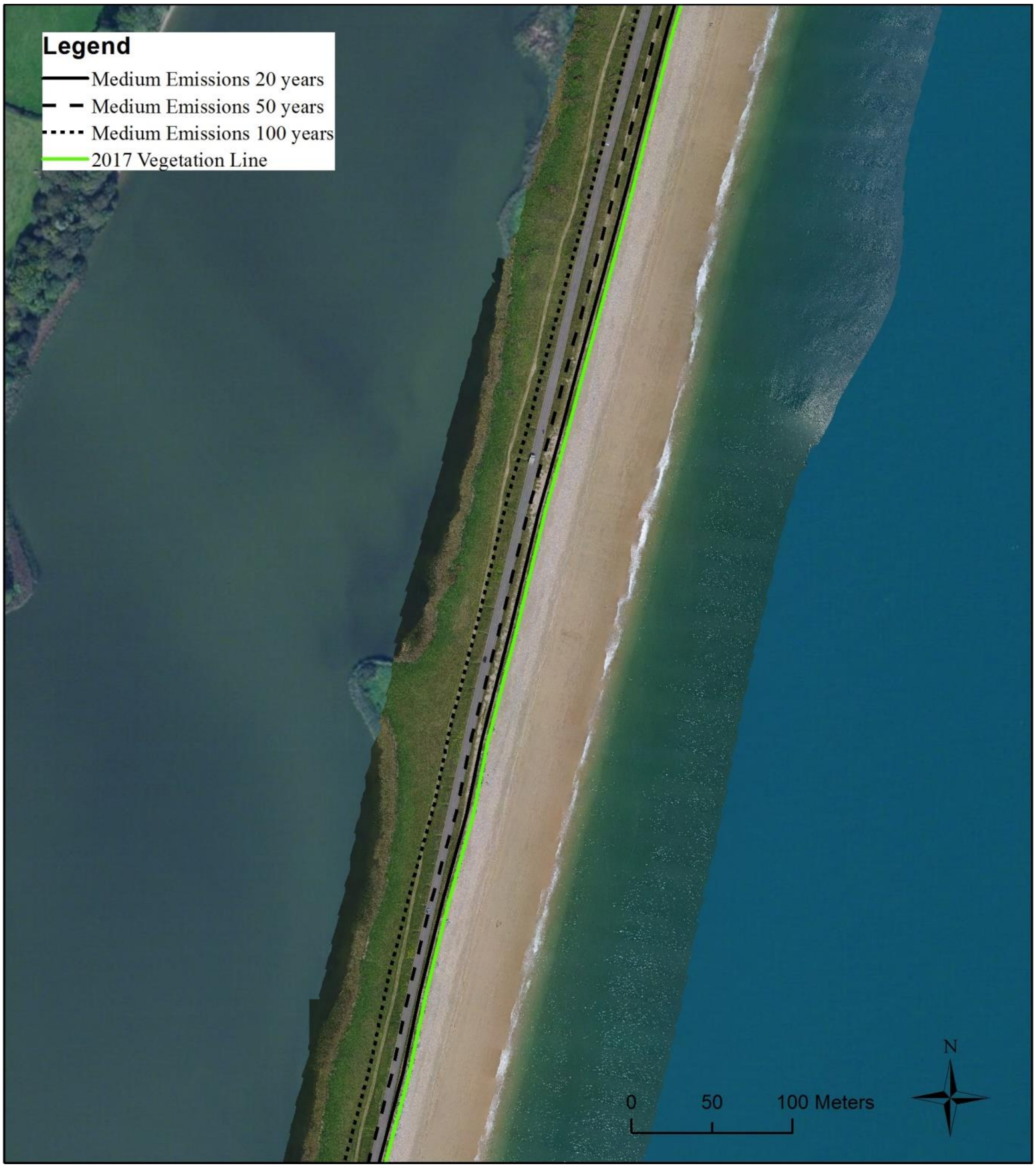

Figure B-4. Predicted retreat distance of Slapton barrier under rising sea-level rise from a medium emissions scenario (50th percentile prediction). Barrier section 4 of 5 is shown, where 1 = Strete, and 5 = Torcross.

Figure B-5. Predicted retreat distance of Slapton barrier under rising sea-level rise from a medium emissions scenario (50th percentile prediction). Barrier section 5 of 5 is shown, where 1 = Strete, and 5 = Torcross.

Appendix C. Predicted Barrier Retreat Under UKCP09 High Emissions Scenario

Figure C-1. Predicted retreat distance of Slapton barrier under rising sea-level rise from a high emissions scenario (50th percentile prediction). Barrier section 1 of 5 is shown, where 1 = Strete, and 5 = Torcross.

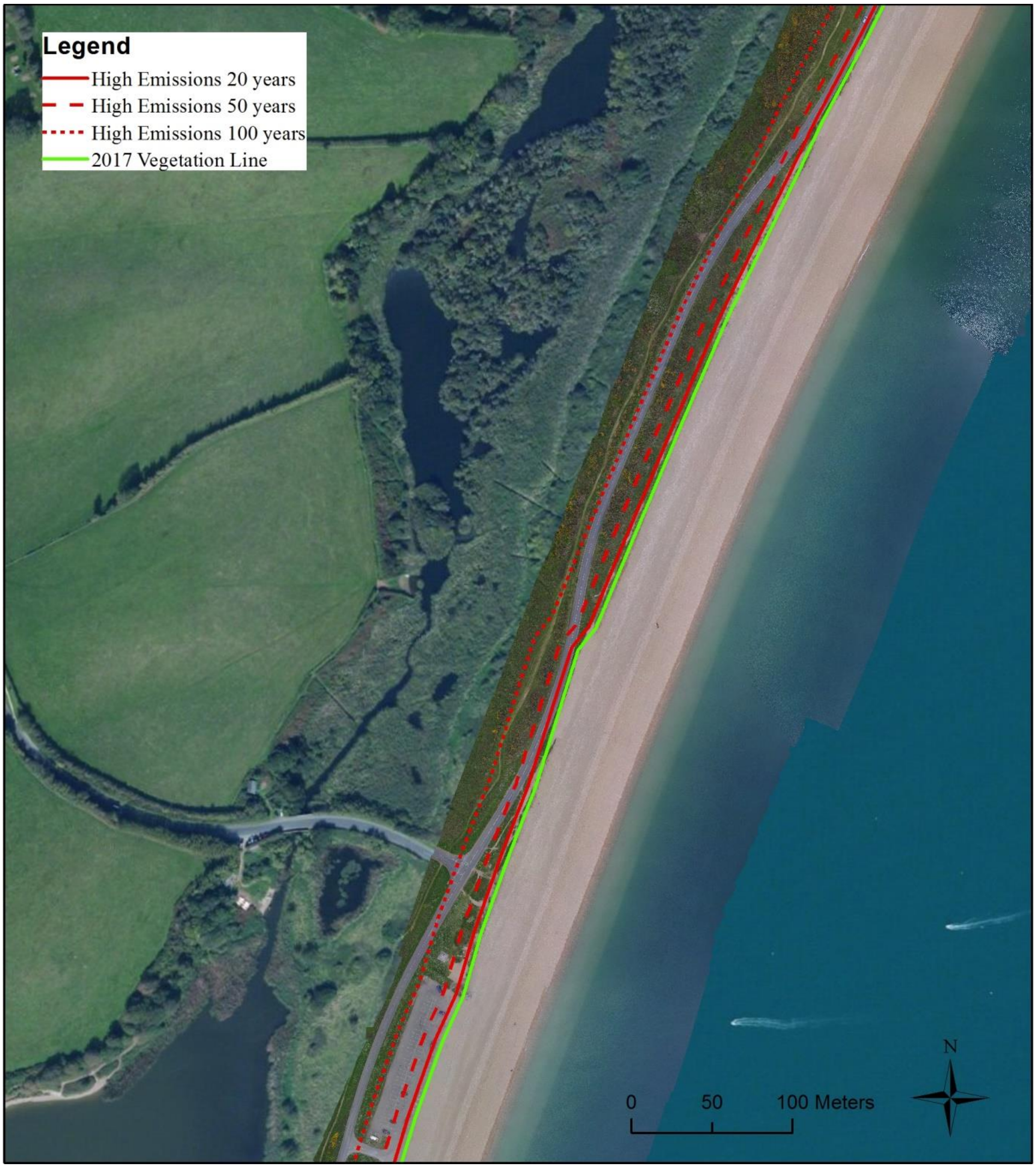

Figure C-2. Predicted retreat distance of Slapton barrier under rising sea-level rise from a high emissions scenario (50th percentile prediction). Barrier section 2 of 5 is shown, where 1 = Strete, and 5 = Torcross.

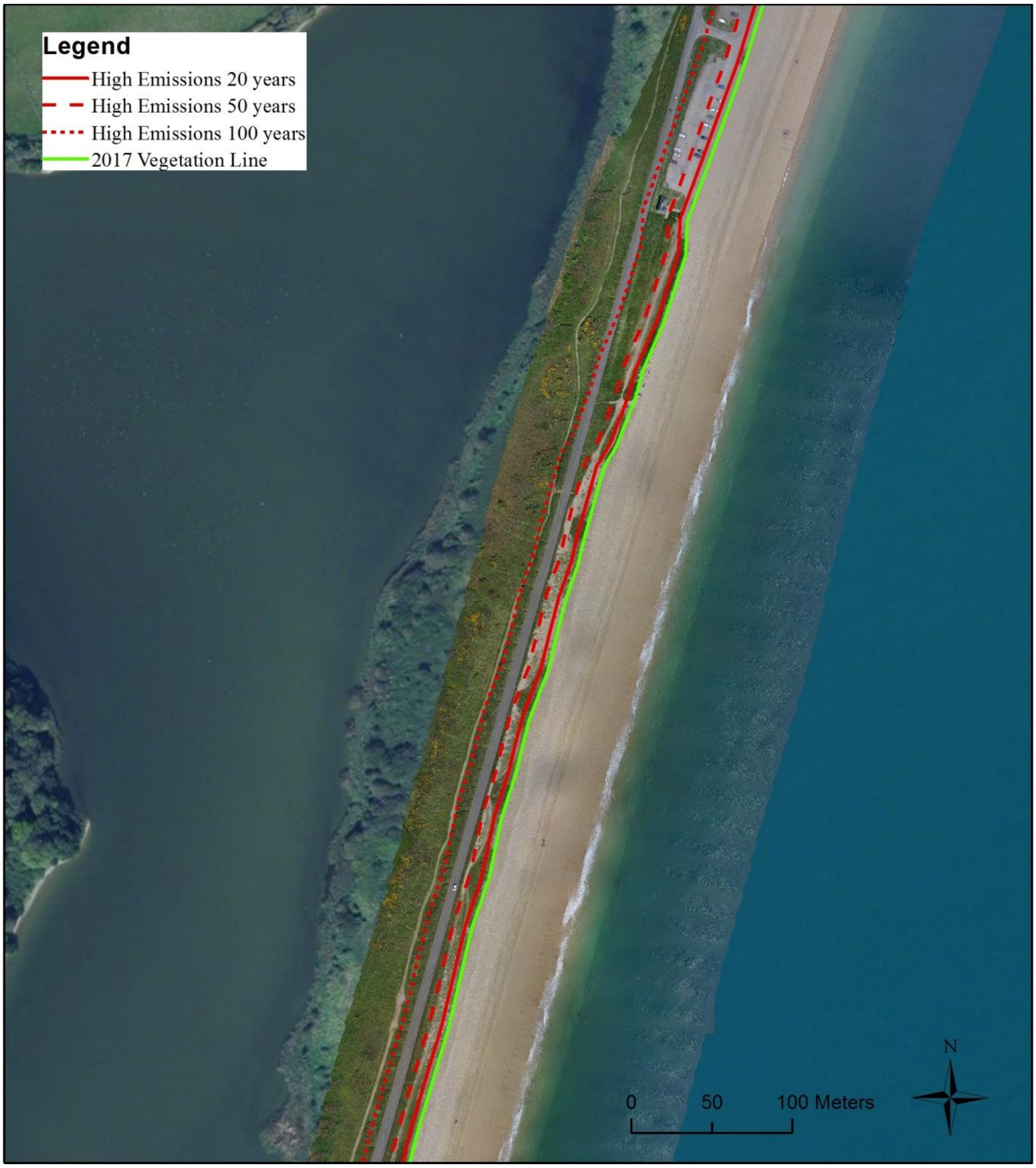

Figure C-3. Predicted retreat distance of Slapton barrier under rising sea-level rise from a high emissions scenario (50th percentile prediction). Barrier section 3 of 5 is shown, where 1 = Strete, and 5 = Torcross.

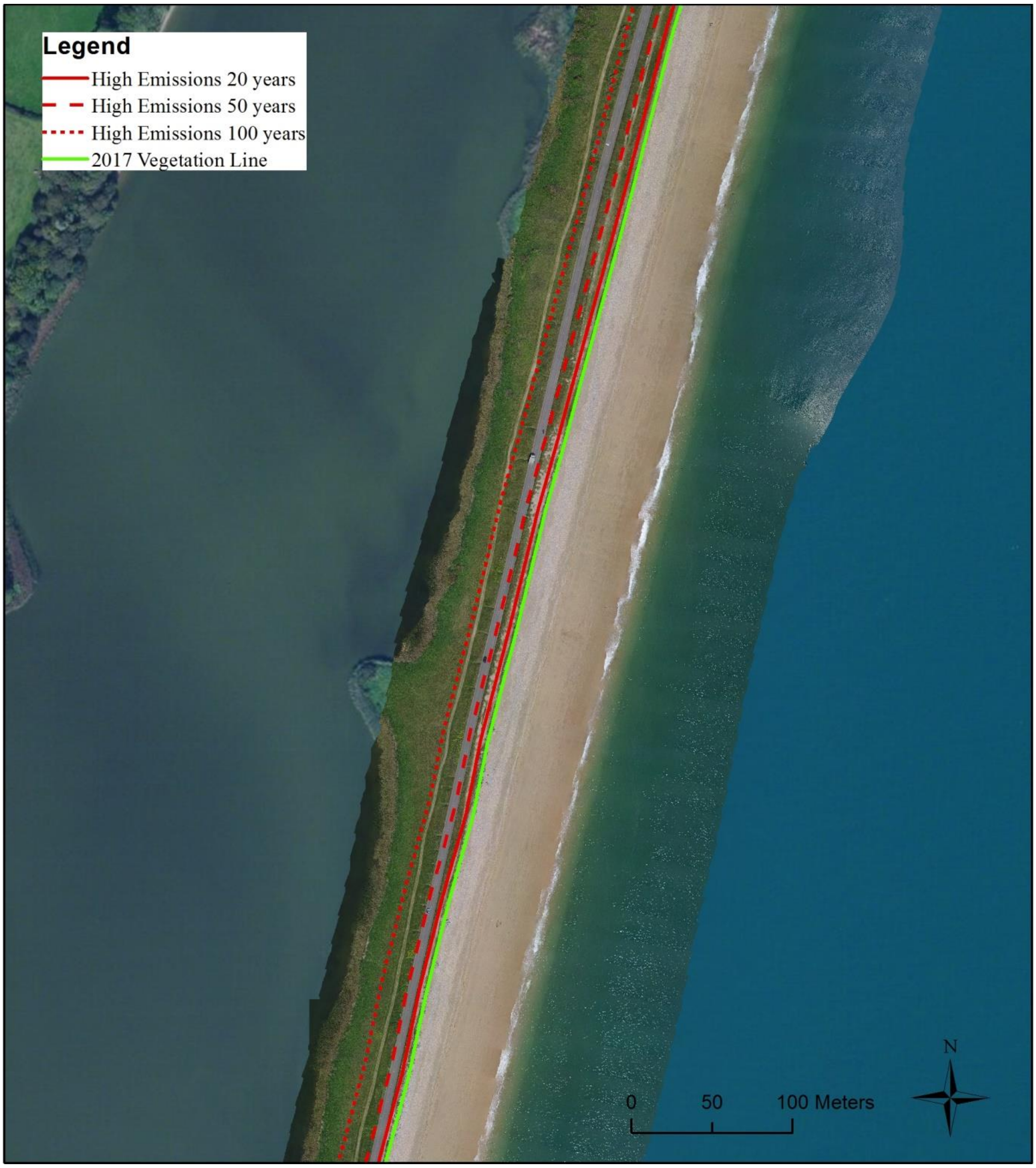

Figure C-4. Predicted retreat distance of Slapton barrier under rising sea-level rise from a high emissions scenario (50th percentile prediction). Barrier section 4 of 5 is shown, where 1 = Strete, and 5 = Torcross.

Figure C-5. Predicted retreat distance of Slapton barrier under rising sea-level rise from a high emissions scenario (50th percentile prediction). Barrier section 5 of 5 is shown, where 1 = Strete, and 5 = Torcross.